

Contents

1	Introduction	3
1.1	The Mott transition	4
1.1.1	The Mott insulator	4
1.1.2	The strongly-correlated metal	5
2	Brief introduction to Dynamical Mean Field Theory	7
2.1	Properties of tight-binding models in infinite coordination lattices	7
2.2	Reduction to a single site problem	10
2.3	Mapping onto an impurity model	13
2.4	Cluster extensions of DMFT	14
3	The Kondo effect and the physics of the Anderson impurity model	15
3.1	The Anderson Impurity Model	16
3.1.1	Perturbation theory	19
3.1.2	Mean-field analysis of the interaction	23
3.2	From the Anderson to the Kondo model	25
3.2.1	The emergence of logarithmic singularities and the Kondo temperature	26
3.2.2	Anderson's scaling theory	28
3.3	The impurity model from weak to strong repulsion and the DMFT results	31
3.3.1	DMFT scenario for the Mott transition	32
A	Brief introduction to scattering theory	34
A.0.2	Three dimensional example	37
A.1	General analysis of the phase-shifts	39
B	The Gutzwiller variational approach to the AIM	41
B.1	Variation of the electron number	41
B.2	Energy variation	42
B.3	The Gutzwiller wavefunction	45

C	Fermi liquid theory of the Anderson impurity model	48
C.1	Application to the single-orbital AIM	54
4	Brief introduction to the Wilson numerical renormalization group and to Conformal Field Theory	55
4.1	Reduction to a one dimensional model	55
4.2	The Wilson Numerical Renormalization group	58
4.2.1	The simplest example: the single-channel Kondo effect	61
4.3	Conformal Field Theory applied to impurity models	62
4.3.1	Some simple CFT results	63
5	The fate of the Kondo effect in impurity clusters and speculations on cluster DMFT	71
5.1	The impurity dimer	73
5.1.1	The isolated impurities	73
5.1.2	The breakdown of perturbation theory	75
5.1.3	The dimer phase diagram	76
5.1.4	The phase diagram away from particle-hole symmetry	84
5.1.5	A more realistic dimer model	86
5.2	The dimer model versus DMFT	87

Chapter 1

Introduction

More than fifty years after its proposal, the Mott transition remains an issue of current and broad interest, continually revived by the discovery of strongly correlated materials which display anomalous phenomena in the vicinity of a Mott insulating phase, high T_c superconductivity in cuprates being just the most spectacular example.

The Mott transition is known to escape any simple single-particle-like description, including the Hartree-Fock and the DFT-LDA theories. Indeed these theories are only able to deal with band-insulators characterized by an energy gap separating totally filled from unfilled bands. Therefore they can describe a Mott insulator only if a symmetry breaking order parameter is assumed, which turns effectively a Mott- into a conventional band-insulator. The typical example is the single-band Hubbard model at half-filling. This model should always have an insulating phase at sufficiently large repulsion. Yet, in order to make this phase accessible for instance to Hartree-Fock theory, one is obliged to assume an antiferromagnetic order parameter that doubles the unit cell so to fulfil the necessary requirement for a band-insulator to have an even number of electrons per unit cell. In this way, the Mott phenomenon, which solely involves freezing of charge fluctuations, is completely masked by magnetism. Since also conventional perturbation theory is inadequate, being the Mott transition inherently non-perturbative, *ad hoc* schemes have been developed during the years, starting from Hubbard himself. Among them, Dynamical Mean Field Theory (DMFT) and numerical quantum-simulations have been the most successful in uncovering the basic features of the Mott transition disentangled from un-necessary complications as magnetism.

However, once we accept the idea that the Mott phenomenon is well distinguishable from the on-set of symmetry breaking that usually arises in the insulating phase, then even the latter becomes far less trivial, as we are going to discuss.

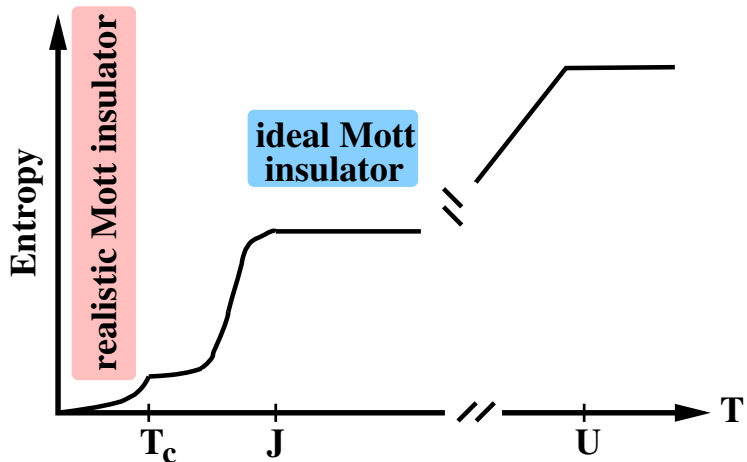


Figure 1.1: Qualitative behavior of the entropy of a Mott insulator.

1.1 The Mott transition

As we know the interaction-driven Mott metal-to-insulator transition emerges out of the competition between the tendency of the electrons to delocalize throughout the crystal so to maximize the band-energy gain and the Coulomb repulsion among the same electrons which, on the contrary, tends to suppress valence fluctuations by localizing the carriers. If the band-energy gain, which can be identified with the “bare” bandwidth W is small enough with respect to the short-range Coulomb repulsion, commonly parametrized by an on-site Hubbard U , and the electron-density is commensurate with the lattice, charges get localized and the system is a Mott insulator. On the contrary, if the bandwidth is larger than a critical value or if the electron-density is incommensurate, the pure system without disorder has to remain a metal, although a strongly-correlated one. Let us discuss on very general grounds the behavior of the entropy in both cases..

1.1.1 The Mott insulator

In Fig. 1.1 we sketch very roughly the expected behavior of the entropy well inside a Mott insulating phase, $U \gg W$. At high temperature $T \sim U$, the entropy related to valence fluctuations is suppressed and the system enters a regime with approximately constant entropy that could be defined as the *ideal* Mott insulator. Here only charge degrees of freedom are locked while all other degrees of freedom, like the spins and eventually the orbitals, are still completely free. However, at some lower temperature, other energy scales come into play, whose role is to lock these additional degrees of freedom so to rid the Mott insulator of their entropy. These energy scales include for instance the on-site Coulomb exchange, responsible of the Hund’s rules, the

inter-site direct- or super-exchange, the crystal field, the coupling to the lattice and so on and so for. We will denote these energy scales collectively as J , which has to be identified as the temperature at which the entropy of the residual degrees of freedom of the ideal Mott insulator starts to be suppressed. Consequently, at low temperature, a *realistic* insulating phase is established, which is usually accompanied by a symmetry breaking phase transition at $T = T_c \leq J$, for instance a magnetic ordering. Below T_c , the entropy decreases to zero as $T \rightarrow 0$ either exponentially or with a power law with an exponent generically greater than one, if a continuous symmetry is broken and gapless Goldstone modes exist.

Recently a lot of research activity has focused on the possibility that different symmetry broken phases may compete in the insulator, leading to exotic low temperature phenomena. Here we will discard completely this event and concentrate on a different competition which emerge in the metallic phase adjacent the Mott insulator.

1.1.2 The strongly-correlated metal

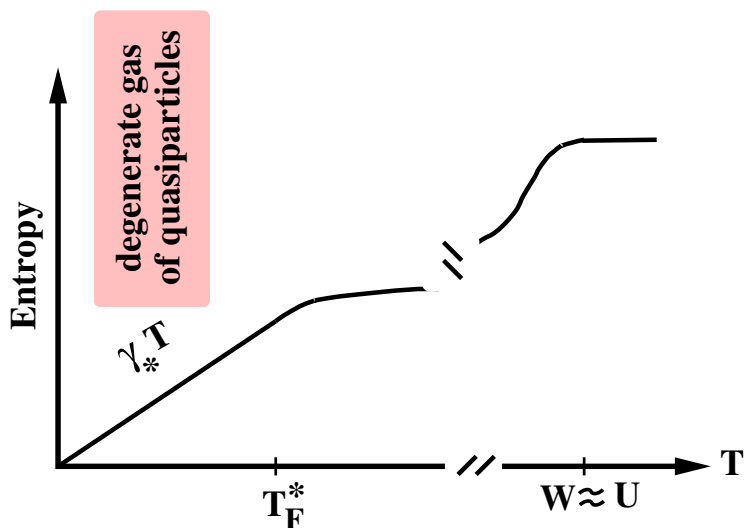


Figure 1.2: Qualitative behavior of the entropy of a strongly-correlated metal.

Let us move now on the metallic side of the Mott transition, where the band-energy gain W is slightly larger than its critical value $W_c \simeq U$ or the density is not commensurate. In Fig. 1.2 we draw what would roughly be the entropy behavior of the strongly-correlated Fermi-liquid-like metal in the absence of any symmetry breaking. As before we expect that the charge-fluctuation entropy is, this time only partially, reduced at some high temperature of order $W \simeq U$. The rest of the charge-fluctuation entropy as well as the entropy of the other degrees of freedom are instead suppressed by the formation of the degenerate quasi-particle gas. This occurs below a

temperature T_F^* , that can be identified as the effective quasi-particle Fermi temperature. Since quasiparticles carry the same quantum numbers of the electrons, the entropy quenching involves all degrees of freedom at the same time, including the charge. Below T_F^* the entropy should therefore vanish linearly, $S(T) \simeq \gamma_* T$, with a specific heat coefficient γ_* generically larger than its non-interacting value $\gamma \sim 1/W$.

Let us suppose that the Mott metal-to-insulator transition (MIT) is continuous and try to argue how it can happen. Obviously, since quasi-particles disappear at the transition, we should expect that $T_F^* \rightarrow 0$ at the MIT. Therefore at some value of $W \geq W_c$, the quasi-particle Fermi temperature T_F^* should become smaller than J . Therefore, by continuity with the insulating side, we should expect that part of the spin and eventually orbital entropy is already suppressed at temperatures of order J before the on-set of degeneracy. This would imply some kind of pseudo-gap opening above T_F^* , which is a bit at odds with the conventional Landau-Fermi-liquid theory. One way out, apart from a first-order MIT, is that something new happens when $T_F^* \simeq J$. Indeed the presence of J provides the metallic phase with an alternative mechanism to freeze spin and, eventually, orbital degrees of freedom independently of the charge ones, which becomes competitive with the on-set of a degenerate quasiparticle gas when $T_F^* \simeq J$. This competition more likely leads to an instability of the Landau-Fermi-liquid towards a low-temperature symmetry-broken phase, like in the insulating side, but it may also signal a real break-down of Fermi-liquid theory.

Notice that, unlike the competition between different symmetry broken Mott-insulating phases, which requires fine tuning of the Hamiltonian parameters that may only accidentally occur in real materials, this new type of competition should be accessible whenever it is possible to move gradually from a Mott insulator into a metallic phase, for instance by doping or applying pressure. We also know several examples where this competition is argued to be the origin of very appealing phenomena. For instance in heavy fermion materials the Kondo effect, favoring the formation of a coherent band of heavy quasiparticles, competes with the RKKY interaction. Here this competition is supposedly the key to understand the anomalies which appear at the transition between the heavy fermion paramagnet and the magnetically ordered phase. Another popular example are just the cuprates, where the role of J is presumably played by the super-exchange and is believed by many people to be the origin of superconductivity.

Since this competition occurs nearby the Mott transition, it is very difficult to investigate with conventional many-body techniques. Fortunately a lot of insights can still be gained by resorting to Dynamical Mean Field Theory.

Chapter 2

Brief introduction to Dynamical Mean Field Theory

In these lectures we discuss some general aspects of Dynamical Mean Field Theory which are needed for what will follow. This theory was formulated by Georges and Kotliar in 1992 starting from some previous observations by Metzner and Vollhardt about the properties of lattice models of interacting electrons in the limit of infinite coordination lattices.

2.1 Properties of tight-binding models in infinite coordination lattices

Since we do not pretend to give here a complete overview, let us discuss for simplicity the case of electrons hopping to nearest neighbor sites in a Bethe Lattice, which is the limit of infinite connectivity $z \rightarrow \infty$ of a Cayley tree, shown for instance with $z = 3$ in Fig. 2.1. The results, apart from some details, are generic to any infinite coordination lattices. Let us start by calculating the density of states (DOS) of a Cayley tree with nearest neighbor hopping $-t/\sqrt{z}$ in the limit $z \rightarrow \infty$ (the normalization of the hopping is needed to obtain a meaningful result, as shown below). The on-site Green's function of a given site, denoted as site 0, satisfies the Dyson equation with complex frequency ζ

$$G_{00}^{-1}(\zeta) = \zeta - \frac{t^2}{z} \sum_{i,0} G_{ii}^{(0)}(\zeta),$$

where the sum is over the z nearest neighbors of 0, and $G_{ii}^{(0)}(\zeta)$ denotes the local Green's function at site i with site 0 removed. In the limit $z \rightarrow \infty$, $G_{ii}^{(0)}$ should become equal to the true local Green's function $G = G_{00}$, leading to the self-consistency equation

$$G^{-1}(\zeta) = \zeta - t^2 G(\zeta).$$

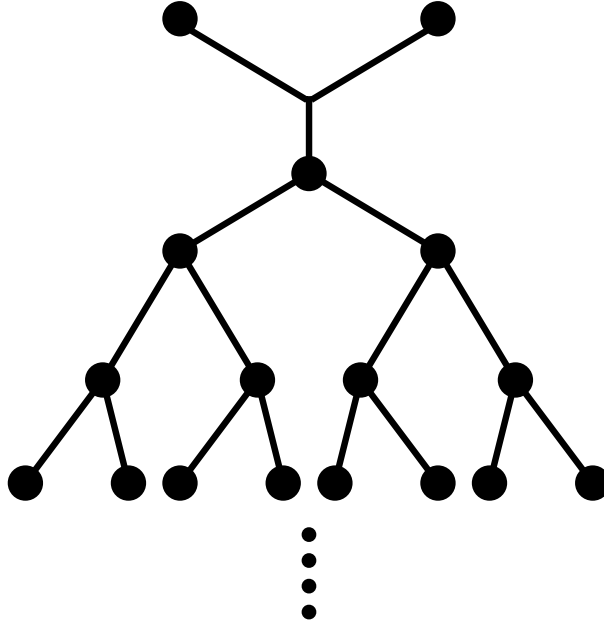


Figure 2.1: The Cayley tree for connectivity $z = 3$

Indeed the Dyson equation has a well defined limit for $z \rightarrow \infty$ thanks to the proper normalization of the hopping. The solution is

$$G(\zeta) = \frac{1}{2t^2} \left(\zeta - \sqrt{\zeta^2 - 4t^2} \right), \quad (2.1)$$

with the convention that

$$\lim_{|\zeta| \rightarrow \infty} \sqrt{\zeta^2 - 4t^2} = \zeta.$$

The DOS is obtained through

$$D(\epsilon) = -\frac{1}{\pi} \Im m G(\zeta \rightarrow \epsilon + i0^+) = \frac{\sqrt{4t^2 - \epsilon^2}}{2\pi t^2}. \quad (2.2)$$

The advantage of using the Bethe lattice is that its DOS is non-zero only on a finite energy-range, hence it is a sensible representation of the DOS of a generic tight-binding model in finite-dimensional lattices (apart from accidental model-dependent features as Van Hove singularities). For instance the DOS of a hypercubic lattice with nearest neighbor hopping $-t/\sqrt{2d}$ (the coordination number $z = 2d$) in the limit of infinite dimensions $d \rightarrow \infty$ is a gaussian

$$D(\epsilon) = \frac{1}{\sqrt{2\pi t^2}} e^{-\epsilon^2/2t^2},$$

which is non-zero for any value of the energy.

Two sites, i and j , are connected in the Cayley tree by just a single path, whose length is denoted as $R(i, j)$. In other words, an electron at i has to hop $R(i, j)$ times to reach j , each hopping bringing with itself a factor $1/\sqrt{z}$. As a result the Green's function G_{ij} scales with z as

$$G_{ij} \sim \left(\sqrt{\frac{1}{z}} \right)^{R(i,j)}. \quad (2.3)$$

Since this scaling behavior with the coordination number is just consequence of the normalization of the hopping amplitude, it is generic to any d -dimensional lattices when $d \rightarrow \infty$. Moreover we do not expect that this behavior does change if a short-range interaction is included.

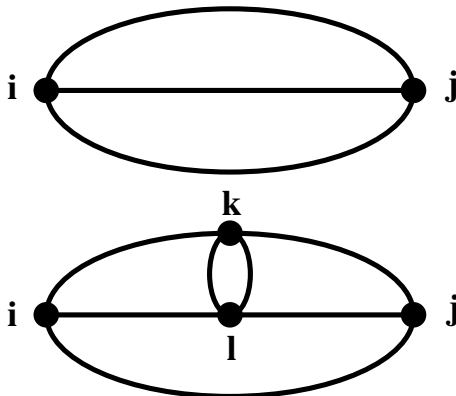


Figure 2.2: Example of two self-energy diagrams which collapse to a single site

Let us analyse the consequences of (2.3) within the skeleton perturbation expansion of the single-particle self-energy $\Sigma_{ij}(i\epsilon_n)$. In Fig. 2.2 we draw the second- and the fourth-order skeleton diagrams of the self-energy Σ_{ij} . Each dot corresponds to the on-site interaction vertex and is labelled by the site-index, while the lines are the fully-interacting Green's functions. In the second order diagram, site i and j are connected by three lines, which means through (2.3) a factor $z^{-3R(i,j)/2}$. If we were to do a Fourier transform, we should take fixed for instance i and sum over all j 's. Since the number of sites j which have the same distance $R(i, j) = R$ from i scales as z^R , we get to the conclusion that only the term with $R = 0$, namely $i = j$, survives. Let us consider now the fourth-order diagram. Again we can realize that each pair of sites can be joined at least by three independent paths. As a result the only non-zero contribution for $z \rightarrow \infty$ arises again when $i = j = k = l$. The same conclusion can be shown to hold at any order in perturbation theory. The consequence is that the self-energy in the skeleton expansion is only functional of the local Green's function, hence it is itself local, namely

$$\Sigma_{ij}(i\epsilon_n) = \delta_{ij} \Sigma(i\epsilon_n), \quad (2.4)$$

hence its Fourier transform is momentum independent,

$$\Sigma(\mathbf{k}, i\epsilon_n) = \Sigma(i\epsilon_n). \quad (2.5)$$

As a by-product, let us consider the irreducible vertex $\Gamma_{ij;kl}^0$ in some scattering channel. We know that, considering the self-energy as functional of the fully-interacting Green's function, the following relation holds:

$$\Gamma_{il;kj}^0 = \frac{\delta \Sigma_{ij}[G]}{\delta G_{kl}}.$$

Since we just demonstrated that the self-energy is local and functional only of the local Green's function, it derives that all irreducible vertices are local too, i.e.

$$\Gamma_{il;kj}^0 = \Gamma^0 \delta_{ij} \delta_{ik} \delta_{il}. \quad (2.6)$$

We conclude by some definitions. Since the self-energy is only frequency dependent, the local Green's function is the Hilbert transform

$$G(i\epsilon_n) = \tilde{D}(\zeta) \equiv \int d\epsilon D(\epsilon) \frac{1}{\zeta - \epsilon}, \quad (2.7)$$

where $\zeta = i\epsilon_n + \mu - \Sigma(i\epsilon_n)$, μ being the chemical potential. In other words ζ is the inverse Hilbert transform of G , namely

$$\zeta = R\left(\tilde{D}(\zeta)\right) = R(G). \quad (2.8)$$

In the case of the Bethe lattice, one can easily show that

$$\tilde{D}(\zeta) = \frac{1}{2t^2} \left(\zeta - \sqrt{\zeta^2 - 4t^2} \right), \quad (2.9)$$

with the same convention as before

$$\lim_{|\zeta| \rightarrow \infty} \sqrt{\zeta^2 - 4t^2} = \zeta.$$

Inverting this formula leads to

$$\zeta = i\epsilon_n + \mu - \Sigma(i\epsilon_n) = R(G) = t^2 G + \frac{1}{G}. \quad (2.10)$$

2.2 Reduction to a single site problem

Let us now consider the interacting Hamiltonian on the Cayley tree

$$\mathcal{H} \left[c^\dagger, c \right] = -\frac{t}{\sqrt{z}} \sum_{\langle ij \rangle, a} c_{ia}^\dagger c_{ja} + H.c. + \sum_i \mathcal{H}_{int} \left[c_i^\dagger, c_i \right],$$

where c_{ia}^\dagger and c_{ia} are creation and annihilation operators at site i , a is a multilabel for spin and eventually orbitals, and \mathcal{H}_{int} is an on-site interaction term. Within the path-integral formalism the imaginary-time action is

$$\mathcal{S} = \int_0^\beta d\tau \sum_{i,a} \bar{c}_{ia}(\tau) (\partial_\tau - \mu) c_{ia}(\tau) + \mathcal{H}[\bar{c}(\tau), c(\tau)],$$

where $\bar{c}(\tau)$ and $c(\tau)$ are Grassmann variables at imaginary time τ . Let us focus on a particular site, for instance site 0, and write

$$\mathcal{S} = \mathcal{S}_0 + \mathcal{S}_{0-bath} + \mathcal{S}_{bath},$$

where

$$\mathcal{S}_0 = \int_0^\beta d\tau \sum_a \bar{c}_{0a}(\tau) (\partial_\tau - \mu) c_{0a}(\tau) + \mathcal{H}_{int}[\bar{c}_0(\tau), c_0(\tau)],$$

is the action of the isolated site 0,

$$\mathcal{S}_{0-bath} = -\frac{t}{\sqrt{z}} \sum_{\langle i0 \rangle, a} \int_0^\beta d\tau \bar{c}_{ia}(\tau) c_{0a}(\tau) + \bar{c}_{0a}(\tau) c_{ia}(\tau),$$

is the coupling between site 0 and the other sites, described by the action \mathcal{S}_{bath} . The effective action for site 0 can be obtained by integrating over all the other sites within a perturbative expansion in \mathcal{S}_{0-bath} . By means of the linked-cluster theorem one finds that

$$\mathcal{S}_0^{eff} = \mathcal{S}_0 + \Delta\mathcal{S}_0,$$

where (we drop for simplicity the multilabel a)

$$\begin{aligned} \Delta\mathcal{S}_0 &= \sum_{n=1}^{\infty} \Delta\mathcal{S}_0^{(n)} = \sum_{n=1}^{\infty} \left(\frac{t}{\sqrt{z}}\right)^{2n} \sum_{i_1, \dots, i_n, i'_1, \dots, i'_n}^{\text{n.n.'s of 0}} \int_0^\beta \prod_{j=1}^n d\tau_j d\tau'_j \\ &\quad \bar{c}_0(\tau_1) \bar{c}_0(\tau_2) \dots \bar{c}_0(\tau_n) c_0(\tau'_n) \dots c_0(\tau'_2) c_0(\tau'_1) \\ &\quad G_{i_1, \dots, i_n, i'_n, \dots, i'_1}^{(0)}(\tau_1, \tau_2, \dots, \tau_n, \tau'_n, \tau'_{n-1}, \dots, \tau'_1), \end{aligned} \quad (2.11)$$

being $G_{i_1, \dots, i_n, i'_n, \dots, i'_1}^{(0)}(\tau_1, \tau_2, \dots, \tau_n, \tau'_n, \tau'_{n-1}, \dots, \tau'_1)$ the n -particle connected Green's function of the fully interacting model with site 0 removed. Notice that, in the Cayley tree, once site 0 has been removed there is no path connecting two different nearest neighbor sites of 0. Therefore the only non-zero fully-connected n -particle Green's functions appearing in (2.11) are those with $i_1 = i_2 = \dots = i_n = i'_n = \dots = i'_1$. As a result, the summation reduces only to the sum over

the z nearest neighbors. Since the n -th order term is proportional to z^{-n} , the only one which survives for $z \rightarrow \infty$ has $n = 1$, namely

$$\Delta \mathcal{S}_0 = \Delta \mathcal{S}_0^{(1)} = \frac{t^2}{z} \sum_{i \text{ n.n.'s of } 0} \int_0^\beta d\tau d\tau' \bar{c}_0(\tau) G_{ii}^{(0)}(\tau, \tau') c_0(\tau').$$

In the limit $z \rightarrow \infty$ the local Green's function with site 0 removed should not differ from the local Green's function G with site 0 present, which is obviously site-independent. Hence

$$\Delta \mathcal{S}_0 \rightarrow t^2 \int_0^\beta d\tau d\tau' \bar{c}_0(\tau) G(\tau, \tau') c_0(\tau'),$$

and

$$\begin{aligned} \mathcal{S}_0^{eff} &= \int_0^\beta d\tau \sum_a \bar{c}_{0a}(\tau) (\partial_\tau - \mu) c_{0a}(\tau) + \mathcal{H}_{int}[\bar{c}_0(\tau), c_0(\tau)] \\ &+ t^2 \int_0^\beta d\tau d\tau' \bar{c}_0(\tau) G(\tau, \tau') c_0(\tau'). \end{aligned} \quad (2.12)$$

This action describes a single site with a non-interacting single-particle Green's function

$$\mathcal{G}_0^{-1}(i\epsilon_n) = i\epsilon_n + \mu - t^2 G(i\epsilon_n), \quad (2.13)$$

in the presence of an instantaneous interaction \mathcal{H}_{int} . \mathcal{G}_0 plays actually the same role played by the Weiss field in classical Mean-Field Theory. Let us suppose we were able to solve this single-site problem and find the fully-interacting single-particle Green's function

$$\mathcal{G}^{-1}(i\epsilon_n) = \mathcal{G}_0^{-1}(i\epsilon_n) - \Sigma(i\epsilon_n), \quad (2.14)$$

where Σ is the self-energy of the single-site problem. Since site 0 is equivalent to any other site, it immediately follows that

$$\mathcal{G}(i\epsilon_n) \equiv G(i\epsilon_n), \quad (2.15)$$

namely that

$$G^{-1}(i\epsilon_n) \equiv i\epsilon_n + \mu - t^2 G(i\epsilon_n) - \Sigma(i\epsilon_n). \quad (2.16)$$

Comparing (2.16) with (2.10) we discover that the self-energy of the single-site problem coincides with the momentum independent self-energy of the lattice model. The same equivalence holds for any infinite-coordination-lattice model, where the single-site non-interacting Green's function, also called the Weiss field, takes the general form

$$\mathcal{G}_0^{-1}(i\epsilon_n) = i\epsilon_n + \mu + G(i\epsilon_n)^{-1} - R(G(i\epsilon_n)), \quad (2.17)$$

being $R(G)$ the inverse Hilbert transform with the appropriate DOS. Eq. (2.17) reduces to (2.13) in the Bethe lattice.

2.3 Mapping onto an impurity model

We have shown that for infinite coordination lattices one can determine the single-particle self-energy, which is purely local, by solving an auxiliary single-site problem with action (2.12). The self-energy of this problem is identical to the lattice self-energy. In order to gain some physical insights, let us try to reformulate the Lagrangian problem (2.12) into an Hamiltonian one.

Let us consider the following Anderson impurity model:

$$\mathcal{H}_{AIM} = \mathcal{H}_{bath} + \mathcal{H}_{imp} + \mathcal{H}_{imp-bath}, \quad (2.18)$$

where

$$\mathcal{H}_{bath} = \sum_{\epsilon a} \epsilon c_{\epsilon a}^\dagger c_{\epsilon a}, \quad (2.19)$$

describes a non-interacting bath,

$$\mathcal{H}_{imp} = -\mu \sum_a d_a^\dagger d_a + \mathcal{H}_{int} [d^\dagger, d], \quad (2.20)$$

is the Hamiltonian of the isolated impurity, and

$$\mathcal{H}_{imp-bath} = \sum_{\epsilon a} V_\epsilon d_a^\dagger c_{\epsilon a} + H.c., \quad (2.21)$$

is the hybridization of the impurity with the bath. Within the path-integral formalism, upon integrating out the conduction electrons we would arrive to an action for the impurity of the same form as (2.12) with the non-interacting Green's function given by

$$\mathcal{G}_0^{-1}(i\epsilon_n) = i\epsilon_n + \mu - \Delta(i\epsilon), \quad (2.22)$$

where $\Delta(i\epsilon)$ is the so-called hybridization function, as discussed later,

$$\Delta(i\epsilon) = \sum_\epsilon \frac{|V_\epsilon|^2}{i\epsilon_n - \epsilon}.$$

Therefore, if we impose that the hybridization function is related to the fully-interacting impurity Green's function by the self-consistency requirement

$$\Delta(i\epsilon) = \sum_\epsilon \frac{|V_\epsilon|^2}{i\epsilon_n - \epsilon} = t^2 \mathcal{G}(i\epsilon_n), \quad (2.23)$$

then the solution of the impurity model coincides with the solution of the lattice model.

A big advantage of the mapping onto an Anderson impurity model is that the latter is very well known and can provide a useful guidance to interpret the behavior of the lattice model. Therefore it is convenient to begin our analysis from the Anderson impurity model *per se*, before discussing the behavior of a strongly correlated lattice models as emerges out of DMFT. However, before we start presenting the physics of the Anderson impurity model, it is convenient to briefly overview the extension of DMFT from the single-site to a cluster.

2.4 Cluster extensions of DMFT

We have shown that, in the limit of infinite-coordination lattices, a lattice model of electrons interacting with an on-site potential can be mapped onto a single Anderson impurity model subject to a self-consistency requirement. Although in finite coordination lattices the mapping is no more exact, one can still use DMFT as a mere approximation. Indeed, if one is convinced that what really matters close to a Mott transition is the frequency dependence of the self-energy and not its momentum dependence, then one can assume $\Sigma(\mathbf{k}, i\epsilon_n) \simeq \Sigma(i\epsilon_n)$ and search for an Anderson impurity model built so to have the same self-energy as the local-one in the lattice model. If one builds up this procedure in a consistent way, the resulting self-consistency requirement is just Eq. (2.17). However, we already mentioned that an interesting piece of physics may emerge in the metallic phase when the quasi-particle Fermi temperature, T_F^* , becomes of the same order as the processes, J , that rid the *ideal* Mott insulator of its residual entropy. Since in many relevant models these processes are inter-site, like the super-exchange in the Hubbard model, this physics is lost in the single-site DMFT approximation.

There have been recently several attempts to extend DMFT approximation to include partially spatial correlations. The idea underneath is the same for all these extensions. Essentially, instead of focusing on a single site, within cluster-DMFT one considers a cluster of sites and solve an auxiliary model of a cluster of Anderson impurities embedded into a bath, with an hybridization function to be determined self-consistently. However, since there is no obvious limiting case in which a cluster extension of DMFT becomes exact, as it was the infinite-coordination limit in the single-site formulation, the self-consistency requirement is not uniquely defined and differs from one version of cluster-DMFT to another.

It is not our purpose to discuss in detail all these extensions. We only want to point out that, as the single impurity *per se* can be used as a guideline to interpret the single-site DMFT results, analogously the knowledge of the general properties of clusters of Anderson impurities may turn useful in connection with cluster-DMFT. In particular we will show that the above mentioned competition T_F^* versus J , that we aim to explore, has a very simple and inspiring analogy in impurity-clusters.

Chapter 3

The Kondo effect and the physics of the Anderson impurity model

The Anderson impurity model was originally introduced in the 60's to explain the behavior of magnetic impurities (Fe, Mn, Cr) diluted into non magnetic metals.

We know that the thermodynamics and transport properties of good metals with a large Fermi temperature, $T_F \sim 10^4$ K, are dominated at low temperatures, $T \ll T_F$, by the Pauli principle. For instance, magnetic susceptibility is roughly constant, $\chi \sim 1/T_F$, and one should in principle heat the sample to very high temperatures $T \gg T_F$ to release the spin entropy and recover a Curie-Weiss behavior $\chi \sim 1/T$. Moreover, the resistivity is an increasing function of temperature, since the channels which may dissipate current, the coupling to the lattice as well as to multi particle-hole excitations, become available only upon heating.

At odds with this expectation, if a very diluted (even few part per million) concentration of magnetic impurities is introduced, the above behavior changes drastically. We just mention three distinct features.

- (1) The magnetic susceptibility shows a Curie-Weiss behavior well below T_F , proportional to the impurity concentration n_i and roughly with the same g -factor of the isolated magnetic impurity, apart from corrections due to the crystal field. Around a very low temperature, called Kondo-temperature, T_K , the Curie-Weiss behavior turns into a logarithmic one and finally the susceptibility saturates at low temperature to a value $\chi(0) \sim n_i/T_K$, with $\chi(T) - \chi(0) \sim -T^2$.
- (2) The resistivity $R(T)$ displays a minimum around T_K , followed at $T < T_K$ by a logarithmic increase. At very low temperatures, $R(T)$ approaches a constant value $R(0) \propto n_i$ with $R(T) - R(0) \sim -T^2$. The value of the residual resistivity $R(0)$ suggests very strong scattering potential, near the so-called *unitary limit*.
- (3) The entropy released above the Kondo temperature, which can be obtained by measuring

the specific heat, includes only spin and eventually orbital degrees of freedom of the isolated impurity but not the charge degrees of freedom. This indicates that the magnetic impurities behave as local moments above T_K .

Explaining this behavior amounts actually to understand (1) how it is possible to sustain a local moment in a metal; and (2) why and how, once the local moment is formed, it disappears at low temperatures.

The earlier attempts, mainly due to Friedel, to tackle these questions using the conventional scattering theory of metals partially failed. As we will discuss in Appendix A, the only possible way to explain within scattering theory a Pauli-like behavior $\chi \sim 1/T_K$ which turns into a Curie-Weiss one at $T_K \ll T \ll T_F$ is by the existence of a narrow resonance, of width T_K , pinned nearby the chemical potential, still on a scale T_K . This explanation is however not satisfying mainly for two reasons. First of all it does not justify why this resonance should always be pinned at the chemical potential for many different host metals and magnetic impurities. Moreover it contradicts the measured entropy-release above T_K . In fact, for temperatures bigger than its width, the full entropy of a resonant state should be recovered, which includes charge degrees of freedom, too.

3.1 The Anderson Impurity Model

Something which is obviously missing in the scattering-theory analysis are local electron-electron correlations around the magnetic ions. A narrow resonance induced by an impurity would be quite localized around the same impurity, being essentially an atomic level broadened by the hybridization with the conduction electrons of the host metal. Therefore, like an atomic level, such a resonance is likely to accomodate only a fixed number of electrons, say N , paying a finite amount of energy for adding or removing electrons. As usual, it is convenient to define a so-called Hubbard repulsion U through

$$U = E(N + 1) + E(N - 1) - 2E(N), \quad (3.1)$$

where $E(M)$ is the total energy when the resonance is forced to have M electrons, N being the equilibrium value. In principle one might include this additional ingredient by adding to the Hamiltonian a term

$$\frac{U}{2} (\hat{n} - N)^2, \quad (3.2)$$

with \hat{n} the occupation number operator of the resonance level. If it were possible to define such an operator, then (3.2) would actually solve one of the puzzles. Indeed, if $U \gg T_K$ and for temperatures $T_K \ll T \ll U$, valence fluctuations with respect to the equilibrium value N would be suppressed, and the only degrees of freedom contributing to the entropy would be those related to the degeneracy of the N -electron configurations at the resonance. Namely, if the

resonance is $2(2L+1)$ -fold degenerate, 2 from spin and $(2L+1)$ from the orbital, the degeneracy of the N -electron state is the binomial

$$C_N^{2(2L+1)} = \binom{2(2L+1)}{N} = \frac{(4L+2)!}{N!(4L+2-N)!},$$

with entropy $S = \ln C_N^{2(2L+1)}$. In other words the resonance would actually behave like a local moment. Unfortunately the resonance occupation number operator is an ill defined object. To overcome this difficulty, Anderson had the idea to represent the resonance as an additional electronic-level inside the conduction band, even if this would be, rigorously speaking, an over-complete basis. This leads to the so-called Anderson Impurity Model (AIM) defined in the simplest case of a single-orbital impurity $L = 0$ as

$$\begin{aligned} \mathcal{H}_{AIM} = & \sum_{\mathbf{k}\sigma} \epsilon_{\mathbf{k}} c_{\mathbf{k}\sigma}^\dagger c_{\mathbf{k}\sigma} + \sum_{\mathbf{k}\sigma} V_{\mathbf{k}} c_{\mathbf{k}\sigma}^\dagger d_\sigma + H.c. \\ & + \frac{U}{2} (\hat{n}_d - 1)^2 + \epsilon_d \hat{n}_d. \end{aligned} \quad (3.3)$$

This model describes a band of conduction electrons with energy dispersion $\epsilon_{\mathbf{k}}$, hybridized with a single level, d_σ , with energy ϵ_d , both $\epsilon_{\mathbf{k}}$ and ϵ_d being measured with respect to the chemical potential, and $\hat{n}_d = \sum_\sigma d_\sigma^\dagger d_\sigma$. This level suffers from an interaction U which tends to lock no more no less than a single electron.

Let us start from the non-interacting model, $U = 0$, to show that it indeed describes a resonance. Before switching the hybridization $V_{\mathbf{k}}$, the conduction electron Green's function in complex frequency z is

$$G_{\mathbf{k}}^{(0)}(z) = \frac{1}{z - \epsilon_{\mathbf{k}}} = \text{-----} \Rightarrow \quad (3.4)$$

and is represented as a dashed tiny line, while the impurity one is

$$\mathcal{G}^{(0)}(z) = \frac{1}{z - \epsilon_d} = \text{—————} \Rightarrow \quad (3.5)$$

and is represented as a solid tiny line. The corresponding Green's functions in the presence of $V_{\mathbf{k}}$,

$$\begin{aligned} G_{\mathbf{k}\mathbf{p}}(z) &= \text{-----} \Rightarrow \\ \mathcal{G}(z) &= \text{—————} \Rightarrow, \end{aligned}$$

are represented as bold lines. Notice that the conduction electron Green's function is no more diagonal in momentum. In addition one has to introduce the mixed Green's functions

$$G_{\mathbf{k}d}(\tau) = -\langle T (c_{\mathbf{k}\sigma}(\tau) d_\sigma^\dagger) \rangle = \text{-----} \Rightarrow \text{—————} \Rightarrow$$

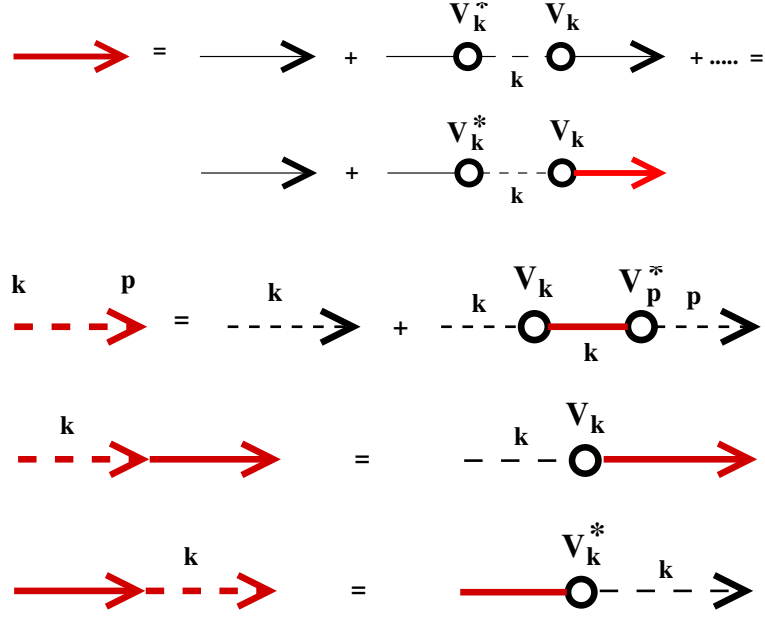


Figure 3.1: Dyson equations for the Green's functions. Bold (red) lines are the Green's functions in the presence of hybridization, represented as a circle, while tiny (black) lines are unperturbed Green's functions.

$$G_{dk}(\tau) = -\langle T(d_\sigma(\tau) c_{k\sigma}^\dagger(\tau)) \rangle = \text{bold arrow} \rightarrow \text{dashed arrow} \rightarrow$$

Through the Dyson equation shown diagrammatically in Fig. 3.1, we find that

$$\mathcal{G}(z) = \frac{1}{z - \epsilon_d - \Delta(z)}, \quad (3.6)$$

where the so-called hybridization function is defined through

$$\Delta(z) = \sum_{\mathbf{k}} \frac{|V_{\mathbf{k}}|^2}{z - \epsilon_{\mathbf{k}}}. \quad (3.7)$$

The conduction electron Green's function is instead

$$G_{\mathbf{k}\mathbf{p}}(z) = \delta_{\mathbf{k}\mathbf{p}} G_{\mathbf{k}}^{(0)}(z) + G_{\mathbf{k}}^{(0)}(z) T_{\mathbf{k}\mathbf{p}}(z) G_{\mathbf{p}}^{(0)}(z), \quad (3.8)$$

where the T -matrix, see Appendix A, is

$$T_{\mathbf{k}\mathbf{p}}(z) = V_{\mathbf{k}} \frac{1}{z - \epsilon_d - \Delta(z)} V_{\mathbf{p}}^*. \quad (3.9)$$

In addition

$$G_{kd}(z) = \frac{V_{\mathbf{k}}}{z - \epsilon_{\mathbf{k}}} \frac{1}{z - \epsilon_d - \Delta(z)}, \quad (3.10)$$

$$G_{d\mathbf{k}}(z) = \frac{V_{\mathbf{k}}^*}{z - \epsilon_{\mathbf{k}}} \frac{1}{z - \epsilon_d - \Delta(z)}. \quad (3.11)$$

We notice that the hybridization function has a branch cut on the real axis since

$$\Im \Delta(z \rightarrow \epsilon \pm i0^+) = \mp \pi \sum_{\mathbf{k}} |V_{\mathbf{k}}|^2 \delta(\epsilon - \epsilon_{\mathbf{k}}) \equiv \mp \Gamma(\epsilon). \quad (3.12)$$

In terms of $\Gamma(\epsilon) > 0$ we can write

$$\Delta(z) = \int \frac{d\epsilon}{\pi} \frac{\Gamma(\epsilon)}{z - \epsilon}.$$

Since we are interested in temperatures/frequencies much smaller than the conduction electron Fermi energy, we will assume for simplicity that $\Gamma(\epsilon) = \Gamma$ for $|\epsilon| < W$ and $\Gamma(\epsilon) = 0$ otherwise, with W of order T_F . Then, if $|z| \ll W$ one readily finds that

$$\Delta(z) = -i\Gamma \operatorname{sgn} \Im z. \quad (3.13)$$

In this approximation the impurity DOS is

$$\rho_d^{(0)}(\epsilon) = -\frac{1}{\pi} \Im \mathcal{G}(\epsilon + i0^+) = \frac{1}{\pi} \frac{\Gamma}{(\epsilon - \epsilon_d)^2 + \Gamma^2}, \quad (3.14)$$

which is just a resonant state trapping a number of electrons of given spin that is

$$N_d = \int_{-\infty}^{+\infty} d\epsilon f(\epsilon) \rho_d^{(0)}(\epsilon). \quad (3.15)$$

According to the scattering theory analysis of Appendix A, this resonance corresponds to a scattering phase shift $\pi/2$ at the chemical potential.

3.1.1 Perturbation theory

Let us consider the case $\epsilon_d = 0$ and switch on the Hubbard repulsion

$$\frac{U}{2} (\hat{n}_d - 1)^2 = \frac{U}{2} + U \hat{n}_{d\uparrow} \hat{n}_{d\downarrow} - \frac{U}{2} \hat{n}_d,$$

to be treated in perturbation theory. To be consistent the perturbation expansion is carried out both in the interaction term as well as in the last term on the right-hand side.

First of all notice that, since the conduction electrons are non-interacting, their Green's function is still of the form

$$G_{\mathbf{k}\mathbf{p}}(z) = \delta_{\mathbf{k}\mathbf{p}} G_{\mathbf{k}}^{(0)}(z) + G_{\mathbf{k}}^{(0)}(z) T_{\mathbf{k}\mathbf{p}}(z) G_{\mathbf{p}}^{(0)}(z), \quad (3.16)$$

where the interacting T -matrix is

$$T_{\mathbf{k}\mathbf{p}}(z) = V_{\mathbf{k}} \mathcal{G}(z) V_{\mathbf{p}}^*. \quad (3.17)$$

with $\mathcal{G}(z)$ the fully-interacting impurity Green's function. It is convenient, for what we are going to show in the following, to introduce the combination of conduction electrons that is actually coupled to the impurity, hence the only one which scatters off the impurity. This is simply

$$c_{0\sigma} = \frac{1}{V} \sum_{\mathbf{k}} V_{\mathbf{k}}^* c_{\mathbf{k}\sigma}, \quad (3.18)$$

where

$$V^2 = \sum_{\mathbf{k}} |V_{\mathbf{k}}|^2,$$

so that the hybridization becomes

$$V \sum_{\sigma} \left(c_{0\sigma}^{\dagger} d_{\sigma} + H.c. \right) \quad (3.19)$$

The Green's function of $c_{0\sigma}$ in the absence of the impurity is given by

$$G_0^{(0)}(z) = \frac{1}{V^2} \sum_{\mathbf{k}} \frac{|V_{\mathbf{k}}|^2}{z - \epsilon_{\mathbf{k}}} = \frac{1}{V^2} \Delta(z), \quad (3.20)$$

and implies a DOS,

$$\rho_0(\epsilon) = \frac{1}{\pi V^2} \Gamma(\epsilon) \rightarrow \frac{1}{\pi V^2} \Gamma. \quad (3.21)$$

the last equality being valid within the approximation leading to (3.13). On the contrary, in the presence of the impurity, the above Green's function transforms, through Eqs. (3.17) and (3.16), into

$$\begin{aligned} G_0(z) &= \frac{1}{V^2} \sum_{\mathbf{k}\mathbf{p}} V_{\mathbf{k}}^* V_{\mathbf{p}} G_{\mathbf{k}\mathbf{p}}(z) \\ &= G_0^{(0)}(z) + G_0^{(0)}(z) T(z) G_0^{(0)}(z), \end{aligned} \quad (3.22)$$

with a T -matrix

$$T(z) = V^2 \mathcal{G}(z). \quad (3.23)$$

It then follows that the phase-shift in the c_0 -scattering-channel, see Appendix A, can be defined as

$$\delta(\epsilon) = \Im m \ln \mathcal{G}(z = \epsilon + i0^+). \quad (3.24)$$

Moreover, the S -matrix at the chemical potential is readily found to be

$$S(0) = 1 - 2 \frac{\rho_d(0)}{\rho_d^{(0)}(0)}, \quad (3.25)$$

where $\rho_d^{(0)}(0)$ is the non-interacting impurity DOS at the chemical potential, see Eq. (3.14), and

$$\rho_d(\epsilon) = -\frac{1}{\pi} \Im m \mathcal{G}(z = \epsilon + i0^+),$$

the interacting DOS. Notice that, in the absence of interaction, $S(0) = -1$ which once more implies a $\pi/2$ -phase shift.

Since everything depends on the impurity Green's function, let us calculate up to second order the self-energy. The first and second order corrections are drawn in Fig. 3.2. One can easily show that the first order correction vanishes, namely the resonance stays pinned at the chemical potential. The calculation of the second order correction is more involved. One can

$\Sigma^{(1)} = \begin{array}{c} \text{---} \sigma \\ \text{---} \text{---} \text{---} \\ \sigma \end{array} - U/2 = 0$

 $\Sigma^{(2)} = \begin{array}{c} \text{---} \text{---} \text{---} \\ \text{---} \text{---} \text{---} \\ \text{---} \text{---} \text{---} \end{array}$

Figure 3.2: First and second order self-energy corrections.

show that, for real frequencies $z \rightarrow \epsilon + i0^+$, $\Re e \Sigma^{(2)}(\epsilon) \sim -\epsilon \left(U \rho_d^{(0)}(0) \right)^2$, namely it vanishes at $\epsilon = 0$. This result remains true at any order in perturbation theory, and it is a consequence of the particle-hole symmetry that we have implicitly assumed using (3.13) and fixing $\epsilon_d = 0$. The

imaginary part

$$\Im m \Sigma^{(2)}(\epsilon) \sim -U^2 \left(\rho_d^{(0)}(0) \right)^3 \epsilon^2.$$

This result is equivalent to the well known behavior of the quasiparticle decay rate and derives from simple phase-space arguments. Indeed one can easily show that, at any order in perturbation theory, the imaginary part of the self-energy decays at least as ϵ^2 . As a result, provided perturbation theory remains valid for any value of U , it should follow that

$$\rho_d(0) = -\frac{1}{\pi} \lim_{\epsilon \rightarrow 0} \Im m \frac{1}{\epsilon + i\Gamma - \Sigma(\epsilon)} = \frac{1}{\pi\Gamma} = \rho_d^{(0)}. \quad (3.26)$$

Were this result true, it would imply that $S(0) = -1$, namely that the phase shift remains $\pi/2$ even in the presence of the Hubbard repulsion. In other words, the resonance that exists right at the chemical potential at $U = 0$, should survive for any U . This perturbative argument is compatible with the low-temperature behavior of diluted magnetic impurities if one assumes that the role of U is to shrink the resonance to a small value of order T_K . Indeed, if we assume that, at small ϵ , the $\Im m \Sigma$ is negligible and

$$\Re e \Sigma(\epsilon) \simeq -\epsilon \left(1 - \frac{1}{Z} \right), \quad (3.27)$$

with $Z < 1$ [$1 - Z \simeq \left(U \rho_d^{(0)}(0) \right)^2$ at second order in U], then

$$\mathcal{G}(\epsilon + i0^+) \simeq \frac{Z}{\epsilon + i Z \Gamma}, \quad (3.28)$$

which implies that the effective resonance-width is $Z\Gamma$, which can become very small if $Z \ll 1$.

In addition, this simple argument can also justify why the resonance remains pinned close to the chemical potential. Indeed, if we introduce back a small ϵ_d , the $\Re e \Sigma(\epsilon = 0)$ becomes finite. If we define a corrected resonance energy as

$$\epsilon_d^* = \epsilon_d + \Re e \Sigma(\epsilon = 0), \quad (3.29)$$

then

$$\mathcal{G}(\epsilon + i0^+) \simeq \frac{Z}{\epsilon - Z \epsilon_d^* + i Z \Gamma}.$$

In other words, the resonance is shifted only by $Z \epsilon_d^*$, which, provided ϵ_d^* is of the same order as ϵ_d , does imply a resonance pinned near the chemical potential.

These perturbative arguments are very suggestive, yet they rely on the assumption that perturbation theory does not break at some critical value of U .

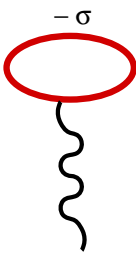
3.1.2 Mean-field analysis of the interaction

In order to understand whether the small U regime is adiabatically connected to the large U one, it is convenient to adopt a different approach more appropriate for strong coupling.

The first question which we address is how strong U should be to move appreciably the model away from the $U = 0$ resonant-level behavior. Let us consider again the case $\epsilon_d = 0$ and switch on the interaction

$$\frac{U}{2} (\hat{n}_d - 1)^2 = U \hat{n}_{d\uparrow} \hat{n}_{d\downarrow} - \frac{U}{2} \hat{n}_d.$$

The second term gives an $\epsilon_d = -U/2$. Let us treat the first term within Hartree-Fock approximation, searching for a magnetic solution. The self-energy for the spin σ impurity electrons is



$$\Sigma_{\sigma}[G] = \text{diagram} = U N_{d-\sigma}$$

Figure 3.3: Self-energy within the Hartree-Fock approximation.

given by, see Fig. 3.3,

$$\Sigma_{\sigma} = U N_{d-\sigma}, \quad (3.30)$$

where

$$N_{d-\sigma} = \langle \hat{n}_{d-\sigma} \rangle,$$

is the average value, which has to be evaluated self-consistently. Therefore the impurity Green's function is

$$\mathcal{G}_{\sigma}(z) = \frac{1}{z - \epsilon_d - \Delta(z) - \Sigma_{\sigma}(z)} = \frac{1}{z + \frac{U}{2} - \Delta(z) - U N_{d-\sigma}}, \quad (3.31)$$

as if $\epsilon_{d\sigma} = -U/2 + U N_{d-\sigma}$. By writing $N_{d\sigma} = 1/2 + m\sigma$ we find through (B.4) the self-consistency condition

$$m = \frac{1}{\pi} \tan^{-1} \frac{U m}{\Gamma}. \quad (3.32)$$

There are two possibilities. If $U \leq \pi\Gamma$ the only solution is $m = 0$. It describes a paramagnetic impurity and corresponds to the previous analysis at $U = 0$. If $U > \pi\Gamma$, there are two stable solutions at finite $m = \pm m_0$, which describe a partially polarized impurity. Since these two solutions are degenerate, the entropy $S = \ln 2$ just reflects the spin degrees of freedom. In other words, the magnetic state $m \neq 0$ describes indeed a local moment. If we assume a density matrix

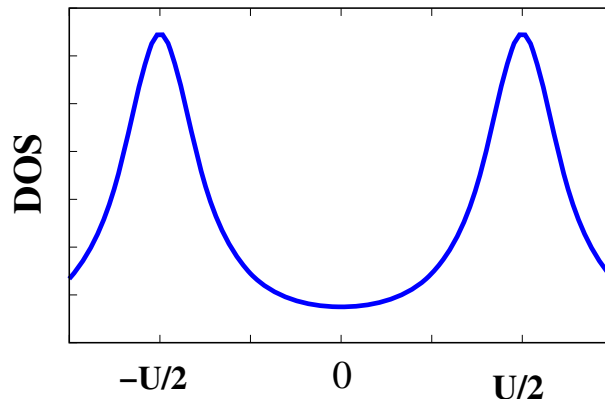


Figure 3.4: DOS of the AIM within the Hartree-Fock approximation.

which is the average of the two degenerate ground states, then the impurity Green's function reads:

$$\mathcal{G}(z) = \frac{1}{2} \left[\frac{1}{z + U m + i\Gamma \text{sign } \mathcal{I}m z} + \frac{1}{z - U m + i\Gamma \text{sign } \mathcal{I}m z} \right], \quad (3.33)$$

and the DOS is composed by two lorentians, one below and one above the chemical potential, which are called the Mott-Hubbard bands. In particular, if $U \gg \Gamma$, $m \rightarrow 1/2$ and the two lorentians are separated by an energy roughly of order U , see Fig. 3.4.

The mean-field solution for large U of the Anderson impurity model shows that, above some value of the repulsion U , the mean-field solution looks indeed very different from the small- U resonant-level behavior. Does this imply an actual breakdown of perturbation theory?

3.2 From the Anderson to the Kondo model

The Hartree-Fock solution of the Anderson impurity model does explain in the large U/Γ -limit the existence of local free moments in a metal well below its Fermi temperature. Nevertheless the degeneracy of the mean-field solution is an artifact of mean-field theory, since the two solutions, in the above example, are not orthogonal and can be coupled through the conduction electrons.

Let us use the fermionic field (3.18) so that the impurity Hamiltonian plus the hybridization become

$$V \sum_{\sigma} \left(c_{0\sigma}^{\dagger} d_{\sigma} + H.c. \right) + \frac{U}{2} (\hat{n}_d - 1)^2. \quad (3.34)$$

In the large U limit the impurity traps a single electron, either with spin up or down, and we can treat the hybridization as a small perturbation lifting the degeneracy between the two spin directions. By second order perturbation theory through intermediate states in which the impurity is empty or doubly occupied, with energy difference equal to $U/2$ for large U , one gets an effective operator lifting the impurity degeneracy given by, apart from constant terms,

$$\begin{aligned} & -\frac{2V^2}{U} \sum_{\sigma\sigma'} c_{0\sigma}^{\dagger} d_{\sigma} d_{\sigma'}^{\dagger} c_{0\sigma'} + d_{\sigma'}^{\dagger} c_{0\sigma'} c_{0\sigma}^{\dagger} d_{\sigma} \\ & = J_K \mathbf{S}_0 \cdot \mathbf{S}_d \end{aligned}$$

where

$$J_K = \frac{8V^2}{U},$$

and

$$\begin{aligned} \mathbf{S}_0 &= \frac{1}{2} \sum_{\alpha\beta} c_{0\alpha}^{\dagger} \boldsymbol{\sigma}_{\alpha\beta} c_{0\beta} \\ &= \frac{1}{2V^2} \sum_{\mathbf{k}\mathbf{p}\alpha\beta} V_{\mathbf{k}} V_{\mathbf{p}}^* c_{\mathbf{k}\alpha}^{\dagger} \boldsymbol{\sigma}_{\alpha\beta} c_{\mathbf{p}\beta}, \end{aligned} \quad (3.35)$$

$$\mathbf{S}_d = \frac{1}{2} \sum_{\alpha\beta} d_{\alpha}^{\dagger} \boldsymbol{\sigma}_{\alpha\beta} d_{\beta}. \quad (3.36)$$

In other words, in the large U limit, the AIM reduces to the so-called Kondo model describing conduction electrons antiferromagnetically coupled to a local moment, a spin-1/2 in our single-orbital AIM example. The Kondo Hamiltonian is therefore

$$\mathcal{H}_K = \sum_{\mathbf{k}\sigma} \epsilon_{\mathbf{k}} c_{\mathbf{k}\sigma}^{\dagger} c_{\mathbf{k}\sigma} + J_K \mathbf{S}_0 \cdot \mathbf{S}_d. \quad (3.37)$$

We notice that this model has built-in a local moment, hence by construction correctly describes the local moment regime for $T_K \ll T \ll T_F$. This local moment provides a scattering potential

for the conduction electrons, with the major difference with respect to a conventional scalar potential that the impurity has internal degrees of freedom. We will show now the consequences of this difference.

3.2.1 The emergence of logarithmic singularities and the Kondo temperature

Let us analyse the role of the Kondo exchange

$$J_K \mathbf{S}_0 \cdot \mathbf{S}_d, \quad (3.38)$$

in perturbation theory. Since (3.38) conserves independently the number of conduction and d -electrons, we use a trick due to Abrikosov and treat the impurity spin in terms of d -electrons with an unperturbed Green's function

$$\mathcal{G}^{(0)}(z) = \frac{1}{z},$$

namely as a resonant state right at the chemical potential with a vanishing broadening, which does contain in the “unperturbed state” just one electron, number which is not going to be changed by (3.38). Since a single electron has a well defined spin, it acts indeed like a local spin-1/2 moment. The Green's function for the conduction electron c_0 is given in (3.20). For convenience let us rewrite (3.38) in a spin-asymmetric form as

$$\sum_{i=x,y,z} J_i S_0^i S_d^i, \quad (3.39)$$

and calculate the first order corrections to the exchange as given by the diagrams in Fig. 3.5. For simplicity we assume that all external lines are at zero frequencies. Each diagram is multiplied by (-1) because of first order perturbation theory. The explicit expression of the diagram (a) is

$$\begin{aligned} \text{(a)} &= - \sum_{i,j=x,y,z} J_i J_j \sum_{\gamma c} S_{\alpha\gamma}^i S_{ac}^i S_{\gamma\beta}^j S_{cb}^j T \sum_n G_0^{(0)}(i\epsilon_n) \mathcal{G}^{(0)}(-i\epsilon_n) \\ &= - \sum_{i,j=x,y,z} \frac{J_i J_j}{V^2} \sum_{\gamma c} S_{\alpha\gamma}^i S_{ac}^i S_{\gamma\beta}^j S_{cb}^j T \sum_n \frac{\Delta(i\epsilon_n)}{-i\epsilon_n} \\ &= -I(T) \sum_{i,j=x,y,z} \frac{J_i J_j}{V^2} \sum_{\gamma c} S_{\alpha\gamma}^i S_{\gamma\beta}^j S_{ac}^i S_{cb}^j, \end{aligned}$$

where the function of temperature $I(T)$ is defined through

$$I(T) = -T \sum_n \frac{\Delta(i\epsilon_n)}{i\epsilon_n}.$$

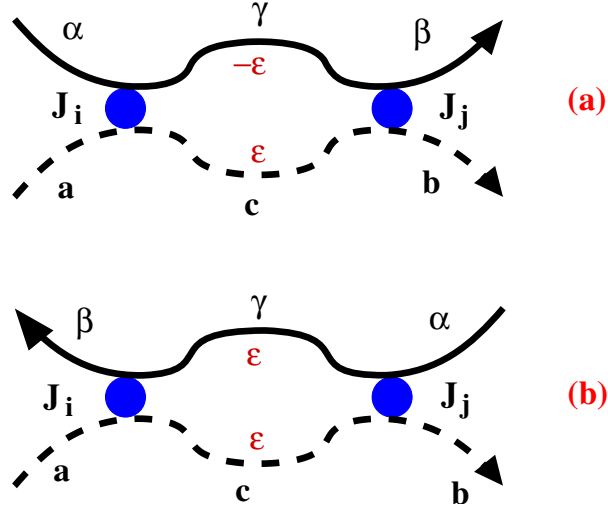


Figure 3.5: First order corrections to the Kondo exchange. Solid and dashed lines indicate impurity and conduction electron Green's functions. Also indicated are the spin labels. All external lines are assumed to be at zero frequency $\epsilon = 0$. The internal frequency, which is going to be summed over, is also indicated.

The diagram (b) is analogously

$$\begin{aligned}
\text{(b)} &= - \sum_{i,j=x,y,z} J_i J_j \sum_{\gamma c} S_{\alpha\gamma}^i S_{cb}^i S_{\gamma\beta}^j S_{ac}^j T \sum_n G_0^{(0)}(i\epsilon_n) \mathcal{G}^{(0)}(i\epsilon_n) \\
&= I(T) \sum_{i,j=x,y,z} \frac{J_i J_j}{V^2} \sum_{\gamma c} S_{\alpha\gamma}^i S_{\gamma\beta}^j S_{ac}^j S_{cb}^i,
\end{aligned}$$

hence the sum is

$$\begin{aligned}
\text{(a)} + \text{(b)} &= I(T) \sum_{i,j=x,y,z} \frac{J_i J_j}{V^2} \sum_{\gamma} S_{\alpha\gamma}^i S_{\gamma\beta}^j \sum_c \left(S_{ac}^j S_{cb}^i - S_{ac}^i S_{cb}^j \right) \\
&= I(T) \sum_{i,j,k=x,y,z} \frac{J_i J_j}{V^2} \sum_{\gamma} S_{\alpha\gamma}^i S_{\gamma\beta}^j i \epsilon_{jik} S_{ab}^k,
\end{aligned}$$

where we used the commutation relations between the spin operators

$$[S^i, S^j] = i \epsilon_{ijk} S^k,$$

where ϵ_{ijk} is the Levi-Civita antisymmetric tensor. Since we sum over i and j , we can also write

$$\begin{aligned}
\text{(a)} + \text{(b)} &= \frac{1}{2} I(T) \sum_{i,j,k=x,y,z} \frac{J_i J_j}{V^2} \sum_{\gamma} S_{\alpha\gamma}^i S_{\gamma\beta}^j i \epsilon_{jik} S_{ab}^k + (i \leftrightarrow j) \\
&= \frac{1}{2} I(T) \sum_{i,j,k=x,y,z} \frac{J_i J_j}{V^2} i \epsilon_{jik} S_{ab}^k \sum_{\gamma} \left(S_{\alpha\gamma}^i S_{\gamma\beta}^j - S_{\alpha\gamma}^j S_{\gamma\beta}^i \right)
\end{aligned}$$

$$= \sum_{k=x,y,z} S_{ab}^k S_{\alpha\beta}^k \left[\frac{1}{2} I(T) \sum_{i,j} \frac{J_i J_j}{V^2} |\epsilon_{ijk}|^2 \right],$$

which provides the first order correction to the exchange constants according to

$$J_k + \delta J_k = J_k + \frac{1}{2} I(T) \sum_{i,j} \frac{J_i J_j}{V^2} |\epsilon_{ijk}|^2. \quad (3.40)$$

In order to evaluate $I(T)$ we use the same integration contour as in Fig. B.1. We recall that the hybridization function has a branch cut approximately given by

$$\Delta(\epsilon + i0^+) - \Delta(\epsilon - i0^+) = -2i\Gamma\theta(W - |\epsilon|),$$

where $\theta(W - |\epsilon|)$ is the Heavyside function and W a cut-off of the order of the conduction bandwidth. We then find that

$$I(T) = - \int_{-W}^W \frac{d\epsilon}{\pi} f(\epsilon) \frac{\Gamma}{\epsilon} \simeq \frac{\Gamma}{\pi} \ln \frac{W}{T},$$

so that e.g. in the isotropic case $J_x = J_y = J_z = J$ we finally get

$$J + \delta J = J + \frac{\Gamma}{\pi V^2} J^2 \ln \frac{W}{T}.$$

In other words the perturbation theory in J generates logarithmic singularities which become visible roughly around a temperature, that has to be identified with the Kondo temperature, when the correction becomes of the same order as J , namely

$$J = \frac{\Gamma}{\pi V^2} J^2 \ln \frac{W}{T_K},$$

leading to

$$T_K = W \exp\left(-\frac{\pi V^2}{\Gamma J}\right) = W \exp\left(-\frac{\pi U}{8\Gamma}\right) \ll W \sim T_F, \quad (3.41)$$

since $U \gg \Gamma$. In agreement with experiments, we do find that the Kondo temperature is much smaller than the host-metal Fermi temperature. Since perturbation theory becomes meaningless below T_K , the next obvious question is how to proceed further.

3.2.2 Anderson's scaling theory

What we have calculated so far is the first order correction to the Kondo exchange for conduction and impurity electrons at zero frequency, which we found to be

$$J_z[W] + \delta J_z[W] = J_z[W] + \frac{\Gamma}{\pi V^2} J_{\perp}[W]^2 \ln \frac{W}{T}, \quad (3.42)$$

$$J_{\perp}[W] + \delta J_{\perp}[W] = J_{\perp}[W] + \frac{\Gamma}{\pi V^2} J_{\perp}[W] J_z[W] \ln \frac{W}{T}. \quad (3.43)$$

In (3.42) and (3.43) we have assumed an easy-axis asymmetry $J_z \neq J_x = J_y \equiv J_{\perp}$, and we have explicitly indicated the dependence upon the bandwidth cut-off W . Clearly the result does not change for finite external frequencies provided they are much smaller than the temperature, otherwise they would cut-off the log-singularity instead of T . Now suppose we have another model with a smaller conduction electron bandwidth cut-off $W(s) = W/s$ with $s > 1$, different J 's but equal Γ/V^2 . In this case, for electrons close to the chemical potential, specifically much closer than the temperature, we would get the first order correction

$$\begin{aligned} J_z[W(s)] + \delta J_z[W(s)] &= J_z[W(s)] + \frac{\Gamma}{\pi V^2} J_{\perp}[W(s)]^2 \ln \frac{W}{sT}, \\ J_{\perp}[W(s)] + \delta J_{\perp}[W(s)] &= J_{\perp}[W(s)] + \frac{\Gamma}{\pi V^2} J_{\perp}[W(s)] J_z[W(s)] \ln \frac{W}{sT}. \end{aligned}$$

On the other hand, it makes not really a big difference for the low energy behavior whether these electrons which lie so close to the chemical potential derive from a band with width W or $W(s)$ provided they suffer the same scattering off the impurity. Therefore we can ask the following question:

what should $J[W(s)]$ be in order for the effective exchange up to first order to be the same as that one with bandwidth W ?

The answer is quite simple, since we can re-write e.g. (3.42) as

$$\begin{aligned} J_z[W] + \delta J_z[W] &= J_z[W] + \frac{\Gamma}{\pi V^2} J_{\perp}[W]^2 \ln(s) + \frac{\Gamma}{\pi V^2} J_{\perp}[W]^2 \ln \frac{W}{sT} \\ &\simeq \left(J_z[W] + \frac{\Gamma}{\pi V^2} J_{\perp}[W]^2 \ln(s) \right) \\ &\quad + \frac{\Gamma}{\pi V^2} \left(J_z[W] + \frac{\Gamma}{\pi V^2} J_{\perp}[W]^2 \ln(s) \right)^2 \ln \frac{W}{sT} + O(J^3), \end{aligned}$$

the equality being valid up to the order at which we have stopped the expansion. Therefore the two models with W and W/s have the same spin exchange up to first order in perturbation theory provided the bare exchange constants satisfy

$$\begin{aligned} J_z[W(s)] &= J_z[W] + \frac{\Gamma}{\pi V^2} J_{\perp}[W]^2 \ln(s), \\ J_{\perp}[W(s)] &= J_{\perp}[W] + \frac{\Gamma}{\pi V^2} J_{\perp}[W] J_z[W] \ln(s), \end{aligned}$$

which can be cast in a differential form

$$\frac{dj_z(s)}{d \ln s} = j_{\perp}(s)^2, \quad (3.44)$$

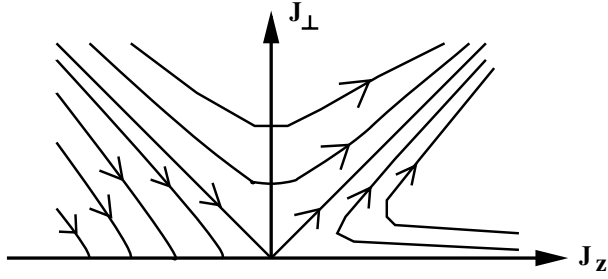


Figure 3.6: Scaling flow of the Kondo exchange constants as the cut-off is sent to zero.

$$\frac{dj_{\perp}(s)}{d \ln s} = j_{\perp}(s) j_z(s), \quad (3.45)$$

having defined

$$J_i [W(s)] \frac{\Gamma}{\pi V^2} \equiv j_i(s).$$

These equations describe how the bare exchange constants have to be modified in order for the model with a reduced bandwidth W/s to have the low-energy scattering amplitudes equal to those of the original model. The idea behind is that, if we are able to follow the evolution of $j_i(s)$ until $W/s \sim T$, at this point we could rely on perturbation theory since $\ln(W/sT) \simeq 0$. This is more or less how Anderson formulated his *poor man's scaling theory* for the Kondo problem in 1970 which is in essence the first implementation of a Renormalization Group transformation.

Let us study the scaling equations. We readily find that, $\ln s = x$,

$$\frac{d^2 j_z}{dx^2} = 2j_{\perp} \frac{dj_{\perp}}{dx} = 2j_z \frac{dj_z}{dx} = \frac{dj_z^2}{dx}.$$

By integrating from $x = \ln s = \ln 1 = 0$, the initial condition $W(s) = W$, to same $x > 0$ we get

$$\frac{dj_z(x)}{dx} - \frac{dj_z(0)}{dx} = \frac{dj_z(x)}{dx} - j_{\perp}(0)^2 = j_z(x)^2 - j_z(0)^2,$$

namely

$$\begin{aligned} \frac{dj_z(x)}{dx} &= j_z(x)^2 - j_z(0)^2 + j_{\perp}(0)^2, \\ \frac{d \ln j_{\perp}(x)}{dx} &= j_z(x). \end{aligned}$$

In Fig. 3.6 it is shown the scaling flow of the exchange constants $j_z(x)$ and $j_{\perp}(x)$ as $x \rightarrow \infty$. Since the sign of J_{\perp} can be always changed by rotating of an angle π the impurity spin around the z -axis, we have just drawn the flow with $J_{\perp} > 0$, $J_z > 0$ and $J_z < 0$ implying antiferro- and ferro-magnetic Kondo exchange, respectively. We notice that for ferromagnetic exchange $J_z < 0$ with $|J_z| \geq J_{\perp}$, the couplings flow to a line of fixed points, where perturbation theory become valid. In particular for isotropic couplings $J_z = J_{\perp} = J < 0$, the value at $x = \ln W/T \gg 1$ is

$$j(T) = \frac{j}{1 - j \ln W/T} \simeq -\frac{1}{\ln W/T} \rightarrow 0. \quad (3.46)$$

This suggests that the impurity asymptotically decouples from the conduction electrons. For instance the impurity magnetic susceptibility, which can be calculated perturbatively in this case, behaves at low temperatures as

$$\chi(T) \sim \frac{1}{T \ln W/T},$$

almost the Curie-like behavior of a free spin.

For antiferromagnetic $J_z > 0$, as well as for $J_z < 0$ but $|J_z| < J_\perp$, the exchange constants flow to strong-coupling $j_z \simeq j_\perp \rightarrow +\infty$. This implies that the electrons very close to the chemical potential feel a very strong antiferromagnetic exchange with the impurity spin. It is therefore reasonable to assume that one has to diagonalize the Kondo spin-exchange first, Eq. (3.38), and only then treats what is left within perturbation theory. Taking this point of view, the first step leads to assume that the electronic state c_0 , see (3.18), get strongly bound into a spin-singlet with the impurity spin. This singlet state has no internal degrees of freedom, hence it can act only as a scalar potential for the left-over electronic states orthogonal to c_0 . The question is what should be the scattering phase shift induced by this spin-singlet object. Since the impurity traps just one electron, from the Friedel sum rule we expect

$$\delta_\uparrow + \delta_\downarrow = \pi.$$

Since the trapping occurs into a singlet state, which is spin-isotropic, $\delta_\uparrow = \delta_\downarrow$, hence

$$\delta_\uparrow = \delta_\downarrow = \frac{\pi}{2}.$$

In other words, the phase shift is indeed the same as we found at very small U , which supports the hypothesis that perturbation theory does not break down. In reality we do know that this is actually the case thanks to exact solutions obtained either by the Wilson numerical renormalization group or by Bethe Ansatz.

3.3 The impurity model from weak to strong repulsion and the DMFT results

Since the weak coupling regime $U \ll \Gamma$ is adiabatically connected to the strong coupling one, $U \gg \Gamma$, let us discuss more in detail the perturbative expression of the impurity Green's function Eq. (3.28) for very small ϵ , i.e.

$$\mathcal{G}(\epsilon + i0^+) \simeq \frac{Z}{\epsilon + i Z \Gamma}. \quad (3.47)$$

The low energy DOS is still a lorentian with a narrower width $T_K = Z \Gamma$ and total spectral weight Z . The rest $1 - Z$ of the spectral weight should be concentrated into some higher-energy

part. The low-energy peak, commonly called Abrikosov-Suhl or Kondo resonance, has to survive even for very large U , although its spectral weight would become very small, $Z \ll 1$.

On the other hand we have seen that, for very large U , when the mapping onto the Kondo model is valid, most of the spectral weight should be concentrated into two features at energies $\pm U/2$, the so-called Hubbard side-bands, see Fig. 3.4. Therefore the obvious conclusion, supported by numerical results, is that, for $U \gg \Gamma$, the impurity spectral function has three distinct features: two Hubbard side-bands centered at $\pm U/2$ and a very narrow Kondo resonance close to the chemical potential, see Fig. 3.7. This narrow resonance shrinks as U increases and disappears only if $U \rightarrow \infty$.

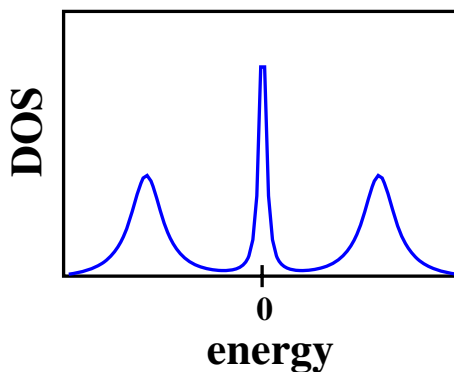


Figure 3.7: The impurity DOS for large U . The central peak is the Kondo resonance, while the other two are the Hubbard bands.

3.3.1 DMFT scenario for the Mott transition

Within DMFT, a single-band Hubbard model in the Bethe lattice can be mapped onto the single-orbital Anderson impurity model (3.3) provided that the hybridization function and the impurity Green's function satisfy the self-consistency relation

$$\Delta(z) = t^2 \mathcal{G}(z). \quad (3.48)$$

The role of self-consistency is crucial. Indeed, as U increases we know that impurity spectral weight is transferred from the central resonance into the Hubbard side-bands and, at the meantime, the central peak shrinks. As a result of self-consistency, the low-frequency component of the hybridization width decreases like the spectral weight of the Kondo resonance. This cooperative effect leads to a vanishing low-frequency hybridization, which implies a vanishing T_K for the impurity model, at a finite value of $U = U_c$, while in the impurity model without self-consistency $T_K \rightarrow 0$ only if $U \rightarrow \infty$. Once $T_k = 0$, only the Hubbard side-bands remain, separated by an energy gap of order U . Since the impurity spectral function corresponds, within

the DMFT mapping, to the local spectral function of the lattice model, the vanishing of T_K corresponds to the opening of a gap in the single-particle spectral function of the lattice model, namely to the Mott transition.

Notice that, since the impurity self-energy $\Sigma(i\epsilon_n)$ is also the lattice self-energy then, in the metallic phase prior to the Mott transition, the low-energy lattice Green's function is, through (3.27),

$$G(\mathbf{k}, i\epsilon_n) = \frac{1}{i\epsilon_n - \epsilon_{\mathbf{k}} - \Sigma(i\epsilon_n)} \simeq \frac{Z}{i\epsilon_n - Z \epsilon_{\mathbf{k}}}, \quad (3.49)$$

and describes low-energy coherent quasiparticles with residue Z , namely effective Fermi temperature Z times smaller than the non-interacting one, $T_F^* = Z T_F$, and renormalized bandwidth ZW , i.e. renormalized mass $m_* = m/Z$. In other words, until the effective impurity model possesses the Kondo resonance, the lattice model describes a metal with coherent quasiparticles. The Mott transition, being signaled by $Z \rightarrow 0$, corresponds to $T_F^* \rightarrow 0$ and, at the same time, $m_* \rightarrow \infty$. This behavior is what is commonly denoted as Brinkmann-Rice scenario for the Mott transition.

The last very important thing to point out is that the Mott transition corresponds to an impurity model with very small $T_K \rightarrow 0$, namely well inside the regime in which the mapping onto a Kondo model is valid.

Appendix A

Brief introduction to scattering theory

We start by showing why the existence of local moments in a metal for $T \ll T_F$ is so puzzling.

Let us consider an impurity imbedded in a normal metal. We only take into account the valence band, described by the Hamiltonian

$$\mathcal{H}_0 = \sum_{\mathbf{k}, \sigma} \epsilon_{\mathbf{k}} c_{\mathbf{k}\sigma}^\dagger c_{\mathbf{k}\sigma}. \quad (\text{A.1})$$

The scattering potential provided by the impurity has the general form

$$\mathcal{V} = \sum_{\sigma} \sum_{\mathbf{k}, \mathbf{p}} V_{\mathbf{k}\mathbf{p}} c_{\mathbf{k}\sigma}^\dagger c_{\mathbf{p}\sigma}, \quad (\text{A.2})$$

where $V_{\mathbf{k}\mathbf{p}}$ are the matrix elements of the impurity potential onto the valence band Bloch waves.

The single-particle Green's function in complex frequency for the full Hamiltonian $\mathcal{H} = \mathcal{H}_0 + \mathcal{V}$ can be formally written as the matrix

$$\hat{G}(z) = \frac{1}{z - \hat{H}}. \quad (\text{A.3})$$

Analogously the unperturbed one is

$$\hat{G}_0(z) = \frac{1}{z - \hat{H}_0}. \quad (\text{A.4})$$

The above operators have the following interpretation. If we consider for instance the inverse of the Green's function \hat{G} , namely

$$\hat{G}(z)^{-1} = z - \hat{H},$$

in the basis set of the valence band Block waves, this is the matrix

$$\left(\hat{G}(z)^{-1}\right)_{\mathbf{k}\sigma,\mathbf{p}\sigma'} = \delta_{\sigma\sigma'} [\delta_{\mathbf{k}\mathbf{p}} z - \delta_{\mathbf{k}\mathbf{p}} \epsilon_{\mathbf{k}} - V_{\mathbf{k}\mathbf{p}}], \quad (\text{A.5})$$

hence the Green's function is the inverse of the above matrix. Suppose that we have diagonalized the full Hamiltonian and got the eigenvalues ϵ_a 's. In the diagonal basis also the Green's function is diagonal with matrix elements

$$G(z)_{ab} = \delta_{ab} \frac{1}{z - \epsilon_a}.$$

Therefore we readily find that

$$\begin{aligned} -\frac{1}{\pi} \lim_{\delta \rightarrow +0} \Im m \operatorname{Tr} \left(\hat{G}(z = \omega + i\delta) \right) &= -\frac{1}{\pi} \lim_{\delta \rightarrow +0} \Im m \sum_{a\sigma} \frac{1}{\omega - \epsilon_a + i\delta} \\ &= \sum_{a\sigma} \delta(\omega - \epsilon_a) \equiv \rho(\omega), \end{aligned}$$

where ω is a real frequency and $\rho(\omega)$ is the density of states (DOS). Since the trace is invariant under unitary transformations, hence also under the transformation which diagonalizes the Hamiltonian, it is generally true that

$$-\frac{1}{\pi} \lim_{\delta \rightarrow +0} \Im m \operatorname{Tr} \left[\hat{G}(z = \omega + i\delta) \right] = \rho(\omega). \quad (\text{A.6})$$

Analogously

$$-\frac{1}{\pi} \lim_{\delta \rightarrow +0} \Im m \operatorname{Tr} \left[\hat{G}_0(z = \omega + i\delta) \right] = \rho_0(\omega) = \sum_{\mathbf{k}\sigma} \delta(\epsilon_{\mathbf{k}} - \omega), \quad (\text{A.7})$$

gives the DOS of the host metal.

Let us formally write the full Green's function as

$$\begin{aligned} \hat{G} &= \frac{1}{z - \hat{H}_0 - \hat{V}} = \frac{1}{\hat{G}_0^{-1} - \hat{V}} \\ &= \frac{1}{\hat{1} - \hat{G}_0 \hat{V}} \hat{G}_0 = \hat{G}_0 + \hat{G}_0 \hat{V} \left[\hat{1} - \hat{G}_0 \hat{V} \right]^{-1} \hat{G}_0 \\ &\equiv \hat{G}_0 + \hat{G}_0 \hat{T} \hat{G}_0, \end{aligned} \quad (\text{A.8})$$

which provides the definition of the so-called T -matrix, namely

$$\hat{T}(z) = \hat{V} \left[\hat{1} - \hat{G}_0 \hat{V} \right]^{-1}. \quad (\text{A.9})$$

From now on we will assume $z = \omega + i\delta$ with δ a positive infinitesimal number, so we will not explicitly indicate the $\lim_{\delta \rightarrow +0}$. We notice that

$$\frac{\partial}{\partial z} \ln \hat{G}(z) = -\hat{G}(z),$$

so that

$$\rho(\omega) = \frac{1}{\pi} \frac{\partial}{\partial z} \left\{ \Im m \operatorname{Tr} \ln \hat{G}(z) \right\}. \quad (\text{A.10})$$

We are interested in the variation of the DOS induced by the impurity, which, by making use of (A.8) and (A.9), is given by

$$\begin{aligned} \Delta\rho(\omega) &= \rho(\omega) - \rho_0(\omega) \\ &= \frac{1}{\pi} \frac{\partial}{\partial z} \left\{ \Im m \operatorname{Tr} \ln \left[\hat{G}(z) \hat{G}_0(z)^{-1} \right] \right\} \\ &= \frac{1}{\pi} \frac{\partial}{\partial z} \left\{ \Im m \operatorname{Tr} \ln \left[\frac{1}{\hat{1} - \hat{G}_0(z) \hat{V}} \right] \right\} \\ &= \frac{1}{\pi} \frac{\partial}{\partial z} \left\{ \Im m \operatorname{Tr} \ln \hat{V}^{-1} \hat{T}(z) \right\}. \end{aligned} \quad (\text{A.11})$$

We define the matrix of the scattering phase shifts

$$\hat{\delta}(z) = \Im m \ln \hat{V}^{-1} \hat{T}(z) = \operatorname{Arg} \left(\hat{V}^{-1} \hat{T}(z) \right), \quad (\text{A.12})$$

through which

$$\Delta\rho(\omega) = \frac{1}{\pi} \frac{\partial}{\partial \omega} \operatorname{Tr} \hat{\delta}(\omega). \quad (\text{A.13})$$

We notice that for $|z| \rightarrow \infty$, $\hat{G}_0(z) \rightarrow 1/z \rightarrow 0$, hence $\hat{T}(z) \rightarrow \hat{V}$ and $\hat{\delta}(z) \rightarrow 0$.

The variation of the total number of electrons, ΔN_{els} , induced by the impurity at fixed chemical potential μ is therefore

$$\Delta N_{els} = \int_{-\infty}^{\mu} d\omega \Delta\rho(\omega) = \frac{1}{\pi} \operatorname{Tr} \hat{\delta}(\mu), \quad (\text{A.14})$$

which is the so-called Friedel sum rule.

Let us go back to the definition of the T -matrix (A.9). One readily finds that its inverse is given by

$$\hat{T}(z)^{-1} = \left[\hat{V}^{-1} - \hat{G}_0(z) \right].$$

Since the Hamiltonian is hermitean, then

$$\left[\hat{T}(z)^{-1} \right]^\dagger = \left[\hat{V}^{-1} - \hat{G}_0(z^*) \right],$$

so that

$$\left[\hat{T}(z)^{-1} \right]^\dagger - \hat{T}(z)^{-1} = \left[\hat{G}_0(z) - \hat{G}_0(z^*) \right].$$

Therefore

$$\begin{aligned} \hat{T}(z)^\dagger \left\{ \left[\hat{T}(z)^{-1} \right]^\dagger - \hat{T}(z)^{-1} \right\} \hat{T}(z) &= \hat{T}(z) - \hat{T}(z)^\dagger \\ &= \hat{T}(z)^\dagger \left[\hat{G}_0(z) - \hat{G}_0(z^*) \right] \hat{T}(z). \end{aligned} \quad (\text{A.15})$$

Since

$$\hat{G}_0(z) - \hat{G}_0(z^*) = -2\pi i \delta(\omega - \hat{H}_0),$$

the Eq. (A.15) implies the following identity

$$T_{\mathbf{k}\mathbf{p}}(\omega) - T_{\mathbf{k}\mathbf{p}}^\dagger(\omega) = -2\pi i \sum_{\mathbf{q}} T_{\mathbf{k}\mathbf{q}}^\dagger(\omega) \delta(\omega - \epsilon_{\mathbf{q}}) T_{\mathbf{q}\mathbf{p}}(\omega), \quad (\text{A.16})$$

which is the so-called *optical theorem*. It also shows that the imaginary part of the T -matrix is finite only within the conduction band.

Let us now analyse the on-shell T -matrix

$$T_{\mathbf{k}\mathbf{p}}(\epsilon),$$

where $\epsilon_{\mathbf{k}} = \epsilon_{\mathbf{p}} = \epsilon$. We can rewrite the on-shell optical theorem as follows

$$\begin{aligned} -2\pi i \delta(\epsilon_{\mathbf{k}} - \epsilon_{\mathbf{p}}) \left[T_{\mathbf{k}\mathbf{p}}(\epsilon) - T_{\mathbf{k}\mathbf{p}}^\dagger(\epsilon) \right] \\ = (-2\pi i)^2 \delta(\epsilon_{\mathbf{k}} - \epsilon_{\mathbf{p}}) \sum_{\mathbf{q}} T_{\mathbf{k}\mathbf{q}}^\dagger(\epsilon) \delta(\epsilon_{\mathbf{k}} - \epsilon_{\mathbf{q}}) T_{\mathbf{q}\mathbf{p}}(\epsilon). \end{aligned}$$

The above equation implies that, if we introduce the so-called on-shell S -matrix through

$$S_{\mathbf{k}\mathbf{p}}(\epsilon) = \delta_{\mathbf{k}\mathbf{p}} - 2\pi i \delta(\epsilon_{\mathbf{k}} - \epsilon_{\mathbf{p}}) T_{\mathbf{k}\mathbf{p}}(\epsilon), \quad (\text{A.17})$$

where, as before, $\epsilon_{\mathbf{k}} = \epsilon_{\mathbf{p}} = \epsilon$, then it follows that the S -matrix is unitary, *i.e.*

$$\hat{S} \hat{S}^\dagger = \hat{I}. \quad (\text{A.18})$$

$S_{\mathbf{k}\mathbf{p}}(\epsilon)$ is the transition probability that an electron in state \mathbf{k} scatters elastically into state \mathbf{p} . Since it is unitary, it follows that only elastic scattering survives.

A.0.2 Three dimensional example

Let us consider the simpler case of a spherical Fermi surface, *i.e.* $\epsilon_{\mathbf{k}} = \epsilon_k$ depending only on the modulus of the wavevector. In addition we assume that the matrix elements $V_{\mathbf{k}\mathbf{p}}$ only depend on the angle between the two wavevectors, $\theta_{\mathbf{k}\mathbf{p}}$, hence can be expanded in Lagrange polynomials

$$V_{\mathbf{k}\mathbf{p}} = \sum_l V_l (2l + 1) P_l(\cos \theta_{\mathbf{k}\mathbf{p}}). \quad (\text{A.19})$$

Then also the T -matrix has a similar expansion

$$T_{\mathbf{k}\mathbf{p}}(z) = \sum_l t_l(z) (2l+1) P_l(\cos \theta_{\mathbf{k}\mathbf{p}}). \quad (\text{A.20})$$

Since

$$\int \frac{d\Omega_{\mathbf{q}}}{4\pi} P_l(\cos \theta_{\mathbf{k}\mathbf{q}}) P_{l'}(\cos \theta_{\mathbf{q}\mathbf{p}}) = \frac{1}{2l+1} \delta_{ll'} P_l(\cos \theta_{\mathbf{k}\mathbf{p}}),$$

the optical theorem transforms into

$$t_l(\omega) - t_l^*(\omega) = 2i\text{Im} t_l(\omega) = -2\pi i \rho(\omega) |t_l(\omega)|^2, \quad (\text{A.21})$$

where $\rho(\omega)$ is the bare conduction electron density of states per spin. Since

$$t_l(\omega) = |t_l(\omega)| e^{i\delta_l(\omega)},$$

it follows that

$$t_l(\omega) = -\frac{1}{\pi\rho(\omega)} \sin \delta_l(\omega) e^{i\delta_l(\omega)}, \quad (\text{A.22})$$

and

$$S_l(\omega) = e^{2i\delta_l(\omega)}. \quad (\text{A.23})$$

If the concentration of impurity is very low, then the scattering rate suffered by the electrons is given by the Fermi-golden rule with the T -matrix, namely

$$\frac{1}{\tau_{\mathbf{k}}} = 2\pi n_i \sum_{\mathbf{q}} T_{\mathbf{k}\mathbf{q}}^\dagger(\omega) \delta(\omega - \epsilon_{\mathbf{q}}) T_{\mathbf{q}\mathbf{k}}(\omega) (1 - \cos \theta_{\mathbf{k}\mathbf{q}}),$$

where n_i is the impurity concentration and the last term is a geometric factor which guarantees that forward scattering, $\theta = 0$, does not contribute to the current dissipation. Since

$$(2l+1)z P_l(z) = (l+1)P_{l+1}(z) + lP_{l-1}(z),$$

we obtain

$$\begin{aligned} \frac{1}{n_i \tau_{\mathbf{k}}(\omega)} &= 2\pi \rho(\omega) \sum_{l'} t_l^*(\omega) t_{l'}(\omega) \int \frac{d\Omega_{\mathbf{q}}}{4\pi} (2l+1) P_l(\cos \theta_{\mathbf{k}\mathbf{q}}) \\ &\quad [(2l'+1) P_{l'}(\cos \theta_{\mathbf{k}\mathbf{q}}) + (l'+1) P_{l'+1}(\cos \theta_{\mathbf{k}\mathbf{q}}) + l' P_{l'-1}(\cos \theta_{\mathbf{k}\mathbf{q}})] \\ &= 2\pi \rho(\omega) \sum_l (2l+1) |t_l(\omega)|^2 + l t_l^*(\omega) t_{l-1}(\omega) + (l+1) t_l^*(\omega) t_{l+1}(\omega), \end{aligned} \quad (\text{A.24})$$

which, as expected, gives a scattering rate independent of momentum. If, as usual, only s -wave scattering occurs, then $t_l(\omega) = \delta_{l0} t(\omega)$ as well as $\delta_l(\omega) = \delta_{l0} \delta(\omega)$, hence

$$\frac{1}{\tau(\omega)} = 2\pi n_i \rho(\omega) |t(\omega)|^2 = \frac{2}{\pi\rho(\omega)} \sin^2 \delta(\omega), \quad (\text{A.25})$$

thus leading to a zero-temperature residual resistivity proportional to $n_i \sin^2 \delta(0)$.

A.1 General analysis of the phase-shifts

Let us keep assuming a spherically symmetric case and in addition only s -wave scattering. Then the phase shift is $\delta_l(\omega) = \delta_{l0} \delta(\omega)$ defined through the $l = 0$ component of the T -matrix

$$\delta(\omega) = \tan^{-1} \frac{\text{Im} t(\omega)}{\text{Re} t(\omega)}.$$

An important role is played by the frequencies at which the real part vanishes.

The first possibility is that this occurs outside the conduction band, either below or above. In this case we know that the imaginary part is zero. This implies that the phase-shift jumps by π at these energies so that the variation of the DOS is δ -like. In this case one speaks about bound states which appear outside the conduction band. Clearly this possibility can not explain a Curie-Weiss behavior for $T \ll T_F$. Indeed at very low temperature the bound state is either doubly occupied, if below the conduction band, or empty, if above, and one needs a temperature larger than the conduction bandwidth, hence larger than T_F , to release its spin entropy.

The other possibility is that the real part vanishes at a frequency ω_* within the conduction band where the imaginary part is non zero. Around ω_* and assuming a real part linearly vanishing and an imaginary part roughly constant we get

$$\delta(\omega) \simeq \tan^{-1} \frac{\Gamma}{\omega - \omega_*},$$

which implies a phase-shift $\delta_L(\omega_*) = \pm\pi/2$ and leads to a Lorentian DOS variation

$$\Delta\rho(\omega) \sim \frac{1}{\pi} \frac{\Gamma}{(\omega - \omega_*)^2 + \Gamma^2}. \quad (\text{A.26})$$

This is called a *resonance*. Clearly, in order for this resonance to contribute at $T \ll T_F$, ω_* should be very close to the chemical potential, in particular $|\omega_* - \mu| \ll T_K$, and, in addition, $\Gamma \simeq T_K$.

Let us therefore assume $\Gamma = T_K$ and for further simplicity that the resonance is right at the chemical potential, i.e. $\omega_* = 0$. The contribution of the resonant state to the magnetic susceptibility is then given by

$$\Delta\chi(T) = -\mu_B g \int d\epsilon \frac{\partial f(\epsilon)}{\partial \epsilon} \frac{1}{\pi} \frac{T_K}{\epsilon^2 + T_K^2}, \quad (\text{A.27})$$

where

$$f(\epsilon) = \left(1 + e^{\beta\epsilon}\right)^{-1},$$

is the Fermi distribution. One readily finds that for $T \gg T_K$,

$$\Delta\chi \simeq \mu_B g \frac{1}{T},$$

while for $T \ll T_K$

$$\Delta\chi \simeq \mu_B g \frac{1}{\pi T_K},$$

similar to the observed behavior. In addition the resistivity would be given through (A.24) by ($\rho(\omega) \sim \rho(0) \equiv \rho_0$)

$$\begin{aligned} R(0) &\propto \frac{1}{\tau(0)} = n_i \frac{2}{\pi \rho_0} \sin^2 \delta(0) \\ &= n_i \frac{2}{\pi \rho_0}, \end{aligned} \tag{A.28}$$

again compatible with the almost unitary limit, $\delta(0) = \pi/2$, observed experimentally. Therefore the existence of a narrow resonance near the chemical potential with width exactly given by T_K would seem the natural explanation to what experiments find.

However this is evidently very strange, since the Kondo behavior is observed in many different host metals as well as for different magnetic impurities, hence it would be really surprising that in all these cases a resonance appears always pinned near the chemical potential.

Moreover this simple single-particle scenario fails to explain the entropy released above T_K . Indeed, for $T \gg T_K$ the resonance is effectively like an isolated level which can be empty, singly occupied with a spin up or down, or doubly occupied. Therefore its entropy should be $S = 2 \ln 2$. On the other hand the experiments tells us that only spin and orbital degrees of freedom are released above T_K , which amounts in the above simplified model to an entropy $S = \ln 2$. In other words a resonance at the chemical potential at temperatures larger than its broadening is not at all the same as a local moment, since the former does have valence fluctuations which are absent in the latter.

Therefore, although the resonance scenario is suggestive, it is not at all the solution to the puzzle.

Appendix B

The Gutzwiller variational approach to the AIM

In this section we will study the AIM by means of a Gutzwiller-type of variational wave-function. However, before that, we need some additional results for the simple resonant level model.

B.1 Variation of the electron number

The variation of the electron number per spin due to the impurity is known to be related to the Green's functions through

$$\begin{aligned}
 \Delta N_{els} &= T \sum_n \left[\mathcal{G}(i\omega_n) + \sum_{\mathbf{k}} G_{\mathbf{k}\mathbf{k}}(i\omega_n) - G_{\mathbf{k}\mathbf{k}}^{(0)}(i\omega_n) \right] e^{i\omega_n 0^+} \\
 &= T \sum_n \frac{1}{i\omega_n - \epsilon_d - \Delta(i\omega_n)} \left[1 + \sum_{\mathbf{k}} |V_{\mathbf{k}}|^2 \left(\frac{1}{i\omega_n - \epsilon_{\mathbf{k}}} \right)^2 \right] \\
 &= T \sum_n \frac{\partial}{\partial i\omega_n} \ln(i\omega_n - \epsilon_d - \Delta(i\omega_n)), \tag{B.1}
 \end{aligned}$$

Let us consider the contour drawn in Fig. B.1. The function $S(z) = \ln(z - \epsilon_d - \Delta(z))$ has a branch cut on the real axis and it is analytic everywhere else. Therefore

$$\oint \frac{dz}{2\pi i} f(z) \frac{\partial}{\partial z} S(z) = 0,$$

because in the region which excludes both axes the function is analytic. On the other hand

$$0 = \oint \frac{dz}{2\pi i} f(z) \frac{\partial S(z)}{\partial z} = T \sum_n \frac{\partial}{\partial i\omega_n} \ln(i\omega_n - \epsilon_d - \Delta(i\omega_n))$$

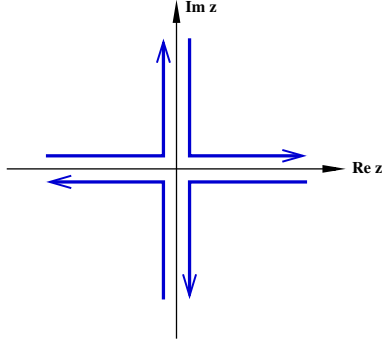


Figure B.1: Integration contour.

$$+ \int_{-\infty}^{+\infty} \frac{d\epsilon}{2\pi i} f(\epsilon) \frac{\partial}{\partial \epsilon} [S(\epsilon + i0^+) - S(\epsilon - i0^+)]$$

Therefore we finally get

$$\Delta N_{els} = - \int_{-\infty}^{+\infty} \frac{d\epsilon}{2\pi i} f(\epsilon) \frac{\partial}{\partial \epsilon} [S(\epsilon + i0^+) - S(\epsilon - i0^+)]. \quad (\text{B.2})$$

Within the previous approximation

$$S(\epsilon + i0^+) - S(\epsilon - i0^+) = \ln(\epsilon - \epsilon_d + i\Gamma) - \ln(\epsilon - \epsilon_d - i\Gamma) = 2i \tan^{-1} \frac{\Gamma}{\epsilon - \epsilon_d},$$

hence, through Eq. (3.15),

$$\Delta N_{els} = \int_{-\infty}^{+\infty} d\epsilon f(\epsilon) \frac{1}{\pi} \frac{\Gamma}{(\epsilon - \epsilon_d)^2 + \Gamma^2} = N_d. \quad (\text{B.3})$$

In other words the change in the number of electrons only comes from those electrons occupying the impurity level. If for instance $\epsilon_{d\uparrow}$ is different from $\epsilon_{d\downarrow}$, at zero temperature the number of electrons at the impurity with spin σ is

$$N_{d\sigma} = \frac{1}{2} - \frac{1}{\pi} \tan^{-1} \frac{\epsilon_{d\sigma}}{\Gamma}. \quad (\text{B.4})$$

B.2 Energy variation

For later convenience, we calculate here the impurity contribution to the total energy. Suppose that we change $V_{\mathbf{k}} \rightarrow \lambda V_{\mathbf{k}}$. The total energy becomes a function of λ , $E(\lambda)$, which, by the Hellmann-Feynmann theorem, satisfies

$$\frac{\partial E(\lambda)}{\partial \lambda} = \langle \Psi_\lambda | \frac{\partial \mathcal{H}}{\partial \lambda} | \Psi_\lambda \rangle$$

$$= \sum_{\mathbf{k}\sigma} \langle \Psi_\lambda | V_{\mathbf{k}} c_{\mathbf{k}\sigma}^\dagger d_\sigma + H.c. | \Psi_\lambda \rangle = 2T \sum_n \sum_{\mathbf{k}} V_{\mathbf{k}} G_{d\mathbf{k}}(i\omega_n; \lambda) + V_{\mathbf{k}}^* G_{\mathbf{k}d}(i\omega_n; \lambda).$$

Here $|\Psi_\lambda\rangle$ is the ground state wavefunction at a fixed λ , and $G(i\omega_n; \lambda)$ are the corresponding Green's functions. Specifically

$$G_{\mathbf{k}d}(z; \lambda) = \lambda \frac{V_{\mathbf{k}}}{z - \epsilon_{\mathbf{k}}} \frac{1}{z - \epsilon_d - \lambda^2 \Delta(z)}, \quad (\text{B.5})$$

$$G_{d\mathbf{k}}(z; \lambda) = \lambda \frac{V_{\mathbf{k}}^*}{z - \epsilon_{\mathbf{k}}} \frac{1}{z - \epsilon_d - \lambda^2 \Delta(z)}, \quad (\text{B.6})$$

with $\Delta(z)$ defined in Eq. (3.7). Therefore

$$\begin{aligned} \frac{\partial E(\lambda)}{\partial \lambda} &= 4T \sum_n \sum_{\mathbf{k}} \lambda \frac{|V_{\mathbf{k}}|^2}{i\omega_n - \epsilon_{\mathbf{k}}} \frac{1}{i\omega_n - \epsilon_d - \lambda^2 \Delta(i\omega_n)} \\ &= 4T \sum_n \lambda \Delta(i\omega_n) \frac{1}{i\omega_n - \epsilon_d - \lambda^2 \Delta(i\omega_n)} = -2T \sum_n \frac{\partial}{\partial \lambda} \ln(i\omega_n - \epsilon_d - \lambda^2 \Delta(i\omega_n)), \end{aligned}$$

so that the energy variation due to the impurity is

$$E(\lambda) - E(0) = -2T \sum_n \ln \left(\frac{i\omega_n - \epsilon_d - \lambda^2 \Delta(i\omega_n)}{i\omega_n - \epsilon_d} \right). \quad (\text{B.7})$$

In addition the average value of the hybridization at fixed λ is

$$E_{hyb}(\lambda) = \sum_{\mathbf{k}\sigma} \langle \Psi_\lambda | \lambda V_{\mathbf{k}} c_{\mathbf{k}\sigma}^\dagger d_\sigma + H.c. | \Psi_\lambda \rangle = \lambda \frac{\partial E(\lambda)}{\partial \lambda}, \quad (\text{B.8})$$

so that the change in the bath energy is given by

$$E_{bath}(\lambda) - E_{bath}(0) = E(\lambda) - E(0) - E_{hyb}(\lambda) = E(\lambda) - E(0) - \lambda \frac{\partial E(\lambda)}{\partial \lambda}. \quad (\text{B.9})$$

To calculate (B.7) we use the same integration contour as in Fig. B.1. By noticing that

$$\ln(\epsilon - \epsilon_d + i0^+) - \ln(\epsilon - \epsilon_d - i0^+) = 2i \tan^{-1} \frac{0^+}{\epsilon - \epsilon_d} = 2\pi i \theta(\epsilon_d - \epsilon),$$

we find

$$E(\lambda) - E(0) = 2 \int \frac{d\epsilon}{\pi} f(\epsilon) \left[\tan^{-1} \frac{\lambda^2 \Gamma}{\epsilon - \epsilon_d} - \pi \theta(\epsilon_d - \epsilon) \right]. \quad (\text{B.10})$$

Let us evaluate this integral in the simple case $\epsilon_d = 0$ at zero temperature, where

$$E(\lambda) - E(0) = 2 \int_{-\infty}^0 \frac{d\epsilon}{\pi} \left[\tan^{-1} \frac{\lambda^2 \Gamma}{\epsilon} - \pi \right] = -\frac{2}{\pi} \lambda^2 \Gamma \ln \frac{We}{\lambda^2 \Gamma}. \quad (\text{B.11})$$

Therefore the full energy gain is

$$\Delta E = -\frac{2}{\pi} \Gamma \ln \frac{We}{\Gamma}, \quad (\text{B.12})$$

which derives from an hybridization gain

$$E_{hyb} = -\frac{4}{\pi} \Gamma \ln \frac{W}{\Gamma}, \quad (\text{B.13})$$

and a bath energy cost

$$\Delta E_{bath} = \frac{2}{\pi} \Gamma \ln \frac{W}{e\Gamma}. \quad (\text{B.14})$$

B.3 The Gutzwiller wavefunction

Armed with the previous results, let us introduce a variational wavefunction for a single-orbital AIM. The Hamiltonian is

$$\mathcal{H}_{AIM} = \sum_{\mathbf{k}\sigma} \epsilon_{\mathbf{k}} c_{\mathbf{k}\sigma}^\dagger c_{\mathbf{k}\sigma} \quad (\text{B.15})$$

$$+ V \sum_{\mathbf{k}\sigma} \left(c_{\mathbf{k}\sigma}^\dagger d_\sigma + H.c. \right) + \frac{U}{2} (n_d - 1)^2 \quad (\text{B.16})$$

$$= \mathcal{H}_{bath} + \mathcal{H}_{hyb} + \mathcal{H}_{int}, \quad (\text{B.17})$$

and is assumed to be particle-hole symmetric. We consider an uncorrelated wave-function, $|\psi_0\rangle$, which is the ground state of a non-interacting impurity with a variational hybridization strength λV . The variational correlated wave-function is defined through

$$|\psi\rangle \equiv \mathcal{P}_G |\psi_0\rangle, \quad (\text{B.18})$$

where the operator \mathcal{P}_G acts only on the impurity and is given by

$$\mathcal{P}_G \equiv \lambda_0 \left(|0\rangle\langle 0| + |2\rangle\langle 2| \right) + \lambda_1 |1\rangle\langle 1|. \quad (\text{B.19})$$

λ_0 and λ_1 are variational parameters and $|n\rangle\langle n|$ is the projector at the impurity site onto a state with n electrons, $|1\rangle\langle 1|$ being the sum of the projectors onto a singly occupied impurity orbital with both spin up and down. Notice that, by construction, \mathcal{P}_G preserves both particle-hole and spin rotational symmetries. Since we can multiply \mathcal{P}_G by any constant, which is absorbed by normalization, without loss of variational freedom we can impose the following condition:

$$\langle \psi_0 | \mathcal{P}_G^2 | \psi_0 \rangle = \langle \psi_0 | \psi_0 \rangle = 1.$$

This implies that

$$1 = \lambda_0^2 \left(P^{(0)}(0) + P^{(0)}(2) \right) + \lambda_1^2 P^{(0)}(1), \quad (\text{B.20})$$

where

$$P^{(0)}(n) = \langle \psi_0 | |n\rangle\langle n| | \psi_0 \rangle = \frac{1}{4} \begin{pmatrix} 2 \\ n \end{pmatrix}$$

are the occupation probabilities of the uncorrelated wavefunction. Notice that $P^{(0)}(0) = P^{(0)}(2)$ because of particle-hole symmetry. Let us define new variational parameters

$$\begin{aligned} P(0) &= \lambda_0^2 P^{(0)}(0), \\ P(1) &= \lambda_1^2 P^{(0)}(1), \end{aligned}$$

$$P(2) = \lambda_0^2 P^{(0)}(2) = P(0),$$

through which (B.20) becomes

$$P(0) + P(1) + P(2) = 2P(0) + P(1) = 1.$$

One can regard $P(n)$ as the correlated occupation probabilities. Indeed it follows that the average impurity occupation

$$\langle \psi_0 | \mathcal{P}_G \left(\sum_n n |n\rangle \langle n| \right) \mathcal{P}_G | \psi_0 \rangle = P(1) + 2P(2) = P(1) + 2P(0) = 1 = \langle \psi_0 | \left(\sum_n n |n\rangle \langle n| \right) | \psi_0 \rangle,$$

which proves not only that the $P(n)$'s do behave as occupation probabilities, but also that, since $\sum_n n |n\rangle \langle n| = \sum_\sigma d_\sigma^\dagger d_\sigma$, and, in addition, spin-rotational symmetry is preserved, the following expression holds:

$$\langle \psi_0 | \mathcal{P}_G^2 d_\sigma^\dagger d_{\sigma'} | \psi_0 \rangle = \langle \psi_0 | d_\sigma^\dagger d_{\sigma'} | \psi_0 \rangle = \frac{1}{2} \delta_{\sigma\sigma'}. \quad (\text{B.21})$$

It implies that, if we select out of the operator \mathcal{P}_G a creation and an annihilation operator and average what is left with the uncorrelated wavefunction, this average is zero. From this property it follows that

$$\langle \psi_0 | \mathcal{P}_G \mathcal{H}_{bath} \mathcal{P}_G | \psi_0 \rangle = \langle \psi_0 | \mathcal{H}_{bath} | \psi_0 \rangle = E_0 + \Delta E_{bath}(\lambda^2 \Gamma), \quad (\text{B.22})$$

where E_0 is the bath energy in the absence of the impurity, Γ is the hybridization width

$$\Gamma = \pi \rho_0 V^2,$$

ρ_0 being the conduction bath DOS, and ΔE_{bath} is given in Eq. (B.14). In addition,

$$\langle \psi_0 | \mathcal{P}_G \mathcal{H}_{hyb} \mathcal{P}_G | \psi_0 \rangle = \sqrt{Z} \langle \psi_0 | \mathcal{H}_{hyb} | \psi_0 \rangle = \frac{\sqrt{Z}}{\lambda} E_{hyb}(\lambda^2 \Gamma), \quad (\text{B.23})$$

see Eq. (B.13). The \sqrt{Z} prefactor is equal to

$$\sqrt{Z} = 2 \langle \psi_0 | \mathcal{P}_G d_\sigma^\dagger \mathcal{P}_G d_\sigma | \psi_0 \rangle \quad (\text{B.24})$$

$$= \sqrt{2P(0)P(1)} + \sqrt{2P(2)P(1)} = 2\sqrt{2P(0)P(1)}. \quad (\text{B.25})$$

Finally, it is straightforward to show that

$$\langle \psi_0 | \mathcal{P}_G \mathcal{H}_{int} \mathcal{P}_G | \psi_0 \rangle = U P(0). \quad (\text{B.26})$$

We easily realize that the uncorrelated wave-function which minimizes the energy has $\lambda = \sqrt{Z}$, implying $\Gamma \rightarrow Z\Gamma$. Therefore the variational energy turns out to be, see Eq. (B.12),

$$E = E_0 + \Delta E(Z\Gamma) + U P(0). \quad (\text{B.27})$$

We define $P(0) = P(2) = d/2$ hence $P(1) = 1 - d$, and $\Gamma_* = Z \Gamma$. Therefore

$$Z = 4d(1 - d).$$

In terms of Γ_*

$$d = \frac{1}{2} - \sqrt{\frac{1}{4} - \frac{\Gamma_*}{4\Gamma}}.$$

For large U , *i.e.* small d as well as small Γ_* ,

$$\frac{\partial d}{\partial \Gamma_*} \simeq \frac{1}{4\Gamma},$$

hence the minimum condition reads

$$\frac{\partial E}{\partial \Gamma_*} = -\frac{2}{\pi} \ln \frac{W}{\Gamma_*} + \frac{U}{8\Gamma} = 0,$$

with solution

$$\Gamma_* = W \exp \left[-\frac{U}{16 \rho_0 V^2} \right]. \quad (\text{B.28})$$

I recall that the Kondo coupling is

$$J_K = 8 \frac{V^2}{U},$$

so that

$$\Gamma = W \exp \left[-\frac{1}{2 \rho_0 J_K} \right], \quad (\text{B.29})$$

which is actually the square root of T_K . Therefore, in spite of the fact that the Gutzwiller wave-function predicts correctly a ground state which looks the same as that of a resonant level model with a reduced hybridization width, quantitatively the energy scale comes out too large.

Appendix C

Fermi liquid theory of the Anderson impurity model

In this Appendix we build up a Fermi liquid theory of a generic AIM closely following the original work by Mihaly and Zawadowskii, and Yoshimori and Zawadowskii.

Let us consider more generally a multi-orbital Anderson impurity model with Hamiltonian

$$\begin{aligned} \mathcal{H}_{AIM} = & \sum_{\mathbf{k}a} \epsilon_{\mathbf{k}a} c_{\mathbf{k}a}^\dagger c_{\mathbf{k}a} + \sum_{\mathbf{k}a} \left(V_{\mathbf{k}a} c_{\mathbf{k}a}^\dagger d_a + H.c. \right) \\ & + \sum_a \epsilon_a d_a^\dagger d_a + \mathcal{H}_{int} \left[d^\dagger, d \right]. \end{aligned} \quad (\text{C.1})$$

The Hamiltonian admits conserved quantities labelled by an index (i),

$$\mathcal{M}^{(i)} = \sum_{\mathbf{k}ab} c_{\mathbf{k}a}^\dagger M_{ab}^{(i)} c_{\mathbf{k}b} + \sum_{ab} d_a^\dagger M_{ab}^{(i)} d_b. \quad (\text{C.2})$$

For convenience we adopt the normalization $\text{Tr} \left(M^{(i)} \cdot M^{(i)} \right) = 1$. By means of the Luttinger-Ward functional one can prove that the variation $\Delta M^{(i)}$ of the average value $M^{(i)} = \langle \mathcal{M}^{(i)} \rangle$ associated with the presence of the impurity is given by

$$\Delta M^{(i)} = \sum_{ab} M_{ab}^{(i)} \oint \frac{dz}{2\pi i} f(z) \frac{\partial}{\partial z} \ln \mathcal{G}_{ba}(z) = \oint \frac{dz}{2\pi i} f(z) \frac{\partial}{\partial z} \text{Tr} \left(M^{(i)} \ln \mathcal{G}(z) \right),$$

where the integration contour encloses clockwise the real axis, $f(z)$ is the Fermi distribution function in the complex plane and $\mathcal{G}(z)$ the matrix of the impurity single-particle Green's functions. Since the latters have a branch cut on the real axis, the above expression is also equal to

$$\Delta M^{(i)} = -\frac{1}{\pi} \int_{-\infty}^{\infty} d\epsilon \frac{\partial f(\epsilon)}{\partial \epsilon} \Im m \text{Tr} \left(M^{(i)} \ln \mathcal{G}(\epsilon + i\delta) \right) \quad (\text{C.3})$$

with δ an infinitesimal positive number. Let us consider one of the conserved operators (to simplify notations we will drop its index). We can always rotate the basis set in such a way to make this operator diagonal

$$\mathcal{M} = \sum_{\mathbf{k}a} M_a c_{\mathbf{k}a}^\dagger c_{\mathbf{k}a} + \sum_a M_a d_a^\dagger d_a, \quad (\text{C.4})$$

leaving unchanged the non-interacting part of the Hamiltonian (C.1). In this representation, if we add to (C.1) a perturbation

$$\delta\mathcal{H}_{AIM} = -h\mathcal{M}, \quad (\text{C.5})$$

the impurity Green's functions become

$$\begin{aligned} \mathcal{G}_{ab}(z, h)^{-1} &= \delta_{ab} \mathcal{G}_a(z, h)^{-1} \\ &= \delta_{ab} \left[\left(\mathcal{G}_a^{(0)}(z, h) \right)^{-1} - \Sigma_a(z, h) \right] = z - \epsilon_a + h M_a - \Delta_a(z, h) - \Sigma_a(z, h), \end{aligned}$$

where

$$\Delta_a(z, h) = \sum_{\mathbf{k}} |V_{\mathbf{k}a}|^2 \frac{1}{z - \epsilon_{\mathbf{k}a} + h M_a} \quad (\text{C.6})$$

is the hybridization function in the presence of the external field h , as opposed to the one in its absence $\Delta_a(z, 0) \equiv \Delta_a(z)$. We notice that

$$\left(\frac{\partial \Delta_a(z, h)}{\partial h} \right)_{h=0} = M_a \frac{\partial \Delta_a(z)}{\partial z},$$

from which it follows that, by defining $\mathcal{G}_a(z, h=0) \equiv \mathcal{G}_a(z)$,

$$\begin{aligned} \left(\frac{\partial \ln \mathcal{G}_a(z, h)}{\partial h} \right)_{h=0} &= - \left(\frac{\partial \ln \mathcal{G}_a(z, h)^{-1}}{\partial h} \right)_{h=0} \\ &= -\mathcal{G}_a(z) \left[M_a \left(1 - \frac{\partial \Delta_a(z)}{\partial z} \right) - \left(\frac{\partial \Sigma_a(z, h)}{\partial h} \right)_{h=0} \right]. \end{aligned}$$

In the presence of the field, also the average value of \mathcal{M} changes, $M \rightarrow M(h)$, as well as its variation in the presence of the impurity $\Delta M \rightarrow \Delta M(h)$. From the above formulas it follows that the variation of the susceptibility $\Delta\chi$ is given by

$$\begin{aligned} \Delta\chi &= \left(\frac{\partial \Delta M(h)}{\partial h} \right)_{h=0} = \sum_a \int_{-\infty}^{\infty} \frac{d\epsilon}{\pi} \frac{\partial f(\epsilon)}{\partial \epsilon} \Im m \left\{ M_a \mathcal{G}_a(\epsilon + i\delta) \right. \\ &\quad \left. \times \left[M_a \left(1 - \left(\frac{\partial \Delta_a(z)}{\partial z} \right)_{z=\epsilon+i\delta} \right) - \left(\frac{\partial \Sigma_a(\epsilon + i\delta)}{\partial h} \right)_{h=0} \right] \right\}. \quad (\text{C.7}) \end{aligned}$$

On the other hand one can prove diagrammatically that

$$\begin{aligned}
\left(\frac{\partial \Sigma_a(i\omega_n)}{\partial h}\right)_{h=0} &= -\frac{1}{\beta} \sum_m \sum_b \Gamma_{a,b;b,a}(i\omega_n, i\epsilon_m; i\epsilon_m, i\omega_n) \mathcal{G}_b(i\epsilon_m)^2 \left(\frac{\partial \left(\mathcal{G}_a^{(0)}(i\epsilon_m, h)\right)^{-1}}{\partial h}\right)_{h=0} \\
&= -\frac{1}{\beta} \sum_m \sum_b \Gamma_{a,b;b,a}(i\omega_n, i\epsilon_m; i\epsilon_m, i\omega_n) \mathcal{G}_b(i\epsilon_m)^2 M_b \left(1 - \frac{\partial \Delta_b(i\epsilon_m)}{\partial i\epsilon_m}\right),
\end{aligned} \tag{C.8}$$

where the interaction vertex is the reducible one.

Using the fact that \mathcal{M} is conserved, the following Ward identity also holds

$$\begin{aligned}
\left[\Sigma_a(i\epsilon + i\omega) - \Sigma_a(i\epsilon)\right] M_a &= -\frac{1}{\beta} \sum_n \sum_b \Gamma_{a,b;b,a}(i\epsilon + i\omega, i\epsilon_n; i\epsilon_n + i\omega, i\epsilon) \\
&\times M_b \mathcal{G}_b(i\epsilon_n + i\omega) \mathcal{G}_b(i\epsilon_n) [i\omega - \Delta_b(i\epsilon_n + i\omega) + \Delta_b(i\epsilon_n)].
\end{aligned} \tag{C.9}$$

It follows that

$$\begin{aligned}
\frac{\partial \Sigma_a(i\epsilon)}{\partial i\epsilon} M_a &= -\frac{1}{\beta} \sum_n \sum_b \Gamma_{a,b;b,a}(i\epsilon, i\epsilon_n; i\epsilon_n, i\epsilon) M_b \mathcal{G}_b(i\epsilon_n)^2 \\
&\quad - \lim_{i\omega \rightarrow 0} \frac{1}{\beta} \sum_n \sum_b \Gamma_{a,b;b,a}(i\epsilon + i\omega, i\epsilon_n; i\epsilon_n + i\omega, i\epsilon) \\
&\quad \times M_b \mathcal{G}_b(i\epsilon_n + i\omega) \mathcal{G}_b(i\epsilon_n) \frac{[-\Delta_b(i\epsilon_n + i\omega) + \Delta_b(i\epsilon_n)]}{i\omega} \\
&= -\frac{1}{\beta} \sum_n \sum_b \Gamma_{a,b;b,a}(i\epsilon, i\epsilon_n; i\epsilon_n, i\epsilon) M_b \mathcal{G}_b(i\epsilon_n)^2 \left(1 - \frac{\partial \Delta_b(i\epsilon_n)}{\partial i\epsilon_n}\right) \\
&\quad + \int_{-\infty}^{\infty} \frac{d\epsilon'}{2\pi} \frac{\partial f(\epsilon')}{\partial \epsilon'} \sum_b \Gamma_{a,b;b,a}(i\epsilon, \epsilon' - i\delta'; \epsilon' + i\delta', i\epsilon) \\
&\quad \times M_b \mathcal{G}_b(\epsilon' + i\delta') \mathcal{G}_b(\epsilon' - i\delta') \Im m \left[\Delta_b(\epsilon' - i\delta') - \Delta_b(\epsilon' + i\delta') \right]
\end{aligned} \tag{C.10}$$

$$\begin{aligned}
&= -\frac{1}{\beta} \sum_n \sum_b \Gamma_{a,b;b,a}(i\epsilon, i\epsilon_n; i\epsilon_n, i\epsilon) M_b \mathcal{G}_b(i\epsilon_n)^2 \left(1 - \frac{\partial \Delta_b(i\epsilon_n)}{\partial i\epsilon_n}\right) \\
&\quad + \int_{-\infty}^{\infty} \frac{d\epsilon'}{\pi} \frac{\partial f(\epsilon')}{\partial \epsilon'} \sum_b \Gamma_{a,b;b,a}(i\epsilon, \epsilon' - i\delta'; \epsilon' + i\delta', i\epsilon) \\
&\quad \times M_b \Gamma_b(\epsilon') \mathcal{G}_b(\epsilon' + i\delta') \mathcal{G}_b(\epsilon' - i\delta'),
\end{aligned} \tag{C.11}$$

where, by definition,

$$\Gamma_b(\epsilon') = \frac{1}{2} \Im m \left(\Delta_b(\epsilon' - i\delta') - \Delta_b(\epsilon' + i\delta') \right)$$

is the non-interacting resonance-width.

By comparing (C.11) with (C.8) we find that

$$\begin{aligned} \left(\frac{\partial \Sigma_a(i\epsilon)}{\partial h} \right)_{h=0} &= \frac{\partial \Sigma_a(i\epsilon)}{\partial i\epsilon} M_a - \int_{-\infty}^{\infty} \frac{d\epsilon'}{\pi} \frac{\partial f(\epsilon')}{\partial \epsilon'} \sum_b \Gamma_{a,b;b,a}(i\epsilon, \epsilon' - i\delta'; \epsilon' + i\delta', i\epsilon) \\ &\times M_b \Gamma_b(\epsilon') \mathcal{G}_b(\epsilon' + i\delta') \mathcal{G}_b(\epsilon' - i\delta'). \end{aligned} \quad (\text{C.12})$$

Going back to the expression for the variation of the susceptibility, Eq. (C.7), and inserting (C.12), we obtain the following result

$$\begin{aligned} \Delta \chi &= \sum_a \int_{-\infty}^{\infty} \frac{d\epsilon}{\pi} \frac{\partial f(\epsilon)}{\partial \epsilon} \Im m \left\{ M_a \mathcal{G}_a(\epsilon + i\delta) \right. \\ &\times \left[M_a \left(1 - \left(\frac{\partial \Delta_a(z)}{\partial z} \right)_{z=\epsilon+i\delta} - \left(\frac{\partial \Sigma_a(z)}{\partial z} \right)_{z=\epsilon+i\delta} \right) \right. \\ &\left. \left. + \int_{-\infty}^{\infty} \frac{d\epsilon'}{\pi} \frac{\partial f(\epsilon')}{\partial \epsilon'} \sum_b \Gamma_{a,b;b,a}(\epsilon, \epsilon'; \epsilon', \epsilon) M_b \Gamma_b(\epsilon') \mathcal{G}_b(\epsilon' + i\delta') \mathcal{G}_b(\epsilon' - i\delta') \right] \right\} \end{aligned} \quad (\text{C.13})$$

in which we have assumed that the reducible vertex is analytic on the real axis.

Let us define the quantity

$$\rho_a^* = \int_{-\infty}^{\infty} \frac{d\epsilon}{\pi} \frac{\partial f(\epsilon)}{\partial \epsilon} \Im m \left\{ \mathcal{G}_a(\epsilon + i\delta) \left[1 - \left(\frac{\partial \Delta_a(i\epsilon)}{\partial i\epsilon} \right)_{i\epsilon \rightarrow \epsilon + i\delta} - \left(\frac{\partial \Sigma_a(i\epsilon)}{\partial i\epsilon} \right)_{i\epsilon \rightarrow \epsilon + i\delta} \right] \right\}, \quad (\text{C.14})$$

which plays actually the role of the quasi-particle DOS at the chemical potential, as opposed to the particle DOS

$$\rho_a = \int_{-\infty}^{\infty} \frac{d\epsilon}{\pi} \frac{\partial f(\epsilon)}{\partial \epsilon} \Im m \mathcal{G}_a(\epsilon + i\delta) \equiv - \int_{-\infty}^{\infty} \frac{d\epsilon}{\pi} \frac{\partial f(\epsilon)}{\partial \epsilon} \rho_a(\epsilon). \quad (\text{C.15})$$

Finally we notice that

$$\mathcal{G}_b(\epsilon' + i\delta') \mathcal{G}_b(\epsilon' - i\delta') = \frac{1}{\epsilon' - \epsilon_b - \Delta_b(\epsilon' + i\delta') - \Sigma_b(\epsilon' + i\delta')} \frac{1}{\epsilon' - \epsilon_b - \Delta_b(\epsilon' - i\delta') - \Sigma_b(\epsilon' - i\delta')}$$

$$\begin{aligned}
&= \frac{1}{\Delta_b(\epsilon' - i\delta') - \Delta_b(\epsilon' + i\delta') + \Sigma_b(\epsilon' - i\delta') - \Sigma_b(\epsilon' + i\delta')} \\
&\quad \times \left(\mathcal{G}_b(\epsilon' - i\delta') - \mathcal{G}_b(\epsilon' + i\delta') \right) \\
&= \pi \rho_b(\epsilon') \frac{1}{\Gamma_b(\epsilon') + \gamma_b(\epsilon')},
\end{aligned}$$

where we have defined

$$\gamma_b(\epsilon') = \frac{1}{2} \Im m \left(\Sigma_b(\epsilon' - i\delta') - \Sigma_b(\epsilon' + i\delta') \right), \quad (\text{C.16})$$

which is related to the quasiparticle decay rate. By means of the above expression and Eq. (C.14), we can rewrite (C.13) as

$$\begin{aligned}
\Delta \chi &= \sum_a M_a^2 \rho_a^* + \sum_{ab} M_a M_b \int_{-\infty}^{\infty} \frac{d\epsilon d\epsilon'}{\pi} \frac{\partial f(\epsilon)}{\partial \epsilon} \frac{\partial f(\epsilon')}{\partial \epsilon'} \\
&\quad \Im m \left\{ \mathcal{G}_a(\epsilon + i\delta) \Gamma_{a,b;b,a}(\epsilon, \epsilon'; \epsilon', \epsilon) \rho_b(\epsilon') \frac{\Gamma_b(\epsilon')}{\Gamma_b(\epsilon') + \gamma_b(\epsilon')} \right\} \\
&= \sum_a M_a^2 \rho_a^* - \sum_{ab} M_a M_b \int_{-\infty}^{\infty} d\epsilon d\epsilon' \frac{\partial f(\epsilon)}{\partial \epsilon} \frac{\partial f(\epsilon')}{\partial \epsilon'} \\
&\quad \times \rho_a(\epsilon) \rho_b(\epsilon') \Gamma_{a,b;b,a}(\epsilon, \epsilon'; \epsilon', \epsilon) \frac{\Gamma_b(\epsilon')}{\Gamma_b(\epsilon') + \gamma_b(\epsilon')}, \quad (\text{C.17})
\end{aligned}$$

where the last expression is obtained by assuming that, for small frequencies, the reducible vertex is real, hence that the only contribution to the imaginary part comes from

$$\Im m \mathcal{G}_a(\epsilon + i\delta) = -\pi \rho_a(\epsilon).$$

Eq. (C.17) has a broad validity, even in cases like DMFT, in which the hybridization functions may be strongly frequency-dependent.

In general the matrix elements of a conserved operators may be either diagonal or, if different states are degenerate, off-diagonal. In the former case only the diagonal elements of the scattering vertex, $\Gamma_{a,b;b,a}$, enter the expression of the susceptibility. More interesting is the case of degenerate levels, $\epsilon_{\mathbf{k}a} = \epsilon_{\mathbf{k}}$ and $\epsilon_a = \epsilon$ in (C.1). Under the assumption that the interaction does not spoil this degeneracy, $\rho_a = \rho$ and $\rho_a^* = \rho^*$. Since we assumed that $\text{Tr}(M \cdot M) = 1$, in a generic basis in which M is not diagonal the susceptibility variation reads

$$\Delta \chi = \rho^* - \sum_{abcd} M_{ba} M_{dc} \int_{-\infty}^{\infty} d\epsilon d\epsilon' \frac{\partial f(\epsilon)}{\partial \epsilon} \frac{\partial f(\epsilon')}{\partial \epsilon'} \rho(\epsilon) \rho(\epsilon') \Gamma_{a,c;d,b}(\epsilon, \epsilon'; \epsilon', \epsilon) \frac{\Gamma(\epsilon')}{\Gamma(\epsilon') + \gamma(\epsilon')}$$

$$\equiv \rho^* [1 - A], \quad (\text{C.18})$$

with the Landau scattering parameters A defined through

$$A \equiv \frac{1}{\rho^*} \sum_{abcd} M_{ba} M_{dc} \int_{-\infty}^{\infty} d\epsilon d\epsilon' \frac{\partial f(\epsilon)}{\partial \epsilon} \frac{\partial f(\epsilon')}{\partial \epsilon'} \rho(\epsilon) \rho(\epsilon') \Gamma_{a,c;d,b}(\epsilon, \epsilon'; \epsilon', \epsilon) \frac{\Gamma(\epsilon')}{\Gamma(\epsilon') + \gamma(\epsilon')}. \quad (\text{C.19})$$

In most common impurity models the hybridization functions have a smooth frequency-dependence and, in addition, perturbation theory does not break down at any value of the interaction. In these cases we have already seen that, at small frequency,

$$\Sigma_a(i\epsilon) \simeq i\epsilon \left(1 - \frac{1}{Z_a}\right),$$

where Z_a is the so-called quasiparticle residue, hence that

$$\rho_a^* = \frac{\rho_a}{Z_a},$$

and $\gamma_a(\epsilon \rightarrow 0) = 0$. Therefore (C.17) simplifies notably:

$$\begin{aligned} \Delta \chi &= \sum_a M_a^2 \rho_a^* - \sum_{ab} M_a M_b \rho_a \rho_b \Gamma_{a,b;b,a}(0, 0; 0, 0) \\ &= \sum_a M_a^2 \rho_a^* - \sum_{ab} M_a M_b Z_a Z_b \rho_a^* \rho_b^* \Gamma_{a,b;b,a}(0, 0; 0, 0). \end{aligned} \quad (\text{C.20})$$

When orbital degeneracy also occurs

$$\Delta \chi = \rho^* [1 - A], \quad (\text{C.21})$$

when this time

$$A = Z^2 \rho^* \sum_{abcd} M_{ba} M_{dc} \Gamma_{a,c;d,b}(0, 0; 0, 0), \quad (\text{C.22})$$

which is the common definition of the Landau A -parameters in terms of the quasiparticle scattering amplitudes.

We conclude by noticing that the variation of the specific heat is, in the degenerate example,

$$\frac{\Delta C_v}{C_{V0}} = \frac{\rho^*}{\rho_0}, \quad (\text{C.23})$$

where C_{V0} and ρ_0 are the specific heat and DOS, respectively, of the conduction electrons in the absence of the impurity. On the other hand, for any conserved quantity, $\mathcal{M}^{(i)}$, by Eq. (C.21) we find that

$$\frac{\Delta\chi^{(i)}}{\chi_0} = \frac{\rho^*}{\rho_0} [1 - A^{(i)}]. \quad (\text{C.24})$$

In other words, we can define for each conserved quantity a corresponding Wilson ratio whose value

$$R^{(i)} = \frac{\Delta\chi^{(i)}}{\chi_0} \frac{C_{V0}}{\Delta C_v} = 1 - A^{(i)}, \quad (\text{C.25})$$

is directly related to the Landau parameters.

C.1 Application to the single-orbital AIM

Let us apply these results to the single-orbital AIM. Two incoming quasi-particles at the same frequency can only be into a singlet state, hence there is a single scattering parameter

$$\Gamma = \Gamma_{\uparrow,\downarrow;\downarrow,\uparrow} = \Gamma_{\downarrow,\uparrow;\uparrow,\downarrow} = -\Gamma_{\uparrow,\downarrow;\uparrow,\downarrow} = -\Gamma_{\downarrow,\uparrow;\downarrow,\uparrow}. \quad (\text{C.26})$$

There are only two conserved quantities, the total charge, with $M_{\sigma\sigma'}^c = \delta_{\sigma\sigma'}/\sqrt{2}$, and the total spin, with $\mathbf{M}^s = \boldsymbol{\sigma}/\sqrt{2}$. Through (C.22) one finds that the charge, A^c , and spin, A^s , Landau parameters are

$$A^c = Z^2 \rho^* \Gamma = -A^s \equiv A. \quad (\text{C.27})$$

We know that, for large U , the charge fluctuations of the impurity are suppressed, hence we can assume that

$$\chi^c = \rho^* [1 - A] = 0,$$

namely that $A = 1$. It follows that

$$\chi^s = \rho^* [1 + A] = 2\rho^*,$$

as well as

$$R^c = 0, \quad R^s = 2.$$

Chapter 4

Brief introduction to the Wilson numerical renormalization group and to Conformal Field Theory

A very powerful way to study impurity models is by combining together the Wilson numerical renormalization group (NRG) and Conformal Field Theory (CFT). The former allows to determine in a very efficient way the low energy spectrum of an impurity model which, unless in simple cases, requires the full machinery of CFT to be interpreted. In the following we are going to briefly discuss both techniques.

4.1 Reduction to a one dimensional model

Let us consider for simplicity a single-orbital AIM, the extension to more orbitals being straightforward,

$$\begin{aligned}\mathcal{H}_{AIM} &= \sum_{\mathbf{k}\sigma} \epsilon_{\mathbf{k}} c_{\mathbf{k}\sigma}^\dagger c_{\mathbf{k}\sigma} + \left(V_{\mathbf{k}} c_{\mathbf{k}\sigma}^\dagger d_\sigma + H.c. \right) + \mathcal{H}_{int} [d^\dagger, d] \\ &= \mathcal{H}_0 + \mathcal{H}_{hyb} + \mathcal{H}_{int}.\end{aligned}\tag{4.1}$$

We already observed that the impurity is actually coupled only to a particular combination of conduction electrons:

$$c_0^\dagger = \frac{1}{V} \sum_{\mathbf{k}} V_{\mathbf{k}} c_{\mathbf{k}}^\dagger,\tag{4.2}$$

where we have dropped for simplicity the spin index and by definition

$$V^2 = \sum_{\mathbf{k}} |V_{\mathbf{k}}|^2.$$

Let us construct the single-particle state

$$|c_0\rangle = c_0^\dagger |0\rangle.$$

This is not an eigenstate of the conduction electron Hamiltonian \mathcal{H}_0 . Indeed we can always define a new state $|c_1\rangle$ orthogonal to $|c_0\rangle$ through

$$t_0 |c_1\rangle \equiv (\mathcal{H}_0 - \epsilon_0) |c_0\rangle,$$

where

$$\epsilon_0 = \langle c_0 | \mathcal{H}_0 | c_0 \rangle,$$

and

$$t_0^2 = \left(\langle c_0 | \mathcal{H}_0 | c_1 \rangle \right)^2 = \langle c_0 | (\mathcal{H}_0 - \epsilon_0)^2 | c_0 \rangle.$$

Analogously, at the next step we introduce a new state $|c_2\rangle$ orthogonal to the previous two through

$$t_1 |c_2\rangle \equiv (\mathcal{H}_0 - \epsilon_1) |c_1\rangle - t_0 |c_0\rangle,$$

where

$$\epsilon_1 = \langle c_1 | \mathcal{H}_0 | c_1 \rangle,$$

and

$$t_1^2 = \left(\langle c_1 | \mathcal{H}_0 | c_2 \rangle \right)^2 = \langle c_1 | (\mathcal{H}_0 - \epsilon_1)^2 | c_1 \rangle - t_0^2.$$

At the n -th iteration of this Lanczos algorithm, we obtain a state $|c_{n+1}\rangle$, orthogonal to the n previous ones, by

$$t_n |c_{n+1}\rangle \equiv (\mathcal{H}_0 - \epsilon_n) |c_n\rangle - t_{n-1} |c_{n-1}\rangle,$$

where

$$\epsilon_n = \langle c_n | \mathcal{H}_0 | c_n \rangle,$$

and

$$t_n^2 = \left(\langle c_n | \mathcal{H}_0 | c_{n+1} \rangle \right)^2 = \langle c_n | (\mathcal{H}_0 - \epsilon_n)^2 | c_n \rangle - t_{n-1}^2.$$

In this way we can rewrite the Hamiltonian (4.1) like

$$\mathcal{H}_{AIM} = \mathcal{H}_{int} [d^\dagger, d] + V \sum_{\sigma} \left(c_{0\sigma}^\dagger d_{\sigma} + H.c. \right) + \sum_{n \geq 0} \epsilon_n c_{n\sigma}^\dagger c_{n\sigma} + t_n \left(c_{n\sigma}^\dagger c_{n+1\sigma} + H.c. \right), \quad (4.3)$$

which describes a semi-infinite chain with the impurity at the edge. Notice that, if the original model has particle-hole symmetry, which implies that for any \mathbf{k} there is a \mathbf{p} such that $V_{\mathbf{k}} = V_{\mathbf{p}}^*$ and $\epsilon_{\mathbf{k}} = -\epsilon_{\mathbf{p}}$, then, for any $n \geq 0$, $\epsilon_n = 0$.

In the most common situations in which the conduction electron DOS and the hybridization function are smooth, the hopping matrix elements t_n converge fastly to a constant value n -independent.

As an example, let us consider a conduction electron DOS $\rho(\epsilon) = \theta(1 - \epsilon^2)/2$, constant within the interval $-1 \leq \epsilon \leq 1$ (in units of half-bandwidth) and zero outside. The chemical potential is $\mu = 0$. In addition we assume that the hybridization matrix elements V_ϵ are equal for any ϵ . In this case the conduction electron Hamiltonian is

$$\mathcal{H}_0 = \int_{-1}^1 d\epsilon \epsilon c_\epsilon^\dagger c_\epsilon,$$

and

$$c_0^\dagger = \sqrt{\frac{1}{2}} \int_{-1}^1 d\epsilon c_\epsilon^\dagger.$$

If we write

$$c_n^\dagger = \sqrt{\frac{2n+1}{2}} \int_{-1}^1 d\epsilon P_n(\epsilon) c_\epsilon^\dagger,$$

with $P_0(\epsilon) = 1$, and assume

$$\int_{-1}^1 d\epsilon P_n(\epsilon) P_m(\epsilon) = \delta_{nm} \frac{2}{2n+1},$$

the recursion equation becomes

$$\sqrt{2n+1} \epsilon P_n(\epsilon) = t_n \sqrt{2n+3} P_{n+1}(\epsilon) + t_{n-1} \sqrt{2n-1} P_{n-1}(\epsilon),$$

which, multiplying both sides by $\sqrt{2n+1}$, is

$$(2n+1) \epsilon P_n(\epsilon) = t_n \sqrt{(2n+3)(2n+1)} P_{n+1}(\epsilon) + t_{n-1} \sqrt{(2n+1)(2n-1)} P_{n-1}(\epsilon).$$

We realize that the above is the recurrence formula for the Legendre polynomials if

$$t_n = \frac{n+1}{\sqrt{(2n+3)(2n+1)}} \simeq \frac{1}{2} \left(1 + \frac{1}{8n^2} \right),$$

which indeed converges soon to $1/2$.

Therefore, instead of studying the full model (4.3), one can equally well consider a simple tight-binding Hamiltonian with constant hopping on a semi-infinite chain. The advantage is that a lot of powerful techniques are available in one dimension, like Conformal Field Theory, which we discuss later.

4.2 The Wilson Numerical Renormalization group

Let us consider again the model with a constant DOS and matrix elements $V_\epsilon = V$. We divide the energy interval $0 \leq \epsilon \leq 1$ into sub-intervals $I_n^{(+)}$, $n \geq 0$, defined in the following way

$$\epsilon \in I_n^{(+)} \quad \text{means} \quad \frac{1}{\Lambda^{n+1}} \leq \epsilon \leq \frac{1}{\Lambda^n},$$

with $\Lambda > 1$. The same is done for $-1 \leq \epsilon \leq 0$, in which case

$$\epsilon \in I_n^{(-)} \quad \text{means} \quad -\frac{1}{\Lambda^n} \leq \epsilon \leq -\frac{1}{\Lambda^{n+1}}.$$

In other words we have performed a logarithmic mesh of the energies. Let us focus on a single interval $I_n^{(+)}$, whose length is

$$L_n = \Lambda^{-n} (1 - \Lambda^{-1}).$$

In this finite interval we can introduce a complete basis of wave-functions in the energy space, defined as

$$\phi_{n,l}^{(+)}(\epsilon) = \sqrt{\frac{1}{L_n}} e^{i\omega_n l \epsilon},$$

where

$$\omega_n = \frac{2\pi}{L_n},$$

and l is an integer. The fermionic operators are

$$a_{n,l}^\dagger = \int_{I_n^{(+)}} d\epsilon \phi_{n,l}^{(+)}(\epsilon) c_\epsilon^\dagger. \quad (4.4)$$

Analogously, within the interval $I_n^{(-)}$ of negative energies, we define the wave-functions

$$\phi_{n,l}^{(-)}(\epsilon) = \sqrt{\frac{1}{L_n}} e^{-i\omega_n l \epsilon},$$

and the corresponding operators

$$b_{n,l}^\dagger = \int_{I_n^{(-)}} d\epsilon \phi_{n,l}^{(-)}(\epsilon) c_\epsilon^\dagger. \quad (4.5)$$

The conduction electron Hamiltonian in the new basis becomes

$$\mathcal{H}_0 = \int_{-1}^1 d\epsilon \epsilon c_\epsilon^\dagger c_\epsilon = \sum_n \sum_{l,l'} E_{n;l,l'} \left(a_{n,l}^\dagger a_{n,l'} - b_{n,l}^\dagger b_{n,l'} \right), \quad (4.6)$$

where

$$\begin{aligned}
E_{n;l'l'} &= \int_{I_n^{(+)}} d\epsilon \epsilon \phi_{n,l}^{(+)}(\epsilon)^* \phi_{n,l'}^{(+)}(\epsilon) \\
&= \int_{I_n^{(+)}} d\epsilon (\epsilon - E_n) \phi_{n,l}^{(+)}(\epsilon)^* \phi_{n,l'}^{(+)}(\epsilon) + E_n \delta_{ll'} \\
&= \Delta E_{n;l'l'} + E_n \delta_{ll'}.
\end{aligned}$$

In the previous formula, if we take E_n as the average energy within the interval, namely,

$$E_n = \frac{1}{2\Lambda^n} \left(1 + \frac{1}{\Lambda} \right), \quad (4.7)$$

then the off-diagonal matrix elements $\Delta E_{n;l'l'}$ vanish in the limit $\Lambda \rightarrow 1$.

The conduction electron operator which is coupled to the impurity becomes in the new basis

$$f_0^\dagger = \sqrt{\frac{1}{2}} \int_{-1}^1 d\epsilon c_\epsilon^\dagger = \sum_n \sqrt{\frac{L_n}{2}} \left(a_{n,0}^\dagger + b_{n,0}^\dagger \right), \quad (4.8)$$

namely involves only the $l = 0$ component within each interval. Therefore, neglecting the off-diagonal elements $\Delta E_{n;l'l'}$, which is rigorously true only for $\Lambda \rightarrow 1$, the $l = 0$ sector decouples from the $l \neq 0$, which remains untouched by the impurity, and one needs to solve only the following Hamiltonian, dropping the label $l = 0$ and inserting back the spin index,

$$\begin{aligned}
\mathcal{H}_{AIM} &= \sum_{n\sigma} E_n \left(a_{n\sigma}^\dagger a_{n\sigma} - b_{n\sigma}^\dagger b_{n\sigma} \right) \\
&+ V \sum_{n\sigma} \sqrt{\frac{L_n}{2}} \left[\left(a_{n\sigma}^\dagger + b_{n\sigma}^\dagger \right) d_\sigma^\dagger + H.c. \right] + \mathcal{H}_{int} \left[d^\dagger, d \right].
\end{aligned} \quad (4.9)$$

Starting by this Hamiltonian with a logarithmic discretization of the energy, we can apply the previously discussed Lanczos algorithm to obtain the tight-binding Hamiltonian

$$\mathcal{H}_{AIM} = \sum_{n \geq 0} \sum_{\sigma} t_n \left(f_{n\sigma}^\dagger f_{n+1\sigma} + H.c. \right) + V \sum_{\sigma} \left(f_{\sigma}^\dagger d_{\sigma} + H.c. \right) + \mathcal{H}_{int} \left[d^\dagger, d \right]. \quad (4.10)$$

Wilson showed that the hopping matrix elements have the expression

$$t_n = \frac{1}{2} (1 + \Lambda^{-1}) \Lambda^{-n/2} \frac{1 - \Lambda^{-n-1}}{\sqrt{(1 - \Lambda^{-2n-3})(1 - \Lambda^{-2n-1})}} = \frac{1}{2} (1 + \Lambda^{-1}) \Lambda^{-n/2} \zeta_n, \quad (4.11)$$

where ζ_n fastly approaches 1, so that in the following we take it to be strictly unity. We notice that, thanks to the logarithmic mesh, the hopping decays exponentially with the chain-length, unlike the uniform mesh in which the hopping saturates to a constant value.

Let us define a set of Hamiltonians

$$\mathcal{H}_N = \Lambda^{(N-1)/2} \left\{ \sum_{n=0}^{N-1} \sum_{\sigma} t_n \left(f_{n\sigma}^{\dagger} f_{n+1\sigma} + H.c. \right) + V \sum_{\sigma} \left(f_{\sigma}^{\dagger} d_{\sigma} + H.c. \right) + \mathcal{H}_{int} [d^{\dagger}, d] \right\}. \quad (4.12)$$

The pre-factor has the effect of making the lowest hopping $\Lambda^{(N-1)/2} t_{N-1}$ of order one. Clearly

$$\mathcal{H}_{AIM} = \lim_{N \rightarrow \infty} \Lambda^{-(N-1)/2} \mathcal{H}_N.$$

These Hamiltonians satisfy the recursion formula:

$$\mathcal{H}_{N+1} = \Lambda^{1/2} \mathcal{H}_N + \frac{1}{2} (1 + \Lambda^{-1}) \sum_{\sigma} \left(f_{N\sigma}^{\dagger} f_{N+1\sigma} + H.c. \right). \quad (4.13)$$

We know that the Kondo temperature is exponentially small at large U/Γ . Therefore, in order to describe correctly the low temperature physics, one would need to go to an exponentially small $T \ll T_K$. In this case, finite-size effects in any physical observable should become negligible only when the typical level spacing Δ becomes smaller than T . In the uniform mesh, $\Delta \sim \pi/N$, where N is the chain length, hence we would need an exponentially large size to access the low temperature properties. On the contrary, thanks to the logarithmic mesh, a chain with $N \gg \ln(1/T)/\ln \Lambda$ is already sufficient. However it is practically impossible to diagonalize completely the Hamiltonian but for the first few N 's. We notice that, after the rescaling by the factor $\Lambda^{1/2}$, typical Λ being $3 \div 5$, the spectrum of \mathcal{H}_N generally contains a bunch of eigenstates with eigenvalues ≤ 1 , separated by a gap from states with higher energies ≥ 10 . The hopping to site $N + 1$ will have negligible effects on the high energy states, so that one can truncate the Hilbert space of the chain with N -site, by keeping only the low energy eigenstates, combine them with the states of the site $N + 1$ and diagonalize \mathcal{H}_{N+1} in this reduced Hilbert space. This procedure is iterated to larger chain sizes, until the recursion formula (4.13) flows to a fixed point Hamiltonian \mathcal{H}_* . Indeed (4.13) describes a renormalization group (RG) transformation, which can be shortly written as

$$\mathcal{H}_{N+1} = T[\mathcal{H}_N], \quad (4.14)$$

In reality it is more appropriate to define the RG transformation within chains of the same parity, namely

$$\mathcal{H}_N = T^2[\mathcal{H}_{N-2}]. \quad (4.15)$$

As N increases the RG transformation flows to a fixed point defined by

$$\mathcal{H}_* = T^2[\mathcal{H}_*]. \quad (4.16)$$

By analysing the spectrum of the fixed point one should be able to identify \mathcal{H}_* . Once this is done, one may perturb $\mathcal{H}_* \rightarrow \mathcal{H}_* + \delta\mathcal{H}_*$, with $\delta\mathcal{H}_*$ limited to the first few sites, and by iterating again the RG procedure, one can determine all scaling operators and their eigenvalues. In most common cases this programme can be actually carried out, but there are situations in which the model flows to non trivial fixed points which require a more sophisticated analysis.

4.2.1 The simplest example: the single-channel Kondo effect

Just as an example, let us discuss how the Numerical Renormalization Group (NRG) works for a single-orbital AIM in the large- U Kondo-regime. At the beginning it is convenient to consider the model in the absence of the impurity, which, as we discussed, is equivalent to a tight-binding model on a semi-infinite chain. At particle-hole symmetry, the number of electrons is equal to the number of sites. For a finite chain of N sites, the appropriate Bloch waves with open boundaries at site $r = 1$ and $r = N$ are of the form $\sin kr$ with

$$k = \frac{\pi}{N+1} n,$$

with $n > 0$ an integer. The single-particle spectrum near the Fermi energy can be linearized, leading to

$$\epsilon_k \simeq \epsilon_F + v_F k = \epsilon_F + v_F \frac{\pi}{N+1} n,$$

and consists of equally spaced levels, with spacing $\Delta = v_F \pi / (N+1)$. The same property holds also for the full multi-particle spectrum. Since the number of electrons is equal to the number of sites, the chains with an even number of sites is obtained by filling with two electrons the lowest $N/2$ levels. The ground state is therefore non-degenerate and is followed by equally spaced excited states. If the number of sites is odd, the ground state is obtained by doubly occupying the lowest $(N-1)/2$ states, and occupying with a single electron the $(N+1)/2$ level. Since this can be done in two different ways, according to the spin of the electron, the ground state has spin $1/2$, namely is doubly degenerate. If, instead of fixing the number of electrons, we keep the chemical potential fixed such that, on average, the number of electrons is equal to the number of sites, then, in the case of even chains, the chemical potential lies in the middle of two consecutive single-particle levels, while, for odd chains, it coincides with a single-particle level. In the latter case, the ground state turns out to be fourfold degenerate, since there are four equally probable states available on the level right at the chemical potential, empty, singly occupied by a spin up electron, singly occupied by a spin down electron, or doubly occupied.

We know that the Kondo effect is identified by a phase shift $\delta_\sigma = \pi/2$ for each spin-channel σ . By the Friedel's sum rule the variation of the electron number at fixed chemical potential is

$$\Delta N_{els} = \frac{1}{\pi} (\delta_\uparrow + \delta_\downarrow) = 1.$$

This implies that the ground state of a chain with N sites has now to accommodate $N+1$ electrons, hence that an even chain will eventually develop a fourfold degenerate state, while an odd chain a non-degenerate one. In other words the NRG flow for even N ,

$$\mathcal{H}_N = T^2 [\mathcal{H}_{N-2}], \tag{4.17}$$

will start from the spectrum of an even chain and flow to the spectrum of an odd chain. Viceversa for odd N 's. This flow is the clear signal of a $\pi/2$ phase-shift typical of the Kondo effect.

In conclusion, the fixed point Hamiltonian still describes a tight-binding semi-infinite chain with equally spaced levels, the impurity being absorbed by the conduction sea into a simple change of boundary conditions. For what concerns the leading scaling operators, the only perturbing terms compatible with particle-hole symmetry are a variation of the first hopping matrix element, $t_0 \rightarrow t_0 + \delta t_0$, and a local interaction term $\delta U f_{0\uparrow}^\dagger f_{0\downarrow}^\dagger f_{0\downarrow} f_{0\uparrow}$.

4.3 Conformal Field Theory applied to impurity models

We have previously shown that an impurity model in any dimension is, for what it concerns the low energy properties, effectively equivalent to a model of electrons hopping with a constant matrix element on a semi-infinite chain, with the impurity sitting at the edge. We also know that one-dimensional gapless fermions have very peculiar features. In particular, the continuum of particle-hole excitations in one-dimension is exhausted by collective acoustic modes, the zero sounds. This property, which holds even if the electrons are interacting, provided the interaction does not open a gap in the spectrum, is the basis of the so-called **Bosonization technique**, which allows to map the gapless fermionic model into a critical quantum field theory, which corresponds to a 1 + 1 dimensional Conformal Field Theory (CFT). In reality, if the electrons are interacting, the proper mapping is into a set of CFT's that reflect the overall symmetry of the Hamiltonian, which is generally lower if interaction is present. For instance, in a single band spin-isotropic model, one has to introduce a CFT that takes care of the charge degrees of freedom, and a non-abelian CFT to describe the $SU(2)$ spin sector, the well-known spin-charge separation which occurs in one dimension. This procedure, which is called *conformal embedding*, can be rigorously carried out by comparing, in the absence of interaction, the partition functions in the different representations.

In the specific example of impurity models, the conduction electrons are assumed to be non-interacting, hence by construction the fermionic model is massless and should be representable in terms of a CFT. Indeed, since the chain is semi-infinite, it actually maps into a CFT with an appropriate conformally invariant boundary condition (BC) at the edge. A single impurity obviously can not induce any bulk gap so that, even in its presence, the model should still correspond to a CFT with the same number of massless degrees of freedom, namely the same central charge c . Moreover, the impurity can not even change the sound velocity, in this non interacting case simply the Fermi velocity, since the latter is also a bulk property. The only thing that may change are the BC's, which still have to be conformally invariant. The change of boundary conditions has two effects. First it modifies the fine structure of the low-energy spectrum, namely the sequence and degeneracy of levels at finite but long chain-length. In addition, it may change the scaling properties of boundary operators. Both effects can be computed exactly by CFT once the new boundary conditions are known, and compared directly with NRG results.

This procedure encounters two main difficulties. The first is that the actual symmetry in

the presence of the impurity is generally lower than the large symmetry of the free conduction bath. This implies that one has to identify the proper conformal embedding, which in some cases may not be simple to uncover. The second difficulty is to determine the conformally invariant BC's that are compatible with the embedding. This is accomplished by the so-called *fusion hypothesis*, according to which conformally invariant BC's can be obtained by *fusing* the spectrum of a known BC with the primary fields, which are the scaling operators of the theory. By *fusion* one means the product of two primary fields, which yields a combination of primary fields according to some specific rules, called *fusion rules*. In principle, if we were able to classify all allowed BC's, by comparing their CFT spectra with the NRG results we could identify which BC is actually realized.

We do not aim to give here a detailed introduction to CFT, but just want to show in some non-trivial cases how it works. If readers desire to acquire a deeper knowledge, a useful textbook is *Conformal Field Theory*, by P. Di Francesco, P. Mathieu and D. Senechal, hereafter denoted as DMS book.

4.3.1 Some simple CFT results

We know that the first step of Bosonization in one-dimension is the linearization of the free-electron spectrum around the Fermi momentum. This linearization is not expected to affect the low energy behavior provided the perturbations are weak compared to the band-width. Therefore let us consider, instead of a tight-binding model, free spinless Dirac fermions, which have indeed a linear spectrum, on a chain of length L with anti-periodic boundary conditions. We will consider Dirac fermions moving only in one direction, namely with a single chirality, because this is the case relevant to a semi-infinite chain. Indeed, as we have seen, the wave-functions with negative momenta of a semi-infinite chain are not independent from those with positive momenta.

The single-particle wave-functions for a chiral Dirac fermion are plane waves with momentum

$$k = \frac{\pi}{L} (2n - 1),$$

with integer n . The Hamiltonian in momentum space reads

$$\mathcal{H} = v_F \sum_k k c_k^\dagger c_k, \quad (4.18)$$

where v_F has to be identified with the Fermi velocity of the original tight-binding model. Let us define for positive k

$$\begin{aligned} a_k &= c_k, \\ b_k &= c_{-k}^\dagger, \end{aligned}$$

so that, apart from an actually infinite constant, the Hamiltonian becomes

$$\mathcal{H} = v_F \sum_{k>0} k \left(a_k^\dagger a_k + b_k^\dagger b_k \right). \quad (4.19)$$

The partition function at temperature T is simply

$$Z_{Dirac} = \prod_{k>0} \left[1 + \exp(-\beta v_F k) \right]^2 = \prod_{n \geq 1} \left(1 + q^{n-1/2} \right), \quad (4.20)$$

where conventionally q is defined as

$$q = \exp\left(-\beta \frac{2\pi}{L}\right) \equiv e^{2\pi i\tau}.$$

One can show that

$$Z_{Dirac}(q) = \frac{\theta_3(q)}{\phi(q)}, \quad (4.21)$$

where θ_3 is the third Jacobi theta-function

$$\theta_3(q) = \sum_{n=-\infty}^{\infty} q^{n^2/2},$$

and ϕ the Euler function

$$\phi(q) = \prod_{n \geq 1} (1 - q^n).$$

On the other hand, we know by Bosonization that, if we define for positive $p = 2\pi n/L$ the operators

$$b_p = -i\sqrt{\frac{2\pi}{pL}} \rho(p) = -i\sqrt{\frac{2\pi}{pL}} \sum_k c_k^\dagger c_{k+p}, \quad b_p^\dagger = i\sqrt{\frac{2\pi}{pL}} \rho(-p),$$

they satisfy bosonic commutation relations. In addition their equation of motion can be reproduced by the Hamiltonian

$$\mathcal{H} = \frac{\pi v_F}{L} \sum_p \rho(p) \rho(-p) = v_F \sum_{p>0} p b_p^\dagger b_p + \frac{\pi v_F}{L} \Delta N^2, \quad (4.22)$$

where we assumed that $\rho(p=0)$ is the variation ΔN of the electron number with respect to a reference value. The partition function of this bosonic model is the product of the bosonic term

$$\prod_{p>0} [1 - \exp(-\beta v_F p)]^{-1} = \prod_{n>0} (1 - q^n)^{-1} = \phi(q)^{-1}$$

plus the contribution of the ΔN which is simply, assuming an infinite reference number,

$$\sum_{n=-\infty}^{\infty} \exp\left(-\beta \frac{v_F \pi}{L} n^2\right) = \sum_{n=-\infty}^{\infty} q^{n^2/2} = \theta_3(q).$$

We immediately recognize that the bosonic partition function does coincide with the fermionic one.

We can proceed further on, and consider spinful Dirac fermions. Obviously the partition function is the square of Z_{Dirac} in Eq. (4.21). However, we would like to consider a perturbation which only preserves independently the spin $SU(2)$ symmetry and the charge isospin $SU(2)$, defined through the generators \mathbf{I} , which are the $q = 0$ components of the so-called isospin current operators

$$\begin{aligned} I_z(q) &= \frac{1}{2} \sum_{k\sigma} \left(c_{k\sigma}^\dagger c_{k+q\sigma} - \delta_{q0} \right), \\ I^+(q) &= \sum_k c_{k\uparrow}^\dagger c_{-k-q\downarrow}^\dagger, \\ I^-(q) &= \left(I^+ \right)^\dagger. \end{aligned}$$

The spin $SU(2)$ current operators are instead

$$\mathbf{S}(q) = \frac{1}{2} \sum_{k\alpha\beta} c_{k\alpha}^\dagger \boldsymbol{\sigma}_{\alpha\beta} c_{k+q\beta}, \quad (4.23)$$

where $\boldsymbol{\sigma}$ are the Pauli matrices. In real space these current operators, $J_a = I_a, S_a$, satisfy the commutation relations

$$\left[J_a(x), J_b(y) \right] = i\epsilon_{abc} \delta(x-y) J_c(x) - ik \frac{1}{4\pi} \delta_{ab} \frac{\partial \delta(x-y)}{\partial x},$$

with $k = 1$. For generic $k \geq 1$, the above commutation relations identify an $SU(2)_k$ CFT, where the label k may be regarded as the number of channels which are used to build up the generators. In general, an $SU(2)_k$ CFT has primary fields $\phi_{2j}^{(k)}$ with spin quantum numbers j , such that $2j = 0, 1, \dots, k$. Their scaling dimension is $x_j = j(j+1)/(k+2)$. The product of two primary fields with spin j and j' yields all primary fields with spin between $|j-j'|$ and $\min(k-j-j', j+j')$. The Hilbert space of the theory is obtained by applying the primary fields on the reference vacuum state and, from this ancestor state, by generating all descendent states applying the current operators with $q < 0$. This is what is called a *conformal tower*. The energy difference between the descendent states and their ancestor is an integer multiple of

the fundamental level spacing. The character $\chi_{2j}^{(k)}$ represents the contribution to the partition function of the conformal tower generated by the primary field $\phi_{2j}^{(k)}$.

This construction may look abstruse but actually has a simple physical interpretation. Let us consider again a single spinful fermion, $k = 1$. Let us further assume that on average the number of electrons is equal to the number of sites, and the latter is even. In this case the ground state is obtained by filling with two electrons of opposite spin all single-particle states below the chemical potential, which lies in the middle of two consecutive single-particle levels, which, we recall, are separated by the fundamental spacing Δ , from now on our energy unit. With this definition, the Hilbert space can be constructed as follows. One can start from the vacuum and act on it with particle-hole excitations, namely with $I_z(q)$ or $\mathbf{J}(q)$ with $q < 0$. In addition one can apply the operators $I^+(q)$ or $I^-(q)$, again with $q < 0$, to change by an even multiple the number of electrons, and then consider all particle-hole excitations on top of these states. In this way we obtain all states which have even number of electrons, like the vacuum state. This is nothing but the conformal tower obtained by the ancestor fields $\chi_0^{(1)}$ in both the charge and spin $SU(2)_1$ sectors, which should contribute to the partition function with the product of characters $\left(\chi_0^{(1)}\right)_{charge} \left(\chi_0^{(1)}\right)_{spin}$.

The rest of the Hilbert space includes all states with odd number of electrons. Since a single electron carries isospin and spin 1/2, all these states have half-odd integer values of I_z and S_z . One realizes that all they can be obtained by applying the product of the isospin and spin primary fields $\phi_{1charge}^{(1)} \times \phi_{1spin}^{(1)}$, which is nothing but the single electron operator, and construct out of it all descendent states. Their contribution to the partition function should then be $\left(\chi_1^{(1)}\right)_{charge} \left(\chi_1^{(1)}\right)_{spin}$. The expression of the $SU(2)_k$ characters, cfr. DMS book page 586, is

$$\chi_l^{(k)}(q) = \frac{1}{\eta(q)^3} \sum_{n=-\infty}^{\infty} \left[2n(k+2) + l + 1 \right] q^{(2n(k+2)+l+1)^2/4(k+2)},$$

where

$$\eta(q) = q^{1/24} \phi(q),$$

is the Dedekind function. In the specific case of $k = 1$,

$$\begin{aligned} \chi_0^{(1)}(q) &= \sqrt{\frac{\theta_3(q)^2 + \theta_4(q)^2}{2\eta(q)^2}}, \\ \chi_1^{(1)}(q) &= \sqrt{\frac{\theta_3(q)^2 - \theta_4(q)^2}{2\eta(q)^2}}, \end{aligned}$$

where

$$\theta_4(q) = \sum_{n=-\infty}^{\infty} (-1)^n q^{n^2/2},$$

is the fourth Jacobi theta-function. Hence we find that

$$\left(\chi_0^{(1)}\right)_{charge} \left(\chi_0^{(1)}\right)_{spin} + \left(\chi_1^{(1)}\right)_{charge} \left(\chi_1^{(1)}\right)_{spin} = \frac{\theta_3(q)^2}{\eta(q)^2} = q^{-1/12} Z_{Dirac}(q)^2, \quad (4.24)$$

which, apart from the vacuum polarization contribution $q^{-1/12}$ is exactly the partition function of two species of Dirac fermions. The spectrum, and correspondingly the partition function, can be represented as in Table 4.1. In that Table we identify each conformal tower by the quantum

I	S	x
0	0	0
1/2	1/2	1/2

Table 4.1: The spectrum of spinful electrons when the ground state contains an even number of particles

numbers of the primary fields which generate the ancestor states. x is energy in units of the fundamental level spacing Δ of the ancestor state with respect to the chemical potential. The descendent levels of an ancestor have energies $x + n$, with n a positive integer. Notice that an important consequence of conformal invariance is that the energy of each state in units of Δ coincide with the scaling dimension of the operator which, applied to the vacuum, yields that state. In particular the single electron excitation has energy $x = 1/2$, $1/4$ from the spin $S = 1/2$ and $1/4$ from the isospin $I = 1/2$ primary fields, because the chemical potentials lies in the middle between two consecutive levels.

Following the same reasoning, one can easily show that the table of the energy spectrum in the case of odd chains at half-filling is the one of Table 4.2. As discussed before the ground state

I	S	$x - 1/4$
1/2	0	0
0	1/2	0

Table 4.2: The spectrum of spinful electrons when the ground state contains an odd number of particles

is indeed fourfold degenerate, the chemical potential coinciding with a single-particle level.

Following the *fusion hypothesis*, the Kondo fixed point should be obtained by fusing the spectrum in the absence of the impurity with a primary field of the embedded theory. Since, in the large U -limit, the Kondo exchange only involves the spin $SU(2)_1$ degrees of freedom, and since, apart from the identity $S = 0$, the only primary field has $S = 1/2$, we would predict that, upon fusion with the latter, the Kondo fixed point should be reproduced. This is actually

the case. Indeed, if we fuse the spectrum of even chains with the spin field $\phi_1^{(1)}$ we do get the spectrum of odd chains, and viceversa. CFT also tells us that, in order to identify the local scaling operators, we have to double fuse the starting spectrum. Each row of the resulting table corresponds to a local scaling operator, whose dimension is the sum of the dimensions of each primary field involved. Descendent operators have dimensions which increase by unity. An operator is relevant if its dimension is < 1 , marginal if it is exactly 1, and irrelevant otherwise. In the single-channel example, if, for instance, we double fuse the even chain spectrum, we obtain it back. This implies that the lowest dimension operators allowed by symmetry are scalar products of current operators with dimension 2, hence they are irrelevant.

The two channel model

Since it will be important for what follows, let us conclude by considering the case of two channels of spinful fermions. The partition function is the square of the partition function (4.24) of a single channel, and can be written for even chains as

$$Z = \sum_{n_1, n_2=0,1} \left(\chi_{n_1}^{(1)} \chi_{n_2}^{(1)} \right)_{charge} \left(\chi_{n_1}^{(1)} \chi_{n_2}^{(1)} \right)_{spin}, \quad (4.25)$$

where n_1 refers to channel 1 and n_2 to channel 2. For odd chains one readily finds that

$$Z = \sum_{n_1, n_2=0,1} \left(\chi_{n_1}^{(1)} \chi_{n_2}^{(1)} \right)_{charge} \left(\chi_{1-n_1}^{(1)} \chi_{1-n_2}^{(1)} \right)_{spin}. \quad (4.26)$$

These expressions manifestly show that the free two-channel conduction electrons are invariant under independently spin or isospin $SU(2)$ transformations for each channel, namely under a large symmetry $SU(2) \times SU(2) \times SU(2) \times SU(2)$.

Let us suppose that the impurity couples only to the spin-current operators in such a way that only the overall $SU(2)$ symmetry is preserved. Therefore, while the charge degrees of freedom can still be represented by two $SU(2)_1$ CFT's, the appropriate conformal embedding for the spin sectors should involve an $SU(2)_2$ CFT, since the total spin current is made up of two channels, times the coset CFT, namely

$$SU(2)_1 \times SU(2)_1 \rightarrow SU(2)_2 \times \frac{SU(2)_1 \times SU(2)_1}{SU(2)_2}.$$

Since the central charge is conserved and each $SU(2)_k$ has a central charge $3k/(k+2)$, the coset theory should have $c = 1/2$, namely the central charge of an Ising CFT. This can be proved rigorously by the character decomposition.

The Ising CFT has three primary fields, the identity I , with dimension 0, the energy field ϵ , with dimension $1/2$, and the spin field σ with dimension $1/16$. The fusion rules are, see DMS

book,

$$I \times I = I, \quad \epsilon \times \epsilon = \epsilon, \quad \sigma \times \sigma = I + \epsilon, \quad I \times \epsilon = \epsilon, \quad I \times \sigma = \sigma, \quad \epsilon \times \sigma = \sigma.$$

The characters χ_x^I , where x is the dimension of the primary field, are explicitly given by (all functions are assumed to depend on the variable q , even when not indicated)

$$\begin{aligned} \chi_0^I &= \frac{1}{2} \left[\sqrt{\frac{\theta_3}{\eta}} + \sqrt{\frac{\theta_4}{\eta}} \right], \\ \chi_{1/2}^I &= \frac{1}{2} \left[\sqrt{\frac{\theta_3}{\eta}} - \sqrt{\frac{\theta_4}{\eta}} \right], \\ \chi_{1/16}^I &= \sqrt{\frac{1}{2}} \sqrt{\frac{\theta_2}{\eta}}, \end{aligned}$$

where the second Jacobi function is defined by

$$\theta_2 = \sum_{n=-\infty}^{\infty} q^{(n-1/2)^2/2}.$$

One can show that the product of characters of two $SU(2)_1$ CFTs, $\chi_{2j}^{(1)} \chi_{2j'}^{(1)}$, can be related to the product of characters of an $SU(2)_2$ and an Ising CFTs, $\chi_{2l}^{(2)} \chi_x^I$, by

$$\begin{aligned} \chi_0^{(1)} \chi_0^{(1)} &= \chi_0^{(2)} \chi_0^I + \chi_2^{(2)} \chi_{1/2}^I, \\ \chi_0^{(1)} \chi_1^{(1)} &= \chi_1^{(1)} \chi_0^{(1)} = \chi_1^{(2)} \chi_{1/16}^I, \\ \chi_1^{(1)} \chi_1^{(1)} &= \chi_0^{(2)} \chi_{1/2}^I + \chi_2^{(2)} \chi_0^I. \end{aligned}$$

By means of the above decomposition one can write the tables of the spectra for even and odd chains, as given in Table 4.3. By these tables we can easily realize the spectrum of even chains can be turned into that of odd chains, and viceversa, either by fusion with the $SU(2)_2$ primary field of spin 1, or by fusion with the Ising field ϵ .

I_1	I_2	S	$Ising$	x
0	0	0	0	0
0	0	1	1/2	1
1	0	1/2	1/16	1/2
0	1	1/2	1/16	1/2
1	1	0	1/2	1
1	1	1	0	1

I_1	I_2	S	$Ising$	$x - 1/2$
0	0	0	1/2	0
0	0	1	0	0
1	0	1/2	1/16	0
0	1	1/2	1/16	0
1	1	0	0	0
1	1	1	1/2	1

Table 4.3: The spectra of two channels on even chains, right table, and odd chains, left table. I_1 and I_2 are the values of the isospins of each channel, S the value of the total spin and $Ising$ refers to the Ising primary fields.

Chapter 5

The fate of the Kondo effect in impurity clusters and speculations on cluster DMFT

In the previous sections we have discussed quite in detail the physics of a single-orbital Anderson impurity model in connection with DMFT. We have seen that already the simple single-site formulation of DMFT provides interesting results about the Mott transition. Most notably, we have shown that DMFT predicts this transition to occur by the gradual narrowing and disappearing of a quasiparticle peak within well preformed Mott-Hubbard side-bands. This behavior implies for instance that the effective impurity model used to solve the lattice problem is well inside the Kondo regime before the MIT, with a Kondo temperature approaching zero right at the transition.

As we discussed in the Introduction, we expect that new physics emerges when we move to cluster DMFT in order to account for short-range spatial correlations. How does this new physics translates in the corresponding impurity clusters? In the case of the single-site DMFT all the physics was exhausted by knowing whether, after self-consistency, in the effective impurity model Kondo effect takes place or does not. If the self-consistent hybridization function is finite around the chemical potential, the impurity is Kondo-screened, which translates into a Landau-Fermi liquid behavior of the lattice model. On the contrary, if the self-consistent hybridization function develops a gap at the chemical potential, the impurity stays unscreened and the lattice model is insulating. However, an insulator with unscreened local moments is a poor description of a Mott insulator, which may be appropriate only at high temperature. At low temperature, inter-site exchange processes come always into play and provide a screening mechanism within the insulating phase. These processes are not well described within the single-site DMFT, which motivates its extension to cluster-DMFT.

Let us consider therefore a typical cluster of impurities that would represent a lattice model

within cluster-DMFT. Each impurity, besides being hybridized with the conduction bath, is also coupled to the other impurities, generally by a single-particle hopping. Since we still expect the Mott transition to occur when the impurities are well inside the Kondo regime, we can equally well consider a cluster of impurity-spins that are Kondo coupled by an exchange J_K to a conduction bath and, in addition, coupled among themselves by an exchange J , generally antiferromagnetic. In this situation new possibilities arise. If $J_K \gg J$, conventional Kondo screening occurs and the lattice model should be metallic with well defined Landau's quasiparticles. On the contrary, if $J \gg J_K$, the impurities strongly bound together into an overall singlet configuration, if their number is even, in which case no Kondo screening is needed anymore, or, if their number is odd, into a spin-1/2 configuration, in which case a partial Kondo screening can still take place. We will argue that, in both situations, the impurity behavior is not at all trivial. For instance, the impurity spectral function contains, besides the Hubbard side-bands, a low energy incoherent feature which displays either a deep or a singularity right at the chemical potential. When full self-consistency is carried out, two possibilities may arise. The first and boring one is that the insulating phase occupies the whole $J > J_K$ region. This would mean that the incoherent feature is not self-consistent in the DMFT scheme and would likely imply a first order phase transition from the metal to the Mott insulator. The second and more intriguing scenario is that the incoherent feature survives DMFT self-consistency, leading to a strange metallic behavior near the MIT. If this were the case, then we should also expect a transition in the metallic phase from a conventional Fermi-liquid metal, at $J_K \gg J$, into a less conventional metal at $J \gg J_K$.

One may immediately realize that this is the *impurity* analogue of what we discussed in the Introduction about a realistic MIT. Actually, the competition we envisaged between the effective quasiparticle Fermi temperature T_F^* and the energy scale J , that identifies the strength of the terms which quench the residual entropy of the ideal Mott insulator, has its counterpart into the competition between the Kondo temperature and the inter-impurity exchange in impurity clusters. Indeed, the Kondo energy gain is related to the impurity coherently tunneling among all degenerate configurations, and it is greater the more degenerate the impurity ground state is. The inter-impurity exchange instead splits this degeneracy, hence competes against Kondo screening. It turns out that this competition may lead to an unstable fixed point, which separates the Kondo screened phase from the unscreened one. The occurrence of this critical point might actually be the signal that, within cluster-DMFT, the Fermi-liquid metal does encounter an instability before the MIT takes place, as we discussed previously.

Let us speculate a bit more on this hypothesis. Let us suppose, as we will demonstrate in several examples, that, in an impurity cluster, the Kondo screened phase is indeed separated from the unscreened one by an unstable fixed point. The latter will be necessarily characterized by several instability channels, namely by several relevant operators of dimension smaller than one. In turns, this would correspond to singular, if the dimension is smaller than 1/2, or otherwise strongly enhanced impurity contribution to the susceptibilities in the corresponding channels, which also means strongly enhanced irreducible vertices at the impurity site. As we

have learned, the lattice irreducible vertices in DMFT are local and coincide with the impurity ones. Therefore, if these vertices are inserted into the Bethe-Salpeter equation for the lattice susceptibilities, it is reasonable to expect that the impurity instability will turn into a true bulk instability of the lattice model, leading to a symmetry breaking in the dominant channel. This is the channel in which the enhanced irreducible vertex and the Green's function bubble cooperate at most to a bulk instability. Obviously, this instability will affect a whole region around the impurity unstable fixed point, leading to a symmetry broken phase before the MIT takes place. In most cases, however, the cluster of impurities contains by construction small terms which are nevertheless relevant at the unstable fixed point. As a result, the phase transition through the unstable fixed point would turn into a crossover. Yet, if this crossover is sharp, we should still expect that an instability arises when DMFT self-consistency is carried out.

At this stage what we have discussed so far is merely a conjecture but at least suggests that, just like in the single-site DMFT, the knowledge of the physical behavior of impurity clusters *per se* might be of great help to interpret cluster-DMFT results.

5.1 The impurity dimer

The first and simpler impurity cluster that one can discuss is a dimer. In particular we consider the Hamiltonian

$$\begin{aligned} \mathcal{H} = & \sum_{\mathbf{k}\sigma} \sum_{a=1}^2 \epsilon_{\mathbf{k}} c_{\mathbf{k}a\sigma}^\dagger c_{\mathbf{k}a\sigma} + \sum_{\mathbf{k}\sigma} \sum_{a=1}^2 \left(V_{\mathbf{k}} c_{\mathbf{k}a\sigma}^\dagger d_{a\sigma} + H.c. \right) \\ & + \frac{U}{2} \sum_{a=1}^2 (n_a - 1)^2 + V (n_1 - 1) (n_2 - 1) + J \mathbf{S}_1 \cdot \mathbf{S}_2. \end{aligned} \quad (5.1)$$

In this expression

$$n_a = \sum_{\sigma} d_{a\sigma}^\dagger d_{a\sigma}, \quad \mathbf{S}_a = \frac{1}{2} \sum_{\alpha\beta} d_{a\alpha}^\dagger \boldsymbol{\sigma}_{\alpha\beta} d_{a\beta},$$

where $\boldsymbol{\sigma}$ are the Pauli matrices. The Hamiltonian describes two impurities, each one hybridized with its own bath, and coupled together by a charge repulsion term $V > 0$ and by an antiferromagnetic exchange $J > 0$. For simplicity we assume the two conduction baths degenerate and particle-hole symmetric. This implies that both the orbital and the particle-hole symmetries remain, even in the presence of the impurities.

5.1.1 The isolated impurities

Let us start by considering the case of an isolated dimer, i.e. $V_{\mathbf{k}} = 0$. As we will assume always a large U , the ground state of the two impurities in the absence of hybridization lies in the

two-electron sector, which contains six states. It is convenient to introduce pseudo-spin-1/2 operators even in the orbital sector, so that

$$T_z = \frac{1}{2} \sum_{\sigma} (n_{1\sigma} - n_{2\sigma}), \quad T^+ = \sum_{\sigma} d_{1\sigma}^{\dagger} d_{2\sigma}, \quad T^- = \sum_{\sigma} d_{2\sigma}^{\dagger} d_{1\sigma}.$$

Among the six two-particle states, there is a spin-triplet with quantum numbers $S = 1$ and $T = 0$, and energy

$$E(S = 1, T = 0) = V + \frac{J}{4}.$$

The other three states are spin-singlets but form an orbital-triplet, $T = 1$. In particular the states with different $T_z = -1, 0, 1$ are

$$\begin{aligned} |T_z = -1\rangle &= d_{2\uparrow}^{\dagger} d_{2\downarrow}^{\dagger} |0\rangle, \\ |T_z = 0\rangle &= \sqrt{\frac{1}{2}} \left(d_{1\uparrow}^{\dagger} d_{2\downarrow}^{\dagger} + d_{2\uparrow}^{\dagger} d_{1\downarrow}^{\dagger} \right) |0\rangle, \\ |T_z = +1\rangle &= d_{1\uparrow}^{\dagger} d_{1\downarrow}^{\dagger} |0\rangle. \end{aligned}$$

However the interaction lowers the pseudo-spin $SU(2)$ down to $O(2)$, so that the two states with $T = 1$ but $T_z = \pm 1$ are still degenerate, with energy

$$E(S = 0, T = 1, T_z = \pm 1) = U,$$

but the state with $T_z = 0$ has a different energy

$$E(S = 0, T = 1, T_z = 0) = V - \frac{3}{4} J.$$

Provided $V < U + 3J/4$, which is a reasonable assumption, the lowest energy state of the isolated dimer is the spin-singlet with $T_z = 0$, namely the intersite singlet. The next lowest energy state will be the doublet of singlets if $V > U - J/4$, and the spin-triplet otherwise.

Since an incoming pair of electrons has the same quantum numbers of the two electron states, we can define by symmetry three particle-particle scattering vertices, in the triplet channel, Γ^1 , in the singlet channels with $T_z = \pm 1$, Γ_{\pm}^0 , and finally in the singlet channel with $T_z = 0$, Γ_0^0 . Their bare values are

$$\begin{aligned} \Gamma^1 &= V + \frac{1}{4} J, \\ \Gamma_{\pm}^0 &= U, \\ \Gamma_0^0 &= V - \frac{3}{4} J. \end{aligned} \tag{5.2}$$

Notice that the bare Γ_0^0 is attractive only if $V < 3J/4$.

5.1.2 The breakdown of perturbation theory

In the opposite limit of very weak U , J and V , one can do perturbation theory on the non-interacting state, which simply represents two uncoupled resonant level models. As we know, each bath acquires a phase shift $\pi/2$ per spin. Moreover we also know that, at weak coupling, this result does not change. Rather, we have shown that, provided perturbation theory does not break down, the $\pi/2$ phase shift persists up to $U \rightarrow \infty$ in the model with particle-hole symmetry. However, as U increases, the width of the resonance, which is also the Kondo temperature, diminishes and becomes exponentially small for large U . The question is whether perturbation theory actually works for any U or it breaks down at some critical value.

We notice that, if T_K becomes much smaller than the energy gap which separates the ground state of the dimer from the first excited one, the impurities lock into the $T_z = 0$ spin-singlet state. Since this state is non-degenerate, the dimer becomes invisible to the conduction electrons, no Kondo effect is needed anymore. This implies that for very large U , when T_K is very small, the actual phase shift of the conduction channels should be $\delta = 0$. This immediately suggests that something has to occur as U increases. In particular, since $\delta = \pi/2$ and $\delta = 0$ are the only values compatible with particle-hole symmetry, the two extreme cases can not be joined continuously. In other words, a critical point should separate the $\delta = \pi/2$ Kondo screened phase from the $\delta = 0$ unscreened one. Before presenting the NRG plus CFT results, let us use the results of the previous sections to show that this breakdown is actually dramatic for what concerns the impurity.

We have shown that the conduction electron phase shift is given by

$$\delta(\epsilon) = \Im m \ln \mathcal{G}(\epsilon + i0^+), \quad (5.3)$$

where

$$\mathcal{G}(i\epsilon_n)^{-1} = i\epsilon_n + i\Gamma \text{sign}(\epsilon_n) - \Sigma(i\epsilon_n), \quad (5.4)$$

is the impurity Green's function. If we denote as

$$\Sigma'(\epsilon) = \Re e \mathcal{G}(\epsilon + i0^+), \quad \Sigma''(\epsilon) = -\Im m \mathcal{G}(\epsilon + i0^+),$$

then

$$\delta(\epsilon) = -\tan^{-1} \left(\frac{\Gamma + \Sigma''(\epsilon)}{\epsilon - \Sigma'(\epsilon)} \right). \quad (5.5)$$

It is clear from this expression that the only way to obtain a $\delta(\epsilon \rightarrow 0) = 0$ is through a $\Sigma'(\epsilon \rightarrow 0) \rightarrow -\infty$. This shows that a phase-shift $\delta = 0$ is not at all innocuous for the impurity self-energy, whose real part diverges at the chemical potential. Moreover, since the local Landau-Fermi liquid picture should still hold even if $\delta = 0$, simply because the impurity dimer has disappeared at low energy, we should expect that $\delta(\epsilon) \sim \epsilon$, which implies that $\Sigma'(\epsilon) \sim 1/\epsilon$.

Finally we notice that the impurity DOS

$$\rho(\epsilon) = \frac{1}{\pi} \frac{\Gamma + \Sigma''(\epsilon)}{[\epsilon - \Sigma'(\epsilon)]^2 + [\Gamma + \Sigma''(\epsilon)]^2} \sim \epsilon^2, \quad (5.6)$$

namely it vanishes quadratically at the chemical potential. Therefore, moving from $\delta = \pi/2$ to $\delta \rightarrow 0$, the impurity DOS goes from a Kondo-resonance behavior into a pseudo-gapped one.

5.1.3 The dimer phase diagram

The impurity model (5.1) at $V = 0$ was originally studied using NRG by B. Jones and C. Varma in the late 80's. Their results were later interpreted with CFT by I. Affleck and A. Ludwig. The same model but with $V = U$ was studied with NRG by myself and L. De Leo. Indeed, irrespectively of the value of V , provided the lowest energy state is the $T_z = 0$ singlet, the phase diagram remains the same, and is sketched in Fig. 5.1. As expected there are two stable phases,

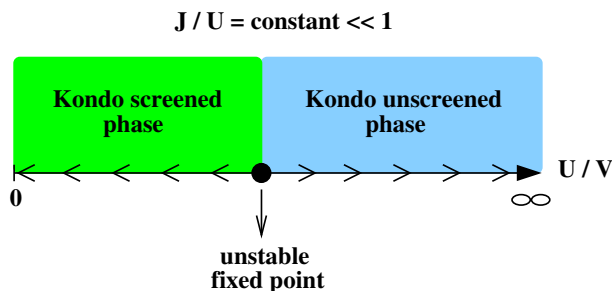


Figure 5.1: Phase diagram of (5.1) as function of U

one Kondo screened below a critical U , and one unscreened above, separated by an unstable fixed point.

CFT analysis

Affleck and Ludwig realized that the NRG spectrum of this fixed point can be reproduced within CFT by fusion of the spectra in Table 4.3 with the Ising primary field σ of dimension $1/16$. The outcome of this fusion is shown in Table 5.1. In the same Table we also list the scaling operators and their dimensions Δ . Apart from the identity, the only operator allowed by symmetry is the second, $(I_1, I_2, S, Ising) = (0, 0, 0, \epsilon)$, with dimension $1/2$. This is the operator which moves away from the fixed point. For instance, if at fixed J the transition occurs when $T_K = T_K^*$, then a change δJ will move away from the fixed point and introduce an energy scale $T_- \sim (\delta J)^{1/(1-\Delta)} = (\delta J)^2$. In order to identify the other relevant operators, we notice that, if

I_1	I_2	S	$Ising$	$x - 1/16$
0	0	0	1/16	0
1	0	1/2	0	3/8
0	1	1/2	0	3/8
0	0	1	1/16	1/2
1	1	0	1/16	1/2
1	0	1/2	1/2	7/8
0	1	1/2	1/2	7/8
1	1	1	1/16	1

I_1	I_2	S	$Ising$	Δ
0	0	0	0	0
0	0	0	1/2	1/2
0	0	1	0	1/2
1	1	0	0	1/2
1	0	1/2	1/16	1/2
0	1	1/2	1/16	1/2
0	0	1	1/2	1
1	1	0	1/2	1
1	1	1	0	1
1	1	1	1/2	3/2

Table 5.1: Left: Spectrum at the unstable fixed point of the model (5.1). Right: Scaling operators with their dimension Δ .

$\mathbf{S}_a(x)$ are the current operators of each channel, then $\mathbf{S}(x) = \mathbf{S}_1(x) + \mathbf{S}_2(x)$ is the current of the $SU(2)_2$ CFT, and

$$\mathbf{M}(x) = \mathbf{S}_1(x) - \mathbf{S}_2(x) \sim \phi_2^{(2)} \epsilon, \quad (5.7)$$

as can be easily understood by checking that both sides have the same dimension 1. This is the third operator in the table. Since it carries spin and is odd under $1 \leftrightarrow 2$, it can not appear in the theory, not only it but also all descendants. Notice that this operator is nothing but the staggered magnetization.

The fourth operator has also dimension 1/2. It is a spin singlet with $I_1 = I_2 = 1$, hence includes both an hopping term among the baths, equivalently among the impurities, namely

$$T = \sum_{\sigma} e^{i\phi} d_{1\sigma}^{\dagger} d_{2\sigma} + H.c., \quad (5.8)$$

and the particle-particle singlet operator

$$\Delta_{SC} = e^{i\phi} \left(d_{1\uparrow}^{\dagger} d_{2\downarrow}^{\dagger} + d_{2\uparrow}^{\dagger} d_{1\downarrow}^{\dagger} \right) + H.c.. \quad (5.9)$$

Again this operator is forbidden by the $O(2)$ orbital symmetry or by particle conservation, hence nor it neither its descendants can appear. The other dimension-1/2 operators correspond to single particle excitation, which does not conserve charge. All the others are marginal or irrelevant.

The relevant operators \mathbf{M} , T and Δ_{SC} have a diverging susceptibility

$$\chi(T) \sim \frac{1}{T_K} \ln \left(\frac{T_K}{T} \right).$$

Away from the fixed point this singularity is cut-off by T_- .

Additional informations can be gained through the so-called modular S -matrix, which is formally defined as follows. If $q = \exp(2i\pi\tau)$ and $\tilde{q} = \exp(2i\pi/\tau)$, then the characters χ_x , where x label primary fields, satisfy

$$\chi_x(\tilde{q}) = \sum_y S_x^y \chi_y(q). \quad (5.10)$$

The matrix elements S_x^y identify the unitary modular S -matrix, which is in general real. Suppose we start from a spectrum in which the ground state belongs to a conformal tower identified by the identity I , and assume that the actual boundary conditions are obtained by fusion with a primary field A . It has been shown in the context of boundary CFT that the ground state degeneracy g_A and residual entropy S_A with the new boundary conditions are

$$g_A = \frac{S_A^I}{S_I^I}, \quad S_A = \ln g_A. \quad (5.11)$$

Next, suppose we want to calculate in the semi-infinite chain the correlation function between an incoming and an outgoing operator, say a primary field B . This correlation function will have obviously the same asymptotic behavior in the new boundary A as in the reference one I . What changes is an overall prefactor, which is the scattering S -matrix $S_B(A|I)$ of the primary field B . It turns out that

$$S_B(A|I) = \frac{S_A^B}{S_A^I} \frac{S_I^I}{S_I^B}. \quad (5.12)$$

In particular, if B is the primary field which enters the decomposition of the single-particle operator, in the two-channel example is the Ising field σ , then the scattering matrix corresponds to the single-particle S -matrix at zero frequency.

In the case under study, the fixed point is obtained by fusion in the Ising sector whose modular S -matrix is, using the convention that it acts on the vector (I, ϵ, σ) , see DMS book page 363,

$$S = \frac{1}{2} \begin{pmatrix} 1 & 1 & \sqrt{2} \\ 1 & -1 & -\sqrt{2} \\ \sqrt{2} & -\sqrt{2} & 0 \end{pmatrix}.$$

One readily finds that the fixed point has a residual entropy $\ln \sqrt{2}$ and a vanishing single-particle S -matrix

$$S(0) = \frac{S_\sigma^\sigma}{S_\sigma^0} \frac{S_0^0}{S_0^\sigma} = 0. \quad (5.13)$$

It turns this implies, from the relation

$$S(0) = 1 - 2 \frac{\rho(0)}{\rho_0(0)},$$

that the impurity DOS at the chemical potential is exactly half of its value in the Kondo screened phase.

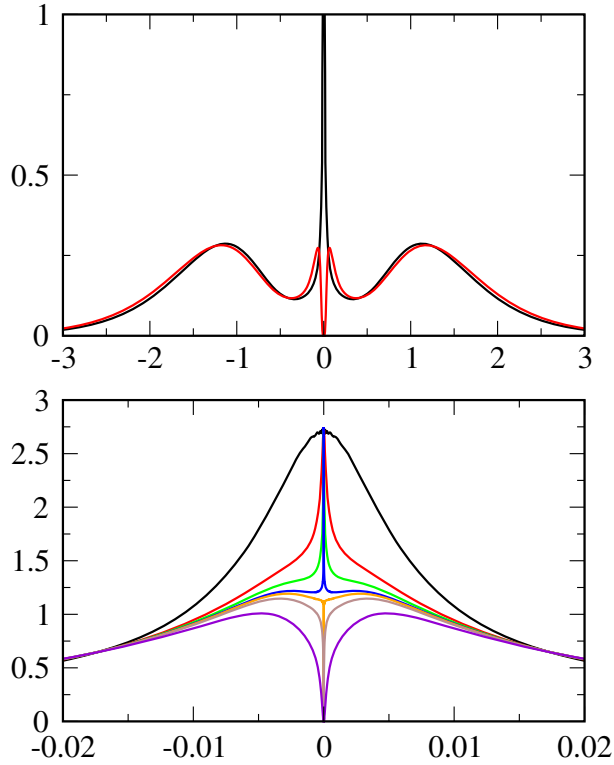


Figure 5.2: Impurity DOS across the unstable fixed point. In the top panel two DOS are shown on the full energy range, with well visible Hubbard-side bands. The bottom panel is a zoom of the low energy part.

NRG results

It is clear that NRG is essential as input of any CFT analysis. In addition NRG provides dynamical informations which are not accessible to CFT, as for instance the whole energy dependence of the impurity spectral function. In Fig. 5.2 we show the DOS of the impurity across the fixed point of the model (5.1) with $V = U$. In the top panel of that Figure we draw the DOSs well inside the Kondo screened phase and the unscreened one on a large energy range, where the Hubbard-side bands are well visible. We notice the Kondo resonance in the screened regime as well as the narrow pseudo-gap in the unscreened one. Yet, in the unscreened regime, even if pseudo-gaped, the DOS has spectral weight within the Hubbard side-bands. In the bottom panel, the low energy part is shown across the fixed point. The DOS has two main features. There is a broad resonance which is smooth across the transition. On top of that, in the screened phase there is a narrower peak which shrinks and vanishes at the transition, where

only the broad resonance survives. Above the transition, in the unscreened phase, the narrow resonance turns into a narrow pseudogap within the broad resonance. Since we know, and it is also confirmed by NRG, that the fixed-point DOS at the chemical potential is half of its value in the Kondo regime, we guessed the following ansatz for the low-energy DOS:

$$\rho_{\pm}(\epsilon) = \frac{\rho_0}{2} \left(\frac{T_+^2}{\epsilon^2 + T_+^2} \pm \frac{T_-^2}{\epsilon^2 + T_-^2} \right), \quad (5.14)$$

where $\rho_0 = 1/(\pi\Gamma)$ is the DOS of the resonant level model in the absence of interaction, and the $+$ refers to the screened phase and the $-$ to the unscreened one. T_+ is the width of the broad resonance, while T_- is that one of the narrow resonance which turns into a narrow pseudogap. T_- has to be identified as the energy scale which controls the deviations δJ from the fixed point, namely $T_- \sim (\delta J)^2$. The model DOS (5.14) has all features we need. At the chemical potential is equal to the non-interacting value ρ_0 in the screened phase, is half of it at the fixed point, and vanishes quadratically in the unscreened regime. The model DOS (5.14) corresponds to a model Green's function at low energy

$$\mathcal{G}(i\epsilon) = \frac{1}{2\Gamma} \left(\frac{T_+}{i\epsilon + iT_+ \text{sign}(\epsilon)} + \frac{T_-}{i\epsilon + iT_- \text{sign}(\epsilon)} \right), \quad (5.15)$$

as well as to a model self-energy

$$\Sigma(i\epsilon) = \mathcal{G}_0(i\epsilon)^{-1} - \mathcal{G}(i\epsilon)^{-1} = i\epsilon + i\Gamma \text{sign}(\epsilon) - \mathcal{G}(i\epsilon)^{-1}. \quad (5.16)$$

If we use (5.16) to fit the actual NRG results, we find an excellent agreement with the fitting parameters T_+ and T_- shown in Fig. 5.3. Indeed T_+ is smooth across the transition, and can be identified as the fixed point value of $J = J_*$, while T_- vanishes quadratically, in accordance with CFT.

In Fig. 5.4 we draw the impurity self-energy $\Im m \Sigma(i\epsilon)$, which is purely imaginary in Matsubara frequencies because of particle-hole symmetry, as function of ϵ in the screened phase, at the fixed point and in the unscreened regime. In the Kondo screened phase

$$\Sigma(i\epsilon) \sim i\epsilon \left(1 - \frac{1}{Z} \right),$$

with

$$Z = \frac{2}{\Gamma} \frac{T_+ T_-}{T_+ + T_-}, \quad (5.17)$$

in accordance with perturbation theory. Notice that the non-interacting limit corresponds to $T_+ = T_- = \Gamma$. As the fixed point is approached, $T_- \rightarrow 0$ and $Z \rightarrow 0$, too. At the fixed point the self-energy is finite at zero frequency

$$\Sigma(i\epsilon \rightarrow 0) = -i\Gamma,$$

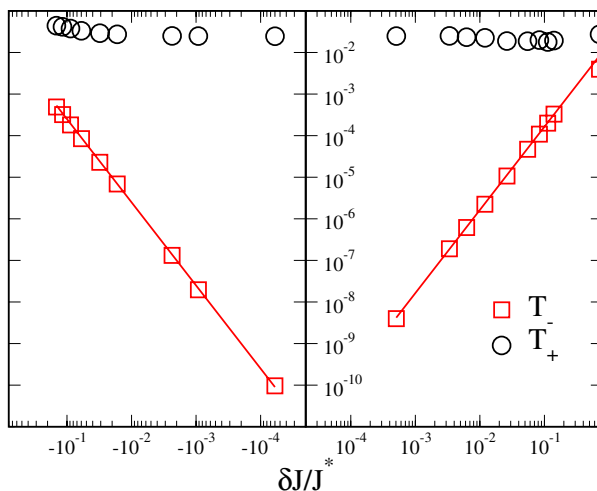


Figure 5.3: Fit values of T_+ and T_- across the fixed point.

like the self-energy of a disordered metal. Finally, in the unscreened phase

$$\Sigma(i\epsilon) \sim -i \frac{2\Gamma}{\epsilon} \frac{T_+ T_-}{T_+ - T_-}.$$

Although the impurity self-energy in the unscreened phase is singular, yet the phase should be describable in terms of a local Fermi liquid theory. Indeed the quasiparticle DOS as given by Eq. (C.14) is perfectly finite even in the unscreened phase

$$\rho_a^* = \int_{-\infty}^{\infty} \frac{d\epsilon}{\pi} \frac{\partial f(\epsilon)}{\partial \epsilon} \Im m \left\{ \mathcal{G}_a(\epsilon+i\delta) \left[1 - \left(\frac{\partial \Delta_a(i\epsilon)}{\partial i\epsilon} \right)_{i\epsilon \rightarrow \epsilon+i\delta} - \left(\frac{\partial \Sigma_a(i\epsilon)}{\partial i\epsilon} \right)_{i\epsilon \rightarrow \epsilon+i\delta} \right] \right\} = \frac{1}{\pi} \left(\frac{1}{T_+} + \frac{1}{T_-} \right), \quad (5.18)$$

since the singularity of the self-energy is compensated by the vanishing DOS. This allows to define an effective $Z = \rho_0/\rho_*$, eventhough, strictly speaking, Z is not determined in the unscreened phase. Notice that ρ_* , defined as above, diverges at the fixed point, implying that a local Fermi liquid description is not possible there.

However, since in the stable screened and unscreened phase a Fermi liquid description is legitimate, one can extract the Landau parameters discussed in C. This is done by calculating with NRG the Wilson ratios of the three conserved quantities, namely the charge (C), the spin (S) and the total T_z (T_z), and, through (C.25) one obtains the Landau parameters in the corresponding particle-hole channels, A_C , A_S and A_{T_z} , respectively. These in turns are related to the scattering amplitudes in the particle-particle channels,

$$A^1 = Z^2 \rho_* \Gamma^1, \quad A_{\pm}^0 = Z^2 \rho_* \Gamma_{\pm}^0, \quad A_0^0 = Z^2 \rho_* \Gamma_0^0,$$

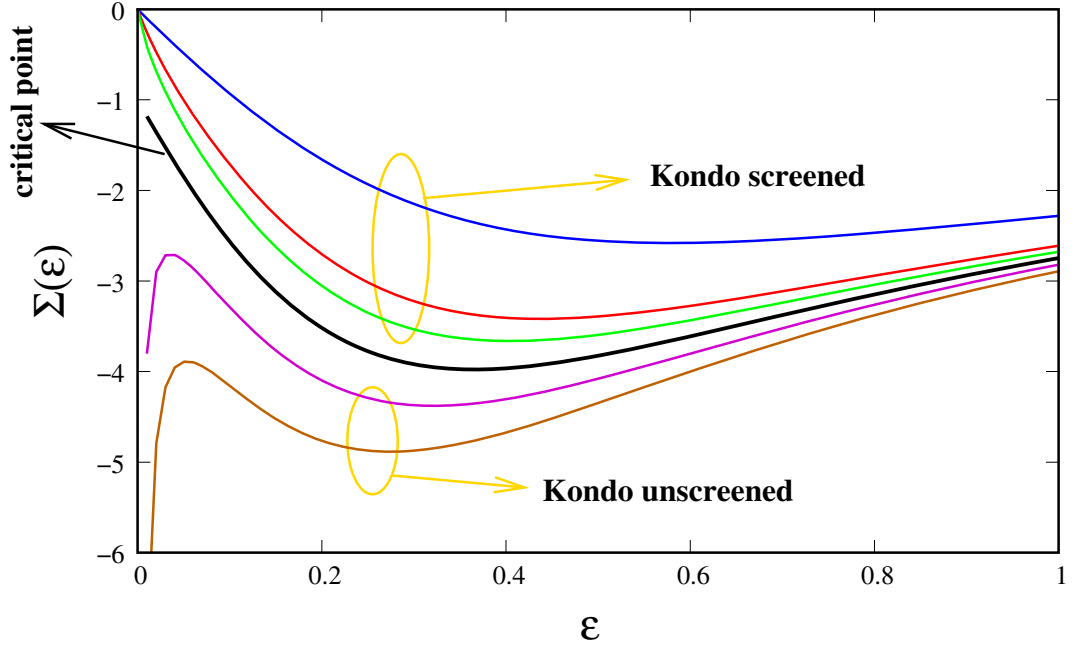


Figure 5.4: Behavior of the self-energy in the different phases.

through

$$\begin{aligned}
 A_C &= \frac{1}{4} \left(6A^1 + 4A_{\pm}^0 + 2A_0^0 \right), \\
 A_S &= \frac{1}{4} \left(2A^1 - 4A_{\pm}^0 - 2A_0^0 \right), \\
 A_{T_z} &= \frac{1}{4} \left(-6A^1 + 4A_{\pm}^0 - 2A_0^0 \right).
 \end{aligned}$$

Since the parameters on the left hand side are known by NRG, one can determine the the scattering amplitudes in the particle-particle channels. In Fig. 5.5 these amplitudes are drawn for the model (5.1) with $V = U$ and both J positive and negative. Notice that, approaching the fixed point from both sides of the transition, $A_0^0 \rightarrow -3$, even though its bare value, see Eq. (5.2), is $\rho_0 (U - 3J/4) \gg 0$ since in that calculation $U/J = 2 \times 10^2$ and $\rho_0 U = 6$. In other words, approaching the fixed point the scattering amplitude in the $S = 0$ $T_z = 0$ Cooper channel from repulsive turns strongly attractive.

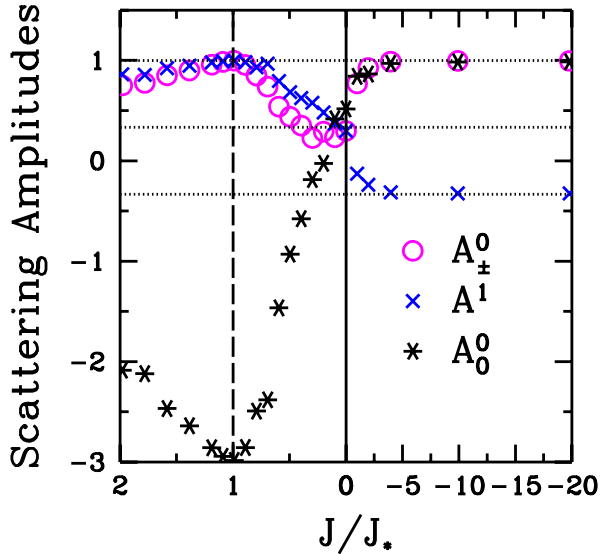


Figure 5.5: Scattering amplitudes in the particle-particle channels.

5.1.4 The phase diagram away from particle-hole symmetry

One may realize that to conjecture the existence of the fixed point we used crucially the particle-hole symmetry to exclude a continuous cross-over from $\delta = \pi/2$ to $\delta = 0$. On the other hand, CFT predicts that ordinary particle-hole symmetry breaking is not a relevant perturbation, hence that the fixed point should survive even when it is broken. In the model (5.1) with $V = U$, we included particle-hole symmetry breaking by

$$\frac{U}{2} \sum_{a=1}^2 (n_a - 1)^2 + V (n_1 - 1) (n_2 - 1) = \frac{U}{2} (n_1 + n_2 - 2)^2 \rightarrow \frac{U}{2} (n_1 + n_2 - 2 + \nu)^2.$$

The role of $\nu > 0$ is to lower the average occupancy of the impurity below 2. However, even in the presence of this perturbation, we still find the same unstable fixed point. The phase diagram as function of J and the average impurity occupancy n , with all other parameters fixed, is sketched in Fig 5.6. The critical line which separates the two stable phases moves at larger J 's as we move away from particle-hole symmetry, and, for $n \rightarrow 1$, merges into a mixed-valence critical point which occurs when $J \simeq U$. The behavior of the DOS across the transition moving the parameter ν is also shown in Fig 5.6. We notice that, as soon as we move away from particle-hole symmetry, the pseudo-gap becomes asymmetric and is gradually filled until, above a critical ν , it turns into a Kondo resonance.

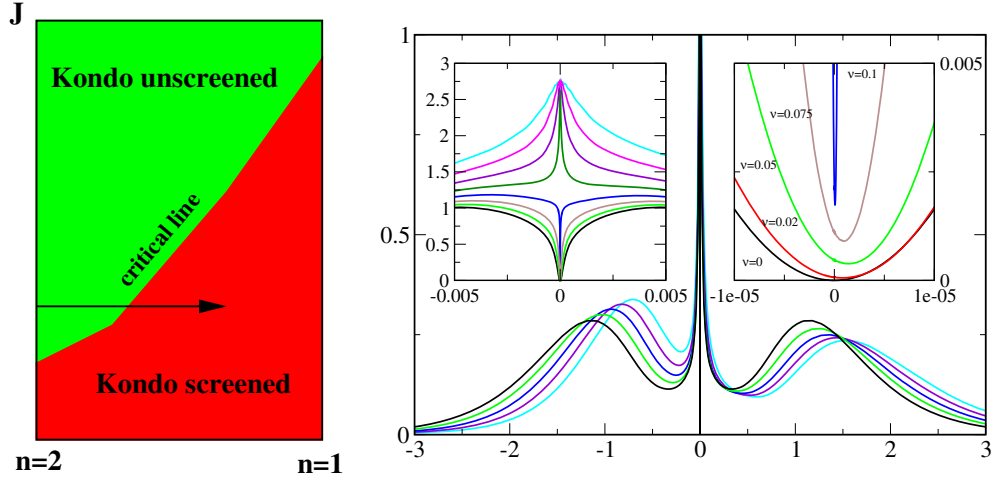


Figure 5.6: Left panel: the phase diagram of the model (5.1) with $V = U$ as function of the average impurity occupancy. Right panel: the impurity DOS along the path drawn in the phase diagram.

The NRG spectrum shows that across the transition there is still a $\pi/2$ jump of the phase shifts, even though on both phases the phase shift is in between 0 and $\pi/2$. Namely, if we assume in the unscreened phase a phase shift δ_- , in the screened phase $\delta_+ = \pi/2 + \delta_-$. In addition we know that the scattering S -matrix is

$$\Re S_{\pm} = \cos 2\delta_{\pm} = 1 - 2\frac{\rho_{\pm}}{\rho_0},$$

from which we obtain

$$\rho_+ - \rho_- = \rho_0 \cos 2\delta_-.$$

From the definition of the phase-shifts in terms of the Green's function, we guessed a model DOS

$$\rho_{\pm}(\epsilon) = \frac{\rho_0}{2} \left[\frac{T_+^2 + \mu_{\pm}^2}{(\epsilon + \mu_{\pm})^2 + T_+^2} \pm \cos 2\delta_- \frac{T_-^2}{\epsilon^2 + T_-^2} \right], \quad (5.19)$$

with $\mu_{\pm} = \pm T_+ \sin 2\delta_-$ which fits well the numerical results. We notice from (5.19) that the second lorentian is always pinned at the chemical potential, so that the filling of the pseudo-gap occurs because the broad resonance is not anymore symmetric.

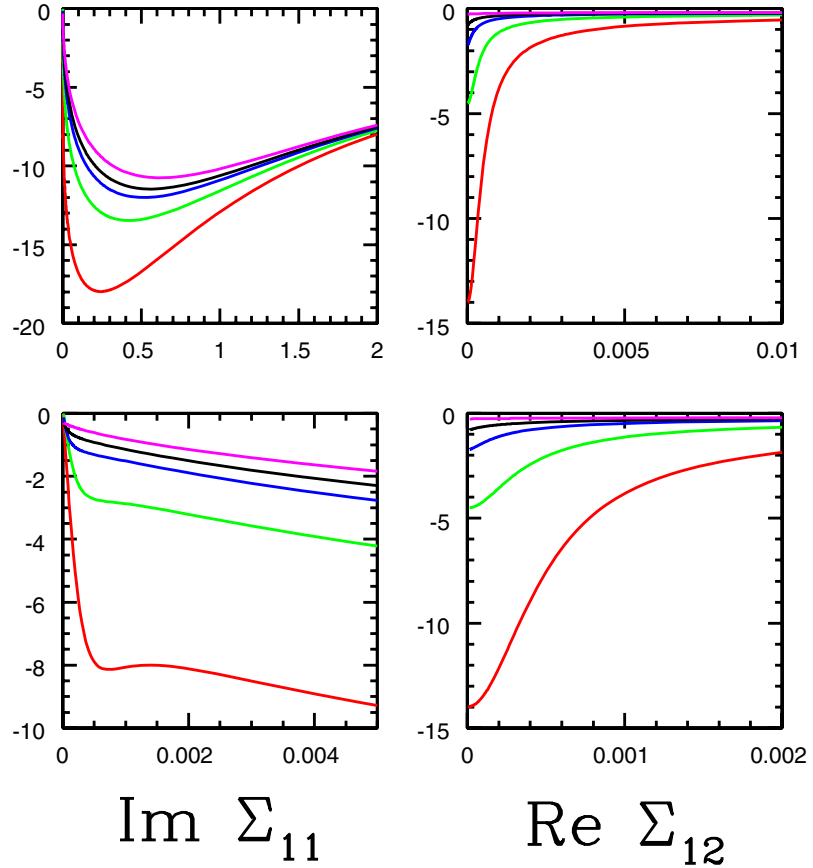


Figure 5.7: Left panels: diagonal self-energy on different energy ranges. Right panels: off-diagonal self-energy.

5.1.5 A more realistic dimer model

We have seen that the unstable fixed point of the dimer model (5.1) is destabilized by a direct hopping between the two impurities. This is however the most realistic situation, and would actually correspond to the impurity model onto which for instance an Hubbard model should be mapped within cluster DMFT. Therefore one may wonder how much of the critical behavior

is left if, instead of (5.1) we considered the impurity model

$$\begin{aligned} \mathcal{H} = & \sum_{\mathbf{k}\sigma} \sum_{a=1}^2 \epsilon_{\mathbf{k}} c_{\mathbf{k}a\sigma}^\dagger c_{\mathbf{k}a\sigma} + \sum_{\mathbf{k}\sigma} \sum_{a=1}^2 \left(V_{\mathbf{k}} c_{\mathbf{k}a\sigma}^\dagger d_{a\sigma} + H.c. \right) \\ & + \frac{U}{2} \sum_{a=1}^2 (n_a - 1)^2 - t \sum_{\sigma} \left(d_{1\sigma}^\dagger d_{2\sigma} + H.c. \right). \end{aligned} \quad (5.20)$$

As we have mentioned several times, the approach to the Mott transition corresponds to an impurity model deep inside the Kondo regime, namely with $U \gg V_{\mathbf{k}}, t$. In this limit, (5.20) can be mapped by a Schrieffer-Wolff transformation onto the Kondo limit of (5.1), with $V = 0$. The Kondo exchange J_K is the same in both models, the impurity exchange is $J = 4t_{\perp}^2/U$. However, at next order in $1/U$, a local direct hybridization V_x among the baths is generated, with $V_x \sim J_k t_{\perp}/U$. Although small, V_x is a relevant perturbation which makes the unstable fixed point of model (5.1) unaccessible in model (5.20). Yet, since $J \gg V_x$, one may expect that a quantum critical region, but not a true quantum critical point, is still well visible.

This is indeed the case. Notice that, in the presence of the hopping, the impurity self-energy has a diagonal part, $\Sigma_{11} = \Sigma_{22}$, which we find is purely imaginary in Matsubara frequencies, and an off diagonal one, $\Sigma_{12} = \Sigma_{21}^*$, which turns out to be real. In Fig. 5.7 we draw the impurity self energy $\Sigma(i\epsilon)$ as function of ϵ with $U = 8$, $t = 0.05$, hence $J = 1.25 \times 10^{-3}$, and $\Gamma = 0.5 \div 0.3$ from the top curve to the bottom one, namely $J_K = 0.08 \div 0.05$, in units of half the conduction bandwidth. There are several interesting things to notice. The first is that a quite sharp cross-over from an “unscreened” phase, with a large $\Im m \Sigma_{11}$ to a “screened” one, with a small $\Im m \Sigma_{11}$, is visible. However, even if in the “unscreened” phase the $\Im m \Sigma_{11}$ seems to be diverging coming from high energy, at very low energy it upturns into a conventional Fermi-liquid behavior, with $\Im m \Sigma_{11} \propto -\epsilon$, although with a very large slope. Also interesting is the behavior of $\Re e \Sigma_{12}$. Indeed, in spite of the fact that the off-diagonal term introduced in the Hamiltonian, $t = 0.05$, is very small, the off-diagonal self-energy becomes very large at small energy, so to compensate the big slope of the diagonal one, inversely proportional to Z . This behavior indicates that, although the fixed point is not accessible, still the cross-over between the two extreme regimes is sharp. This is further confirmed by the plot of the diagonal DOS in the same range of Γ 's, shown in Fig 5.8. We see that the DOS moves from a Kondo-like behavior into a pseudo-gaped one quite sharply.

5.2 The dimer model versus DMFT

In summary, we have shown that a dimer of Anderson impurities includes generally two regimes. One is dominated by the Kondo effect, while in the other the inter-impurity coupling prevails. Consequently, in the former the impurity DOS have a Kondo resonance, but in the latter the DOS have a deep or even a pseudo-gap. In the highly symmetric model (5.1), which possesses

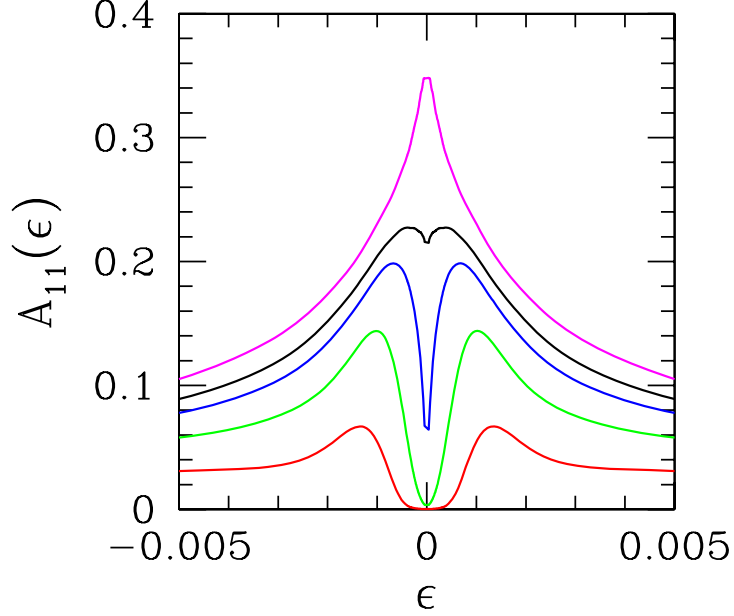


Figure 5.8: Diagonal component of the DOS.

an orbital $O(2)$ symmetry, these two regimes are separated by a true critical point. Right at the critical point there are singular susceptibilities in three relevant channels, namely the staggered magnetization, Eq. (5.9), the channel hybridization, Eq. (5.8), and the inter-channel single Cooper pair, see Eq. (5.7). In the more realistic model (5.20), which includes by construction the relevant interchannel hybridization, the two extreme regimes are separated by a crossover, which however turns out to be quite sharp. This suggests that, although none of the above mentioned susceptibilities ever diverges, yet there should be a finite region where they are strongly enhanced, manifestation of the avoided criticality. Can we make any prediction out of these results about a lattice model which maps by DMFT just on the same class of impurity dimers.

Let us just concentrate on a lattice model which has been actually worked out by DMFT, and corresponds to the lattice generalization of (5.1) with $U = V$, namely with an Hamiltonian

$$\mathcal{H} = -t \sum_{\langle \mathbf{R}\mathbf{R}' \rangle \sigma} \sum_{a=1}^2 \left(c_{\mathbf{R}a\sigma}^\dagger c_{\mathbf{R}'a\sigma}^\dagger + H.c. \right) + \frac{U}{2} \sum_{\mathbf{R}} (n_{\mathbf{R}} - 2)^2 + J \sum_{\mathbf{R}} \mathbf{S}_{\mathbf{R}1} \cdot \mathbf{S}_{\mathbf{R}2}, \quad (5.21)$$

which describes a two-band Hubbard model with an inverted exchange splitting favoring an inter-

orbital singlet state on each site. Within the original single-site DMFT, (5.21) maps onto (5.1), which we know has the right symmetry to encounter the unstable fixed point. The behavior of the Kondo temperature of the impurity after DMFT self-consistency has been carried out can be depicted as in Fig. 5.9. At half-filling, T_K is decreasing with U until, at a critical value, it should

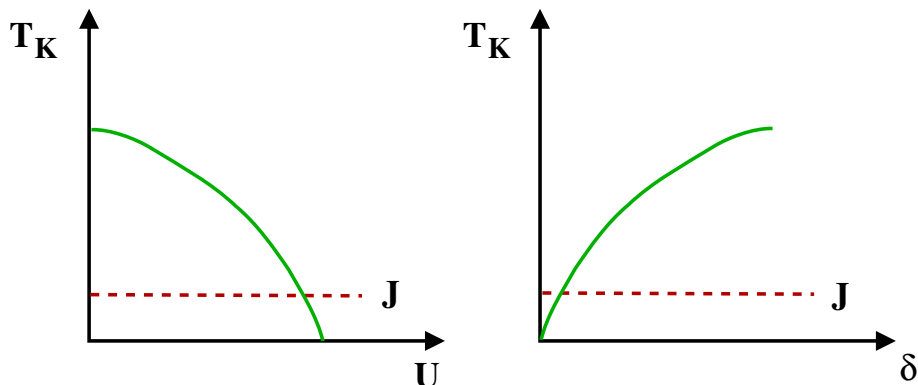


Figure 5.9: Behavior of the DMFT self-consistent Kondo temperature as compared to the inverted exchange J

vanish, signalling the Mott transition. However, before that happens, T_K necessarily becomes of order J which corresponds to the location of the impurity critical point. Analogously, if we start at half-filling from the Mott insulator and dope it, T_K from its insulating value $T_K = 0$, will gradually increase with doping, until, at a critical doping, it will cross the value $T_K \simeq J$ of the critical point, which we know can be crossed also varying the impurity average occupancy. In both cases, the impurity model encounters its critical point before the MIT, and, from what we previously mentioned, one should expect, around this point, a region with symmetry breaking within one of the instability channels of the impurity. The staggered magnetization (5.7) would likely correspond to an antiferromagnetic ordering with opposite staggered magnetization in the two orbitals, while (5.8) to an inter-orbital dimerization, presumably also staggered. Both these instabilities occur in the particle-hole channel. The last one, (5.9), occurs in the particle-particle inter-orbital singlet channel and would correspond to s -wave superconductivity. Since the irreducible vertices in all the three channels are equally singular, which of these instabilities really occurs mainly depends on the Green's function bubbles

$$T \sum_n \sum_{\mathbf{k}} G(i\epsilon_n + i0^+, \mathbf{k} + \mathbf{Q}) G(i\epsilon_n, \mathbf{k}),$$

in the particle-hole channels, where \mathbf{Q} is the modulation wave-vector, as opposed to

$$T \sum_n \sum_{\mathbf{k}} G(i\epsilon_n, \mathbf{k}) G(-i\epsilon_n, -\mathbf{k}),$$

in the Cooper one. While the latter is always singular in a Fermi-liquid phase, the former is singular only if nesting occurs at some \mathbf{Q} , or if a van Hove singularity exists at the chemical potential, in which case $\mathbf{Q} = 0$. If we exclude both these events, which can always be done within DMFT by simply preventing particle-hole instabilities in the self-consistency procedure, only superconductivity might emerge. However, within model (5.21), we should not expect any room for a superconducting instability, especially near the MIT. In fact, the “bare” scattering amplitude in the inter-orbital singlet Cooper channel,

$$A_0^0 = U - 3J/4, \quad (5.22)$$

is always repulsive near the MIT, assuming $J \ll W \simeq U$. This naïve expectation is actually

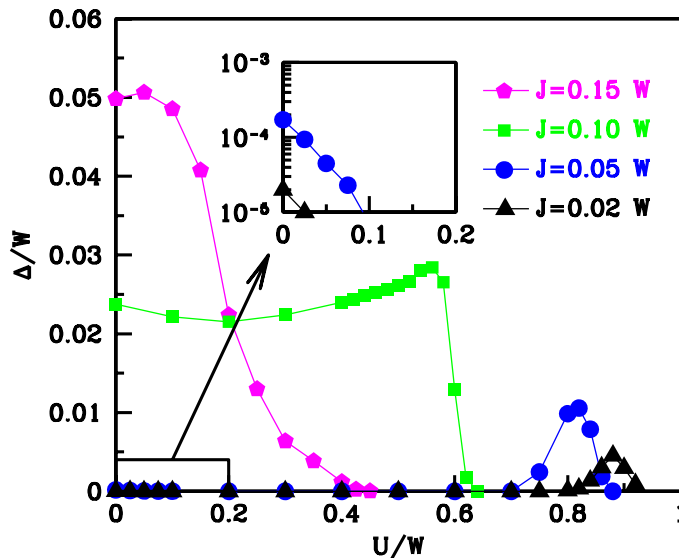


Figure 5.10: Anomalous self-energy at zero frequency as function of U/W for different J 's

wrong. In Fig. 5.10 we draw the anomalous superconducting self-energy at zero-frequency and half-filling as function of U/W for different J 's. For large J/W , as U increases, the anomalous self-energy decreases, in agreement with (5.22), until a first order phase transition from a superconductor to a Mott insulator takes place. For intermediate couplings, the first order transition remains but the off-diagonal self-energy starts to behave non-monotonically, namely

after a first decrease, it increases again. More interesting and surprising is the weak J/W behavior. Here the off-diagonal self-energy decreases until, roughly when $U = 3J/4$, see (5.22), superconductivity disappears into a normal metal behavior. However, just before the MIT, superconductivity reappears with an anomalous self-energy reaching values that are orders of magnitude larger than within the BCS $U = 0$ domain. This behavior might suggest, as we speculated, that this superconducting region before the MIT is just the response of the lattice model to the impurity critical behavior. Indeed, if we prevent superconductivity and calculate numerically the self-energy of the metastable metallic solution, which could be identified as the hypothetical normal phase, we find a behavior very similar to that one of the impurity. By fitting the calculated self-energy with the model one, Eq. (5.16), we can even extract the values of T_- and T_+ as shown in Fig. 5.11. Several things are worth noticing. First, the Landau-Fermi liquid behavior breaks down and turns, before the MIT, into a pseudo-gaped phase. Next, the maximum of the anomalous self-energy occurs right at the point $T_- = 0$, as expected. Finally, the MIT is not accompanied by a vanishing energy scale, as in the Brinkmann-Rice scenario, but occurs when $T_+ = T_-$ within the pseudo-gaped regime. Notice that, the pseudo-gaped phase is semi-metallic, with vanishing Drude weight. On the other hand, this “normal” phase is unstable to superconductivity, which does have a finite Drude weight which vanishes only at the MIT. This implies that, in the pseudo-gaped regime, the on-set of superconductivity is accompanied by an increase of Drude weight, unlike what happens in the BCS regime. This increase of Drude weight, has a counterpart in the impurity model. At the fixed point, the impurity model has a finite entropy, implying that the conduction bath is unable to fully screen the impurity degrees of freedom. If one allows for a bath where anyone of the relevant symmetries is broken, new screening channels open up, that are able to quench also the residual fixed point entropy. The fixed point therefore is washed out, but screening energy is gained. Translated in the lattice model, this screening energy gain does correspond to band energy gain.

In conclusion, at least in model (5.21), the physics of the underneath impurity model translates nicely into the behavior of the lattice model even after full DMFT-self-consistency. This is further supported by the full phase diagram as function of U/W and doping away from half-filling, shown in Fig. 5.12.

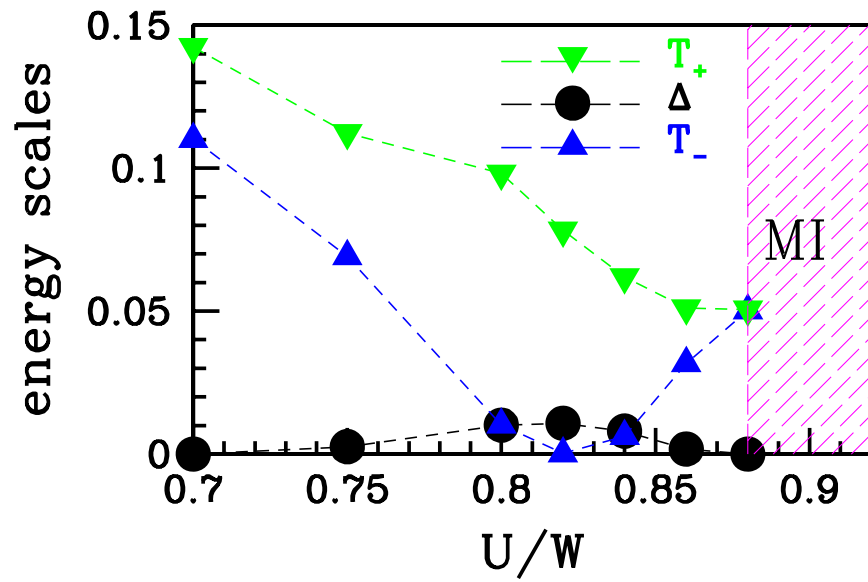


Figure 5.11: Fit values of T_+ and T_- of the normal phase. Also shown is the off-diagonal self-energy

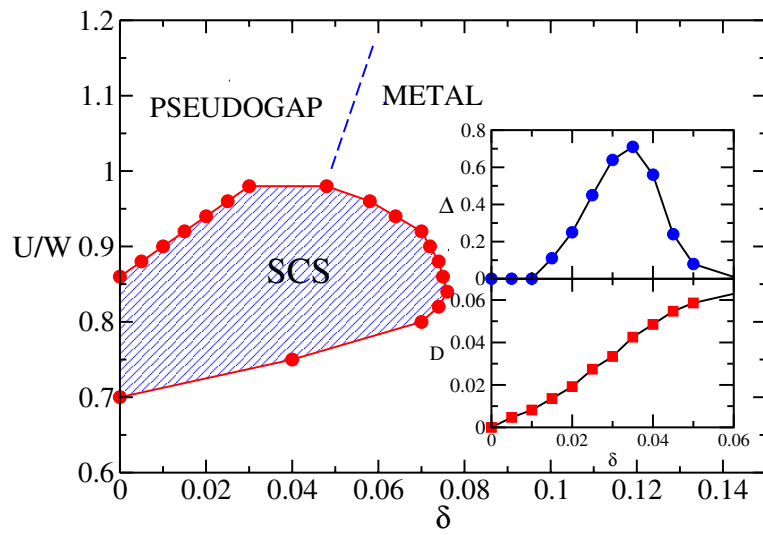


Figure 5.12: Phase diagram of (5.21) with $J/W = 0.02$ as function of U/W and doping $\delta = 2 - n$.